Claudia Eva Maria Schaller

The Autoimmune Regulator (AIRE) and the Early Wave of Apoptosis in Spermatogenesis

Dissertation der Fakultät für Biologie
der Ludwig-Maximilians-Universität München

Department of Microbiology and Immunology
University of California San Francisco

1. Gutachter: Prof. Elisabeth Weiß

2. Gutachter: Prof. Harry MacWilliams

Sondervotum: Prof. Matthias Wabl, University of California San Francisco

Tag der mündlichen Prüfung: 5. July 2010

CHAPTER I: INTRODUCTION

Overview

In 1997 the human autoimmune disorder autoimmune polyendocrinopathy-candidiasis-ectodermal dystrophy (APECED) was linked to mutations in a novel gene, later named the autoimmune regulator (*AIRE*). It soon became clear that AIRE is involved in the expression and presentation of a large variety of peripheral tissue-restricted antigens during T cell development in the thymus. T cells recognizing the self-antigens are eliminated in a process called negative selection, thus establishing central tolerance and helping to prevent autoimmunity.

In addition to the thymus, the testes also are a location that exhibits promiscuous gene expression. This paper presents evidence that AIRE protein is sporadically present in murine spermatogonia and spermatocytes. However, none of the tested genes controlled by AIRE in the thymus were found to be regulated by AIRE in the testis. Nevertheless, *Aire*-deficient male mice are subfertile, and we observed that the essential and scheduled, prepubertal wave of apoptosis is reduced, whereas sporadic apoptosis during adulthood was increased. Excluding an involvement of the adaptive immune system, we suggest a link between the scheduled and sporadic apoptotic processes, and propose that promiscuous gene expression in the testis provides a platform for a negative selection mechanism that keeps the germline stable.

1. AIRE and the immune system

1.1 Immunological background

AIRE plays an essential role in the immune system. To understand the importance of its function within the context of immunity and autoimmunity, an overview of the adaptive immune system is given, thereby focusing on T cell-mediated responses, T cell development and the establishment and breakdown of self-tolerance.

1.1.1 Overview of the adaptive immune response

Vertebrates developed the adaptive immune system, which works together with the ‘first-line’ defense of the innate immune system, to eliminate invading pathogens and any toxic molecules they produce. The innate immune response is non-specific, independent of any previous contact with an antigen, and offers immediate protection during the first critical hours of exposure to a new pathogen.

In the course of its events, the more specific and efficient adaptive immune response is induced by mobilization of antigen-presenting dendritic cells (DCs) that are able to activate T cells (Murphy et al., 2008).

Dendritic cells are located throughout the body and can take up a wide variety of pathogens or their products, either at the site of infection, or in peripheral lymphoid organs. After processing, the pathogen-derived antigens are presented on MHC class I or MHC class II molecules to naive $CD4^+$ or $CD8^+$ T cells in a nearby lymph node (Guermonprez et al., 2002). Besides DCs, also B cells and macrophages serve as antigen-presenting cells (APCs), able to activate T cells (Underhill et al., 1999).

The T cell receptor (TCR) on the naive $CD4^+$ or $CD8^+$ T cell must recognize the foreign-peptide:self-MHC complex together with the particular co-receptor on the APC in order to activate the T cell (Murphy et al., 2008). An additional co-stimulatory signal, provided by the same APC, is necessary for survival and proliferation of the T cell. Cytokines provide a third signal that directs the T cells to differentiate into various subsets of effector cells, which - from that moment on - can respond to the specific target cells without any further co-stimulation (London et al., 2000).

The $CD8^+$ cells differentiate into cytotoxic T cells which attack cells infected with intracellular pathogens such as viruses, some bacteria and parasites. An infected cell displays the foreign antigen bound to MHC class I on its surface. If recognized by the TCR, the primed and cytotoxic T cell induces apoptosis in the target cell (Barry and Bleackley, 2002) via the release of perforin and granzymes, thereby activating pro-apoptotic proteins (Metkar et al., 2002). Cytotoxic T cells also produce FAS ligand that directly induces apoptosis on some FAS-bearing target cells (Trambas and Griffiths, 2003).

Depending on the activation signal, $CD4^+$ cells can differentiate into several types of T-helper (T_H) effector cells: T_H1, T_H2, T_H17 and regulatory T cells (Tregs). T_H1 cells play a central role in macrophage activation. Certain intracellular and extracellular pathogens manage to resist killing after being phagocytosed by the macrophage. T_H1 cells recognize the specific antigen and deliver additional signals activating the macrophage to kill the ingested pathogens (Monney et al., 2002).

The humoral immune response can be induced by T_H1 and T_H2 cells (McHeyzer-Williams et al., 2006). T_H1 cells stimulate B cells to generate strongly opsonizing

IgG antibodies, whereas T_H2 cells are responsible to activate naive B cells to proliferate and secrete specific IgM antibodies. Class switching of B cells to different types of immunoglobulins is as well directed by T_H2 cells (Murphy et al., 2008).

The subset of T_H17 cells produces pro-inflammatory IL-17 and induces fibroblast and epithelial cells to secrete chemokines attracting neutrophils to the site of infection (Veldhoen et al., 2006). Finally, Tregs play a crucial part in regulating peripheral tolerance by suppressing the effector functions of $CD4^+$ and $CD8^+$ T cells (Mempel et al., 2006). They are furthermore found to be able to influence B cell antibody production (Eddahri et al., 2006) and the function and maturation of APCs (Taams et al., 2000).

In order to respond more rapidly and efficient to a possible future encounter with a previous antigen, memory T cells and B cells are generated, providing long-term immunological protection (Murphy et al., 2008). B cells undergo somatic hypermutation and isotype switching, thereby producing high affinity receptors and antibodies. $CD4^+$ and $CD8^+$ memory T cells originate from newly primed and/or differentiated effector cells. The cytokines IL-7 and IL-15 are required for their long-term survival and proliferation needs to be sustained by contact with self-peptide:self-MHC complexes (Murphy et al., 2008).

This illustrates the powerful effector mechanism with which T cells can respond to foreign pathogens. It also becomes clear how important it is that T cells are able to distinguish between the foreign ‘non-self’ macromolecules and the host’s own ‘self’ macromolecules, in order to avoid a dangerous attack against self-tissue. AIRE plays an essential role helping T cells to achieve self-tolerance, as the following sections describe.

1.1.2 Establishment of self-tolerance

Lymphocytes achieve self-tolerance during their development in the thymus and bone marrow (central tolerance) and, once they have left the central lymphoid organs, in the periphery (peripheral tolerance). AIRE establishes central tolerance during T cell development in the thymus by expressing many tissue-restricted self-antigens. Medullary thymic epithelial cells (mTECs) and DCs present those antigens to developing T cells; if responsive, the auto-reactive T cells are deleted during negative selection and central tolerance is established. Together with several mechanisms that build additional peripheral tolerance - some even

suggesting a further involvement of AIRE - a vastly self-tolerant immune system is acquired.

1.1.2.1 Central tolerance: negative and positive selection in the thymus

The morphology of the thymus (figure I.1) is essential for establishment of central tolerance. The unique environment allows developing T cells interactions with other thymic cell types that assist positive and negative selection processes. The outcome is an effective, but non-self-reactive T cell repertoire (Rodewald, 2008).

In mice, thymus development is finished by week 3-4 *post partum*, and in humans at birth; in both, T cell production is highest before puberty and decreases after, although continuing throughout life (Murphy et al., 2008).

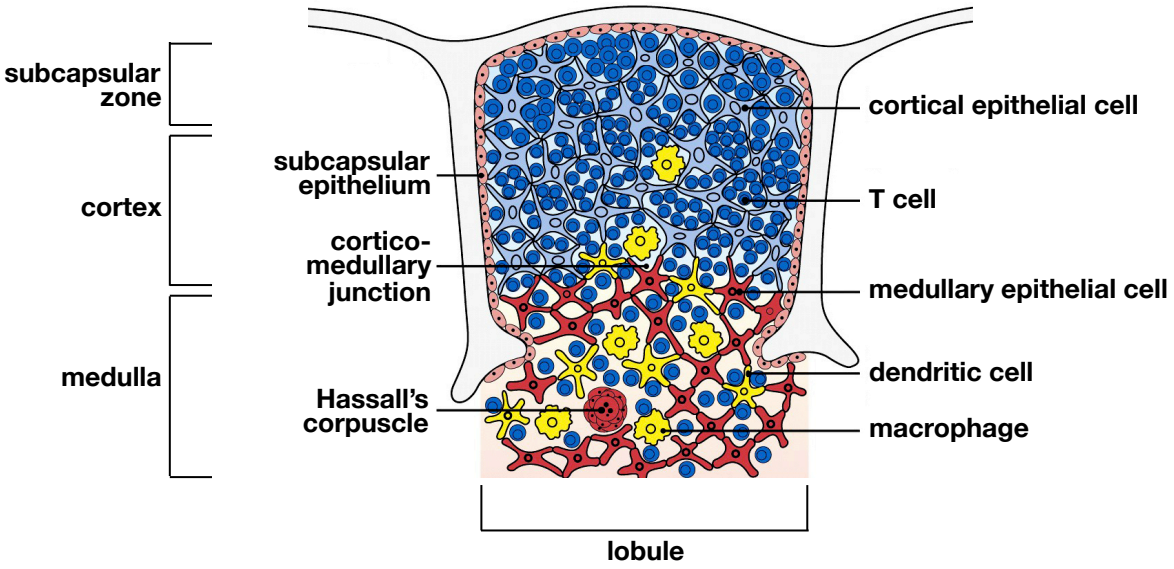

Figure I.1: Cellular organization of the thymus
The thymus consists of numerous lobules, separated by connective tissue. Morphologically, in each lobule an inner lighter zone (the medulla) and an outer darker zone (the cortex) can be distinguished. T cell progenitors enter the thymus through vasculatures that are enriched around the cortico-medullary junction. Therefore, immature, 'double-negative' T cells can be found in the cortex and subcapsular zone of the thymus. During development, T cells become 'double-positive' and undergo positive and negative selection in the cortex by interaction with cortical epithelial cells. Selected mature, 'single-positive' T cells enter the medulla, where negative selection of auto-reactive T cells takes place. AIRE plays an essential role in negative selection by expressing many tissue-restricted self-antigens, which are presented to T cells by medullary epithelial cells and dendritic cells. Macrophages can be found in the cortex and medulla where they clear apoptotic T cells and function as antigen presenting cells; dendritic cells reside in the medulla functioning as well as antigen presenting cells. Via cytokine release, Hassall's corpuscles stimulate dendritic cells to induce regulatory T cell differentiation (Watanabe et al., 2005). Picture from Murphy at al., 2008.

Negative and positive selection are primarily based on the successful assembly of the TCR during T cell development, allowing TCR:MHC interactions (Kyewski and Derbinski, 2004).

T cell precursors, derived from the same lymphoid progenitor as B cells, migrate from the bone marrow into the thymic cortex (Takahama et al., 2006). The $CD3^-4^-8^-$, 'double-negative' cells, give rise to α:β T cells and the minor population of γ:δ T cells. The α:β T cells start VDJ-rearrangement (with help of RAG-1 and RAG-2) of the TCR β-chain locus, and, once successfully synthesized, pair it with a surrogate pre-TCR α-chain (Murphy et al., 2008). During those processes, the T cells migrate, guided by chemokines, toward and then inside the sub-capsular zone of the thymus. Upon assembly of the CD3 co-receptor, the T cells start proliferating, travel back into the outer cortex, and display CD8 and CD4. The 'double-positive' T cells rearrange the TCR α-chain locus and undergo positive and negative selection.

Positive selection ensures specificity of the TCR to the MHC and determines the presentation of either CD4 or CD8 and therefore the effector functions of the mature T cells (Murphy et al., 2008). In order to be positively selected, the α:β TCR with co-receptor of the 'double-positive' T cell has to interact with a self-peptide:self-MHC complex on the cortically thymic epithelial cells (cTECs); recognition of peptides bound to self-MHC class I molecules leads to the production of CD8 and programs the T cell to become a cytotoxic effector cell. TCRs recognizing peptides bound to self-MHC class II molecules generate CD4 and become cytokine-secreting T-helper cells (Murphy et al., 2008). A subset of cells with CD4 and high levels of CD25 develops into Tregs (Fontenot et al., 2005).

The now 'single-positive', either $CD4^+$ or $CD8^+$ T cells, migrate into the medulla where negative selection takes place. Negative selection can occur in the cortex and medulla throughout T cell development, but the medulla with its antigen presenting cells, like macrophages, DCs and mTECs is the specialized site (Hogquist et al., 2005). Negative and positive selection are based on the same principle: the recognition of self-peptide:self-MHC complexes. Weak affinity rescues the T cells and leads to positive selection and further maturation, strong signaling results in negative selection (Bouillet and Strasser, 2002). The negatively selected cells die by apoptosis, mediated by the BCL-2 family member BIM (Sohn et al., 2007), resulting in death of around 95% of T cells (Huesmann et al., 1991).

For negative selection, the APCs not only present ubiquitous antigens and antigens that access via circulation or in association with immigrating cells (Klein and Kyewski, 2000). Peripheral self-antigens, normally only present in specific tissues, need to be expressed and presented, as well. The expression of a large portion of those peripheral-tissue antigens (PTAs) in a distinct subset of mTECs (Hamazaki et al., 2007) is transcriptionally regulated by AIRE (Anderson et al., 2002). The mTECs display the self-antigen:MHC complexes on their surface or release them for uptake and further presentation by DCs (Mathis and Benoist, 2007). The promiscuous gene expression (pGE) in the thymus is highly diverse and represents many organs and developmentally and temporarily regulated genes, which are often clustered and highly conserved between human and mice (Kyewski and Klein, 2006).

After successful positive and negative selection, the naive T cells migrate to the peripheral lymphoid tissue. Circulating between blood and lymph system, the T cells continuously reenter the lymphoid tissue until encountering their specific antigen. If so, the T cell stops circulating, proliferates and differentiates into an effector cell. T cells, which not encounter their specific antigen, die and are replaced, ensuring a constant T cell number combined with TCR diversity (Murphy et al., 2008).

1.1.2.2 Peripheral tolerance

AIRE clearly mediates central T cell tolerance, and some studies also suggest an involvement in the establishment of peripheral tolerance (Sakaguchi et al., 2008; Gardner et al., 2008). Peripheral tolerance completes central tolerance by disarming escaped auto-reactive cells with help of additional selection processes, causing unresponsiveness (anergy) or deletion, or suppression of the auto-reactive T cells by Tregs (Kyewski and Klein, 2006).

Absence of the co-stimulatory signal, which has to be provided by the same APC that activated the TCR, induces anergy and the T cell becomes unresponsive to any future encounter with this antigen. Activation of the TCR can also result in apoptosis of auto-reactive T cells via the FAS/FAS ligand system (Murphy et al., 2008). Tregs execute a dominant peripheral immune regulation by blocking excessive immune responses by suppression of certain types of immune cells (Brusko et al., 2008). Tregs are either produced as functionally mature T cells in the thymus or can be induced from naive T cells in the periphery (Sakaguchi et al., 2008). A role of AIRE in directing auto-reactive T cells in the thymus towards the

Treg cell lineage, rather than their deletion, has been discussed (Aschenbrenner et al., 2007; Sakaguchi et al., 2008). Recently, extrathymic AIRE-producing cells (eTACs) have been identified and found to express a diverse set of antigens in peripheral lymphoid organs, suggesting a role for AIRE in peripheral negative deletion of T cells which were able to escape the thymic selection (Gardner et al., 2008).

The multiple mechanisms of central and peripheral tolerance prevent autoimmunity, though a low level of auto-reactive immune cells remains and is even crucial for normal function of the immune system as the survival of naive T cells and B cells in the periphery requires continuous exposure to autoantigens (Murphy et al., 2008).

1.1.3 Autoimmune diseases

The development of an autoimmune disease is complex and involves usually a combination of different triggers: failure of the above mentioned central and peripheral tolerance mechanism, genetic predisposition and environmental factors, such as infections, all may play a role (Murphy et al., 2008).

The influence of environmental factors is so far not well understood. Infections with certain pathogens can trigger autoimmunity by mimicry of the host's molecules, resulting in cross-reactivity between the pathogen-derived antigen and the self-antigen (Murphy et al., 2008). Also, sequestered proteins, normally sheltered from the immune system can become exposed, and subsequent recognition results in an autoimmune response (Atassi and Casali, 2008).

Autoimmune diseases have a strong genetic component: genetic predisposition for most autoimmune disease is due to the combined effects of multiple genes, especially particular alleles for MHC class II molecules (Atassi and Casali, 2008). Monogenetic autoimmune diseases are very rare, and among them is APECED (autoimmune polyendocrinopathy-candidiasis-ectodermal dystrophy), caused by mutation in the single gene *AIRE* in humans (Ulmanen et al., 2005).

The self-tissue damage is caused by the same effector mechanism as used against pathogens, involving auto-reactive antibodies and T cells that either target specific organs or act systemically (Murphy et al., 2008).

1.2 AIRE (Autoimmune Regulator)

Given the powerful effector mechanisms of the immune systems against pathogens and how harm to self-tissue is avoided by establishing central and peripheral tolerance, the importance of AIRE is emphasized. The following sections will review several aspects how this was discovered and what is known today about the gene, protein, its function and the impact AIRE-deficiency has on mice and also on humans, where it causes the disease APECED.

1.2.1 APECED (autoimmune polyendocrinopathy-candidiasis-ectodermal dystrophy)

The heterogeneous symptoms of this disease were known long before the causative gene was discovered. Thorpe and Handley described the first case in 1929 and APECED appeared since then repeatedly in the literature (Leonard, 1946; Whitaker et al., 1956; Neufeld et al., 1980). APECED (OMIM #240300) is known under various other names, like autoimmune polyendocrine syndrome type-1 (APS-1), polyglandular autoimmune syndrome type I or autoimmune polyendocrinopathy.

1.2.1.1 Genetics

APECED is a rare autoimmune disease, enriched in three genetically isolated populations: the Finnish, the Sardinians and Iranian Jews, where the incidence is approximately 1:25,000 (Ahonen et al., 1990), 1:14,000 (Rosatelli et al., 1998) and 1:9,000 (Zlotogora and Shapiro, 1992), respectively.

Family-based linkage studies in 1994, taking advantage of the high frequency in Finland, surprisingly mapped the locus outside the major histocompatibility complex (MHC) on chromosome 6, to chromosome 21q22.3 (Aaltonen et al., 1994). Because it is an autosomal-recessive condition (Ahonen et al., 1985), it was considered to be a monogenetic disorder, and three years later, two groups identified the responsible gene, named the autoimmune regulator (*AIRE*), by positional cloning (Nagamine et al., 1997; The Finnish-German APECED Consortium, 1997).

Soon, the first pathogenetic mutations were described. So far, over 60 different mutations have been identified in patients, varying from substitutions of single nucleotides to gross deletions, and found throughout the coding region of the human *AIRE* gene (Nagamine et al., 1997; Finnish-German APECED Consortium,

1997; Scott et al., 1998; Heino et al., 2001; Halonen et al., 2002; Meloni et al., 2002). Different *AIRE* mutations seem to have little influence on the complex phenotypes observed in APECED patients. As with all autoimmune diseases, the HLA class II genes (MHC class II, respectively) significantly determine certain disease parameters and therefore the individual clinical picture (Halonen et al., 2002).

1.2.1.2 Clinical features and autoantibodies

APECED patients develop a specific, but also individually variable set of multiple organ-specific autoimmune and infectious diseases (Betterle et al., 1998). With an onset in childhood or early adolescence, the major clinical features are chronic mucocutaneous candidiasis, hypoparathyroidism and adrenocortical failure, also referred to as Addison's disease. To define APECED, two of these three clinical symptoms have to be present (Perheentupa, 2002).

Mucocutaneous candidiasis, caused by *candida albicans*, affects nails, dermis, and various mucous membranes, is the initial manifestation in 60% of the cases, and occurs in all patients at some time (Ahonen et al., 1990). It is potentially followed by hypoparathyroidism, leading to decreased levels of parathyroid hormone (PTH), and later on by Addison's disease (Betterle et al., 1998). In addition to this classical triad of manifestations most patients develop a broad spectrum of associated clinical diseases (Betterle et al., 1998). Autoimmune endocrinopathies like insulin-dependent diabetes mellitus (IDDM) and gonadal dysfunction in female and male patients can be observed (Ahonen et al., 1990). The testicular failure is heterogeneous and occurs in 14% of the APECED patients, who either show azoospermia, primary testicular athropy, or hypergonadotropism (Perheentupa, 2006). Multiple other symptoms were reviewed by Betterle and coworkers, published in 1998.

Immunologically, APECED is characterized by infiltration of lymphocytes into affected organs and the presence of various tissue-specific, circulating autoantibodies (Bjoerses et al., 1998; Peterson et al., 1998). The autoantibodies are directed against proteins and intracellular key enzymes involved in hormone synthesis in organs such as the parathyroid, pituitary and adrenal glands (Nagamine et al., 1997; Bensing et al., 2007). The steroid hormone 17-α-hydroxylase (P450c17) (Krohn et al., 1992), 21-hydroxylase (P450c21) and side-chain cleavage enzyme (P450scc) (Winqvist et al., 1992) are also affected. All three

enzymes are involved in steroid synthesis, and - if targeted by autoantibodies - cause Addison's disease. Gonadal failure is associated with autoantibodies against P450scc and P450c17 (Peterson et al., 2005), and IDDM is linked to autoantibodies against islet cell antigen (ICA), glutamic acid decarboxylase 65 and 67 (GAD65, GAD67), insulin and tyrosine phosphatase-like protein IA-2 (Gylling et al., 2000; Peterson et al., 2004). Anti-interferon autoantibodies have been found recently in 100% of APECED patients (Meager et al., 2006).

1.2.2 Gene

The responsible gene for APECED was identified by two different groups in 1997 (Nagamine et al., 1997; The Finnish-German APECED Consortium, 1997). The human *AIRE* gene is located on chromosome 21q22.2 and consists of 14 exons spanning 11,714 bp of genomic DNA. A promoter with a TATA box is located 35 nucleotides from the first nucleotide of exon 1, and a GC box is immediately upstream of the first exon (Nagamine et al., 1997; The Finnish-German APECED Consortium, 1997). Exon 14 contains the stop codon, followed by a repetitive sequence. Furthermore, exon 14 overlaps with the promoter region of the human phosphofructokinase liver-type (*PFKL*) gene (Levanon et al., 1995). Three splice variant mRNA products have been described, including one which results in a premature stop codon and a transcript predicted to be a candidate for nuclear-mediated decay (Nagamine et al., 1997).

The *Aire* mouse homolog (figure I.2) was isolated 1999 and localized on chromosome 10. The 14 exons span 13,276 bp from the initiation codon to the stop codon (Blechschmidt et al.,1999; Mittaz et al., 1999; Shi et al., 1999). Comparative mapping between mouse and human has shown that human chromosome 21q22.3 shares conserved synteny with mouse chromosomes 10 and 17 (Irving et al., 1994). Eleven alternative splicing forms have been identified (Ruan et al., 1999). Unlike the human homolog, the mouse *Pfkl* gene is located upstream of *Aire* and the DNA methyltransferase 3-like (*Dnmt3l*) gene downstream (Deplus et al., 2002). *Dnmt3l* is positioned in the opposite direction than *Aire* from telomere to centromere and partially overlaps with *Aire* (Shovlin et al., 2007).

The gene organization between the mouse and human homolog is highly conserved, with a nucleotide sequence identity in the coding sequence of 77% (Blechschmidt et al., 1999).

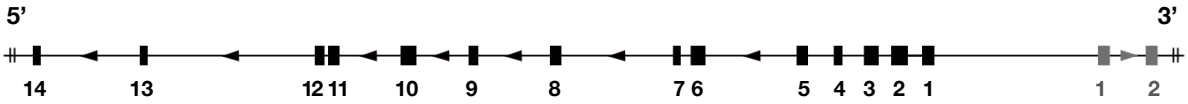

Figure I.2: Schematic *Aire* gene (*mus musculus*)
The 14 exons of the mouse *Aire* gene on chromosome 10 are represented by solid black boxes. The neighboring gene *Dnmt3l* (exon 1 and 2 are represented in grey boxes) is located downstream of *Aire* and orientated in the opposite direction. One of *Dnmt3l*'s splice variants is made with exon 1b which is located between exon 3 and 4 of the *Aire* gene (not shown). Modified after Blechschmidt et al., 1999 and Shovlin et al., 2007.

1.2.3 Protein and domains

The human AIRE protein (545 aa) (Nagamine et al., 1997; The Finnish-German APECED Consortium, 1997) and the mouse AIRE protein (552 aa) (Blechschmidt et al., 1999; Mittaz et al., 1999; Shi et al., 1999), are remarkably conserved and share the same functional domains; their overall identity at the amino acid level is 73% (Blechschmidt et al., 1999).

AIRE contains several domains (figure I.3) characteristic of transcriptional regulators and chromatin binding proteins (Peterson et al., 2008). Its structure is comparable to speckled protein 100 kDa (Sp100) family members, which are involved in transcriptional activation and repression mechanisms (Bloch et al., 2000). Originally, an amino-terminal homogeneously staining region (HSR) was described (Pitkanen et al., 2000), now recently shown to be correspondent to a CARD (caspase recruitment domain) (Ferguson et al., 2007). AIRE's CARD is similar to the one in the apoptosis-procaspase-activating-factor-1 (APAF-1) and might be involved in the oligomerization of AIRE and the formation of protein complexes that function in inflammation and apoptosis (Park et al., 2007). Further downstream a conserved nuclear localization signal (NLS), responsible for nuclear import, and a SAND (SP100, AIRE-1, NUCP41/P75 and DEAF1) domain are found (Peterson et al., 2008). A SAND domain is present in a number of nuclear proteins and functions as a DNA-binding element in some transcription factors (Bottomley et al., 2001), as shown for AIRE *in vitro* (Kumar et al., 2001). Both CARD and SAND domains are important for the protein's ability to form nuclear bodies which associate with the nuclear matrix (Bjorses et al., 1999; Heino et al., 1999; Rinderle et al., 1999; Halonen et al., 2001; Akiyoshi et al., 2004). The SAND domain is followed by two plant homeodomain (PHD)-type zinc fingers (Nagamine et al., 1997), that are often found in proteins involved in the regulation of transcription (Aasland et al., 1995). The first PHD region has been shown to function as an E3 ubiquitin ligase *in vitro* (Uchida et al., 2004) and to interact with unmethylated

histone H3 lysine 4 (H3K4me0) (Koh et al., 2008; Org et al., 2008) and DNA-PK (Liiv et al., 2008). Furthermore a proline-rich-region (PRR) and four nuclear receptor binding LXXLL motifs exist. LXXLL motifs are found in various proteins and mediate binding of co-activators to transcription factors or nuclear receptors, whereas proline-rich-regions can be found in proteins involved in transcription (Helton et al., 2008). Together, the CARD, SAND, PHD1, PHD2 and the carboxy-terminal regions have transcriptional transactivation activity (Meloni et al., 2007).

The importance of the functions of some domains are unveiled by mutations found in APECED patients; of the 19 disease-causing missense mutations, 16 appear to be in the highly conserved CARD and PHD regions of the AIRE protein (Meloni, 2002; Sato et al., 2002; Halonen et al., 2004).

Figure I.3: Schematic domains of the mouse and human AIRE protein
The caspase recruitment domain (CARD) is suggested to work in oligomerization of AIRE and heterodimerizes with other CARD proteins that function in inflammation or apoptosis. The nuclear localization signal (NLS), responsible for nuclear import, is followed by a SAND domain, a putative DNA-binding domain. PHD1 interacts with unmethylated histone H3K4 and DNA-PK and has E3 ubiquitin ligase activity. LXXLL (L) motifs appear in transcriptional co-activator proteins and proline-rich-regions (PRR) in proteins involved in transcription. Modified after Peterson et al., 2008.

1.2.4 Tissue distribution

Prior studies have found AIRE to to be primarily present throughout postnatal life in human and mouse thymus, where it is restricted to a subset of medullary thymic epithelial cells (mTECs) (Heino et al., 2000; Anderson et al., 2002; Gotter et al., 2004; Hubert et al., 2008).

Discordant results have been published about AIRE's presence in peripheral lymphoid organs like lymph nodes and spleen (Blechschmidt et al., 1999; Zuklys et al., 2000; Anderson et al., 2002; Hubert et al., 2008), though a recent study identified extrathymic AIRE-producing cells (eTACs) in peripheral lymph nodes, spleen and Peyer's patches (Gardner et al., 2008). Further inconsistent data have been reported about AIRE's presence in thymic and peripheral DCs (Zuklys et al., 2000; Derbinski et al., 2001; Hubert et al., 2008; Suzuki et al., 2008). In humans, AIRE was found in thymic B cells and 'double-positive' T cells, as well as in

peripheral B cells and activated $CD4^+$ T cells and DCs (Nagafuchi et al., 2006; Suzuki et al., 2008).

However, the detection of AIRE in non-immune related tissues is inconsistent: low levels of human (mRNA) *AIRE,* murine (mRNA) *Aire* and protein were found in gonads, lung, kidney, liver, adrenal glands and brain (Blechschmidt et al., 1999; Ruan et al., 1999; Heino et al., 2000; Halonen et al., 2001; Ramsey et al., 2002; Adamson et al., 2004).

On a subcellular level, AIRE localizes in transiently transfected cells in nuclear bodies, showing a characteristic nuclear dot pattern (Bjorses et al., 1999; Heino et al., 1999; Rinderle et al., 1999; Halonen et al., 2001; Akiyoshi et al., 2004), and associates with the nuclear matrix (Akiyoshi et al., 2004; Tao et al., 2005). Transfected cells expressing (cDNA) *AIRE* show also a cytoplasmatic staining pattern, with the majority of the protein residing in the nucleus (Bjorses et., 1999; Heino et al., 1999; Rinderle et al., 1999; Halonen et al., 2001).

1.2.5 *Aire*-deficient mouse models

The finding that AIRE is strongly produced in mTECs was compelling, because this cell type was suggested to be involved in the presentation of tissue-restricted antigens (TRA) and therefore in negative selection of self-reactive T cells (Kishimoto and Sprent, 1997). Subsequently, *Aire*-knockout mice (Anderson et al., 2002; Ramsey et al., 2002) were generated to unveil AIRE's possible function.

Three different types of *Aire*-knockout mouse-models exist: one was made by Anderson and coworkers at Harvard Medical School, which we designated for our study as the HD-*Aire*-deficient mouse model (Anderson et al., 2002). The second one was generated by Ramsey and coworkers at UCLA Medical School, designated by us as LA-*Aire*-deficient mouse model (Ramsey et al., 2002) (see Materials and Methods 1.14). A third one was created by Kuroda and coworkers and was not used in our experiments (Kuroda et al., 2005).

HD-*Aire*-deficient mice carry a targeted disruption of exon 2, which affects the CARD domain, including portions of the surrounding intron 1 and 3. The strain origins in 129S2/SvPas embryonic stem (ES) cells, and positive clones were injected into C57BL/6 blastocysts. The resulting animals were backcrossed to the C57BL/6 mice strain. Shortened transcripts were detected by RT-PCR in homozygous mutant thymi, but sequence analysis identified a frameshift mutation

resulting from the splicing of exons 1 and 3 that precludes translation past exon 1. LA-*Aire*-deficient mice mimic the most common mutation in Finnish APECED patients (Bjoerses et al., 2000), whose mutation R257X leads to a stop codon in exon 6 (Scott et al., 1998). The disruption of the mouse *Aire* gene was achieved by the insertion of a *Neo*-cassette in the beginning of exon 6. J129 embryonic stem (ES) cells were used and positive ES cells were injected into C57BL/6 blastocysts. Animals were backcrossed to the 129S1 agouti mouse strain. The interruption of (mRNA) *Aire* as well as the early termination of all synthesized polypeptides was confirmed (Ramsey et al., 2002).

The resulting phenotypes are different from each other, and when compared to APECED, similar but not identical (Anderson et al., 2002; Ramsey et al., 2002). The expected symptoms are milder, and none of the most common clinical features of APECED (mucocutaneous candidiasis, hypoparathyroidism, adrenocortical failure), were manifested. The infections with *candida albicans*, which occur in all APECED patients (Ahonen et al., 1990), never affect mice (Mathis and Benoist, 2007). Like APECED patients, mice develop autoantibodies, albeit of different specificity (Poentynen et al., 2006), against multiple peripheral tissues, that are infiltrated by immune cells (Anderson et al., 2002; Ramsey et al., 2002; Liston et al., 2003; Kuroda et al., 2005). A partially overlapping set of organs is affected in mice; most commonly the eye, salivary glands, stomach and liver. $CD4^+$ T cells have been found to be the crucial mediators of the autoimmune response, including tissue infiltration, whereas B cells play a less important role, though still required (Gavanescu et al., 2008; DeVoss et al., 2008). Furthermore, the defect in Treg function, as observed in some APECED patients, hasn't been shown in *Aire*-deficient mice (Kekalainen et al., 2007). In the LA-*Aire* mouse model a significant drop in fertility was described (Ramsey et al., 2002), which is consistent with the infertility manifested in APECED patients (Perheentupa, 2002).

The difference in the mouse-models can be explained by the different genetic background, which has a substantial influence on the disease manifestation (Jiang et al., 2005). This also explains the different targeted spectrum of organs and antibodies in human and mice, since the immune response is subject to HLA/MHC restriction and not all individuals will be able to respond to the same autoantigens (Mathis and Benoist, 2007).

1.2.6 Physiological role

Aire-deficient mice were generated to prove the hypothesis that AIRE is involved in the expression of peripheral-tissue antigens (PTA) by mTECs in the thymus. Using a microarray approach, it was possible to compare the gene expression profiles of isolated mTECs of wild-type and *Aire*-deficient mice, which showed that AIRE indeed promotes transcription of a large number of PTA-encoding genes, among them insulin 2, salivary protein-1 and fatty-acid-binding protein (Anderson et al., 2002; Liston et al., 2003; Anderson et al., 2005, Kont et al., 2008). The number of PTA-encoding genes controlled by AIRE is suggested to be around 1500 (Derbinski et al., 2005), representing nearly all organs in the body (Derbinski et al., 2001), thereby possibly explaining the wide range of autoimmune symptoms in APECED patients. A close connection between disease and AIRE-mediated transcription has been shown for the interphotoreceptor retinoid binding protein (IRBP); *Aire*-deficient mice develop uveitis, which abolishes in *Irbp*/*Aire*-double-knockout mice (DeVoss et al., 2006). Not only does AIRE seem to be responsible for PTA-encoding gene expression in the thymus, but also in the peripheral lymphoid organs, as recently shown (Gardner et al., 2008). The approximately 150 expressed PTA-encoding genes represent a complementary pool of self-antigens, thereby suggesting an additional role for AIRE in establishing peripheral tolerance by negative selection of auto-reactive T cells in peripheral lymphoid organs (Kyewski, 2008). In the thymus though, not all PTA-encoding genes are dependent on expression by AIRE; C-reactive protein and GAD67, against which autoantibodies are found in APECED patients, are among these independent genes (Derbinski et al., 2005). In addition, AIRE doesn't control the transcription of α-fodrin in mTECs, though *Aire*-deficient mice develop autoimmunity against this endogenous self-antigen, implying other roles for AIRE during negative selection (Kuroda et al., 2005). Besides this, AIRE positively or negatively regulates transcription of some genes that do not encode PTA (Sato et al., 2004; Ruan et al., 2007).

The essential question how AIRE promotes the expression of PTA-encoding genes and represses other loci on a molecular level, is still under investigation. AIRE has many features suggestive of a transcriptional activator: first, the protein contains several domains (CARD, SAND, PHDs) known to be involved in transcriptional regulation and nuclear body formation; mutations in those domains decrease AIRE's transactivation ability (Bjorses et al., 2000; Halonen et al., 2004; Ferguson et al., 2008). Second, AIRE binds to proteins functioning in the nucleus, like the transcriptional co-activator CREB-binding protein (Pitkanen et al., 2005) and DNA-PK

(Liiv et al., 2008). DNA-PK is, besides DNA repair, involved in multiple processes like apoptosis and cell survival and has been shown to phosphorylate AIRE (Liiv et al., 2008). Third, AIRE promotes transcriptional elongation by recruiting and binding to the positive transcription elongation factor b (P-TEFb) complex (Oven et al., 2007). P-TEFb activates RNA polymerase II, resulting in activation of gene expression. Finally, though there is limited evidence of direct binding of AIRE to DNA (Kumar et al., 2001; Purohit et al., 2005), it was recently discovered that AIRE interacts with chromatin *in vivo*. By binding to the amino-terminal tail of unmethylated histone H3K4 (H3K4me0) (Koh et al., 2008; Org et al., 2008), a recognition code for silenced genes, AIRE could play a role in epigenetic control of target genes.

A mechanism was recently proposed to explain how all those factors could contribute to AIRE's ability to mediate gene activation (Peterson et al., 2008): AIRE could be recruited to chromatin regions with silenced genes and binds H3K4me0. Recruitment of the P-TEFb complex activates RNA polymerase II and gene expression. AIRE's interaction with CREB-binding protein, which acetylates histones, permits opening of chromatin and DNA. Aire and DNA-PK could collaborate - through the interaction with the nuclear matrix - in the formation of chromatin loops, permitting further activators or suppressors to operate. The observed chromosomal clustering of AIRE-dependent PTA-encoding genes would support this mechanism (Johnnidis et al., 2005).

Though the exact molecular mechanism remains unclear, AIRE's role in mediating the expression of PTA-encoding genes, which translates into negative selection of auto-reactive T cells and induction of T cell tolerance, is established. AIRE also could be involved in other processes in the immune system: instead of negative selection and deletion, AIRE could drive positive selection of certain T cells towards Treg development (Anderson et al., 2005; Mathis and Benoist, 2007). Furthermore, the fast cell death of AIRE-producing mTECs and AIRE's CARD suggest a function in cytotoxicity and direct induction of apoptosis (Gray et al., 2007; Ferguson et al., 2008). The E3 ubiquitin ligase activity of the PHD1 region could influence other nuclear factors by promoting their degradation via the ubiquitin proteasome pathway and indirectly promote apoptosis (Uchida et al., 2004).

This chapter concentrated on AIRE's important role within the immune system. In contrast, our study investigated a possible function of AIRE outside the immune system. We addressed the function of AIRE during germ cell development in the testis.

2. Male germ cells and apoptosis

Overview

AIRE's important role in the immune system as a mediator of promiscuous gene expression leading to negative selection and eventual apoptosis of auto-reactive cells is well established. Not much is known about potential functions of AIRE outside the immune system.

The testes are organs with promiscuous gene expression where apoptosis occurs. The scheduled apoptotic wave during prepuberty is essential for functional spermatogenesis during adulthood, but the underlying reasons are unknown. Our observation that AIRE is present in the testis and that *Aire*-deficiency affects fertility, encouraged us to have a closer look at spermatogenesis and apoptosis to investigate a possible connection between the promiscuous gene expression and an eventual negative selection process of germ cells with mutant genes. To evaluate the potential function of AIRE in testes, an overview of male germ cell development and apoptosis in the context of spermatogenesis is given below.

2.1 Male germ cells

2.1.1 The testis

2.1.1.1 Morphology

The testis with its seminiferous tubules provide the unique environment for spermatogenesis (figure I.4). The tubules are convoluted ducts, surrounded by the *tunica albuginea*, and enmeshed in interstitial connective tissue that is rich in blood- and lymphatic vessels, nerves and Leydig cells (Russell et al., 1990). Each duct straightens between convolutions and travels largely in the long axis of the testis; the two ends terminate over the *tubuli recti* in the *rete testis*, which is connected via several *ductuli efferentes* to the epididymis, where spermatozoa undergo further maturation and storage, and finally exit over *vas deferens* (Russell et al., 1990).

Inside the seminiferous tubules two cell populations can be found: cells of the spermatogenic cell lineage develop from spermatogonial stem cells, which reside

at the basal membrane, into spermatozoa, thereby moving towards the lumen. The second cell type is the stable population of somatic Sertoli cells, and their cytoplasms extend the entire height of the epithelium, thereby forming the blood-testis barrier (Russell et al., 1990).
Besides spermatogenesis in the seminiferous tubules, the mammalian testis performs another major function in a different compartment: the Leydig cells of the interstitium produce testosterone for masculinization and for the onset and maintenance of spermatogenesis (Russell et al., 1990).

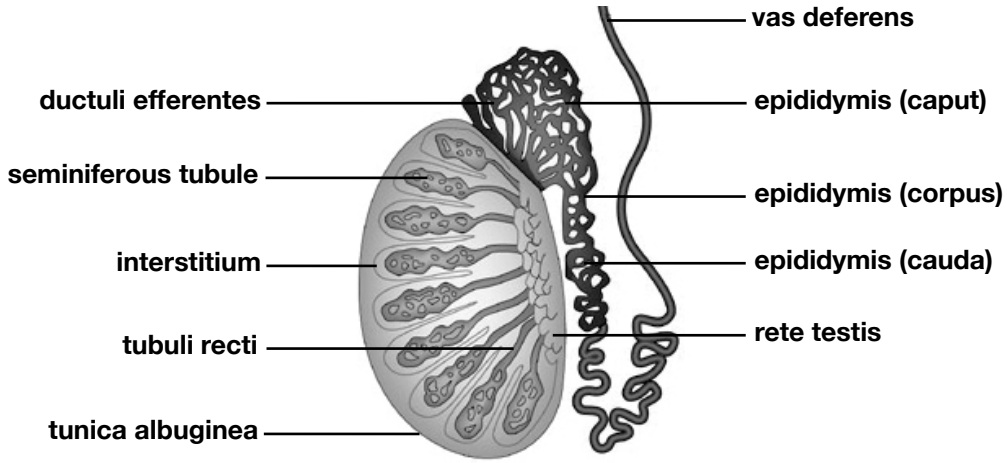

Figure I.4: Simplified overview of the mammalian testis and epididymis
Germ cells develop in seminiferous tubules, which are enmeshed in interstitial tissue and surrounded by the *tunica albuginea*. Spermatozoa leave the seminiferous tubule over the *tubuli recti* in the *rete testis*, and enter the epididymis via *ductuli efferentes*. After further maturation, spermatozoa exit via *vas deferens*. Picture modified after Cooke and Saunders, 2002.

2.1.1.2 Blood-testis barrier

In the context of organ-specific autoimmune diseases with lymphocyte infiltration as caused by *Aire*-deficiency, it is important to know that parts of the male reproductive system are immunologically privileged sites. The blood-testis barrier (BTB) shelters parts of the seminiferous tubules, the *tubuli recti*, *rete testis*, *ductuli efferentes* and epididymis from the immune system to avoid an attack against spermatids and spermatozoa. Due to genetic recombination and their emergence at puberty - a time when immune tolerance has been already established - the haploid cells would be recognized as foreign. The BTB is incomplete, and in healthy mice occasionally lymphocytes and antibodies can be found in the above mentioned reproductive departments, but rarely in the seminiferous tubules (Naito and Itoh, 2008). In there, special tight junctions between Sertoli cells divide the

seminiferous epithelium into the permanent basal and adluminal compartments and the transient intermediate compartment (figure I.5) (Vogl et al., 2000). Spermatogonia and preleptotene spermatocytes reside in the basal compartment where they have access to nutrients during the proliferative phase. Leptotene spermatocytes migrate progressively towards the lumen of the tubules, thereby penetrating the BTB by crossing the intermediate compartment, and enter the sheltered adluminal compartment, where meiosis and spermiogenesis takes place (Russell et al., 1990). To combat potentially infiltrating lymphocytes, Sertoli cells display FAS ligand to induce apoptosis in FAS-bearing lymphocytes (D'Abrizio et al., 2004). FAS is also present on germ cells (Lee et al., 1997). In mice, the BTB closes around day 12 *post partum*, at a time when the first wave of spermatogenesis is about to start (de Kretser et al., 1998).

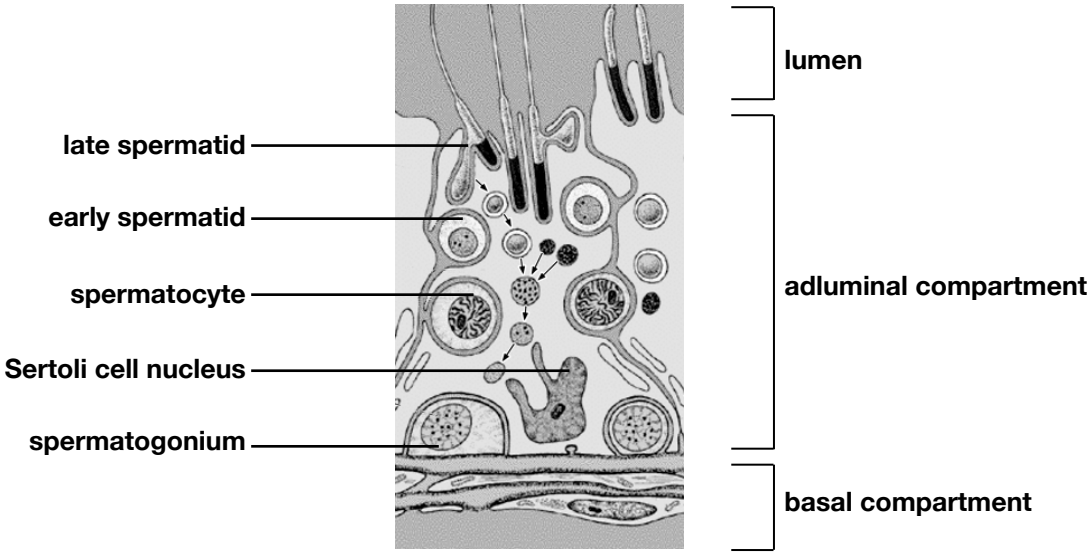

Figure I.5: Simplified, partial cross-section of the seminiferous epithelium
Sertoli cells, extending the entire height of the epithelium, constitute the blood-testis barrier (BTB). Spermatogonia reside in the basal compartment of the seminiferous tubule with access to the interstitium. Developing spermatocytes migrate towards the lumen through the transient intermediate compartment (not shown), thereby crossing the BTB, into the immunologically sheltered adluminal compartment, where they differentiate into spermatids. Picture and text modified after Junqueira and Carneiro, 2003.

2.1.2 Spermatogenesis

Spermatogenesis is defined as the process of morphological and functional differentiation of germ cells over an extended period of time within the boundaries of the seminiferous tubules of the testis (Russell et al., 1990). The process can be divided into three major phases: in the proliferative phase, spermatogonial stem

cells and spermatogonia undergo successive mitotic divisions to assure self-renewal. The stem cells either duplicate themselves, or keep differentiating into spermatocytes which enter meiosis, referred to as meiotic phase. In the third, the haploid or spermiogenic phase, round spermatids transform into elongated spermatozoa, detach from the seminiferous tubule and leave through the lumen. In mice all three phases, from diploid (2n) spermatogonia to haploid (1n) spermatozoa, require about 35 days; in humans 64 days (Russell et al., 1990).

With the onset of puberty around day 30 *post partum* in mice the lifelong process of spermatogenesis starts (deJonge and Barrat, 2006). Before puberty though, an initial round of spermatogenesis occurs, called 'first-wave'-spermatogenesis. For our study this scheduled onset of spermatogenesis was particularly interesting, since it is followed by a massive outburst of apoptosis (Rodriguez et al., 1997) which we found significantly decreased in *Aire*-deficient mice. Adult spermatogenesis is not accompanied by any scheduled apoptotic events, but germ cells show sporadic apoptosis throughout lifetime.

2.1.2.1 Spermatogenic cycle and wave

To reveal AIRE's possible function outside the immune system, we examined cross sections of testes of *Aire*-wild-type and *Aire*-deficient mice. Every cross section shows a precisely defined association of haploid and diploid germ cells, dependent on the stage of the spermatogenic cycle at which the cross section was taken. Along the seminiferous epithelium, 12 cell stages (labeled I-XII) - and therefore different cell associations - can be distinguished in the adult mouse (figure I.6) (Russell et al., 1990). Each stage of the cycle is arranged in an ordered sequence along the length of the seminiferous tubule. The seminiferous tubule is a loop ending with both ends into the *rete testis*, where the segment with the highest stage (stage XII) is located. From there the stages descend to stage I - followed from there by stage XII, XI, X etc. - until the two patterns of descent meet at one point, the 'site of reversal'. The spermatogenic cycle is completed when at one given segment of the seminiferous tubule the same stage reappears; number of stages within the spermatogenic cycle and number of cycles required for completion of spermatogenesis varies between species. The distance between two equal stages in one tubule is called the spermatogenic wave. Both, cycle and wave, assure an even distribution of all stages throughout the seminiferous tubule and a continuous daily output of spermatozoa (Russell et al., 1990).

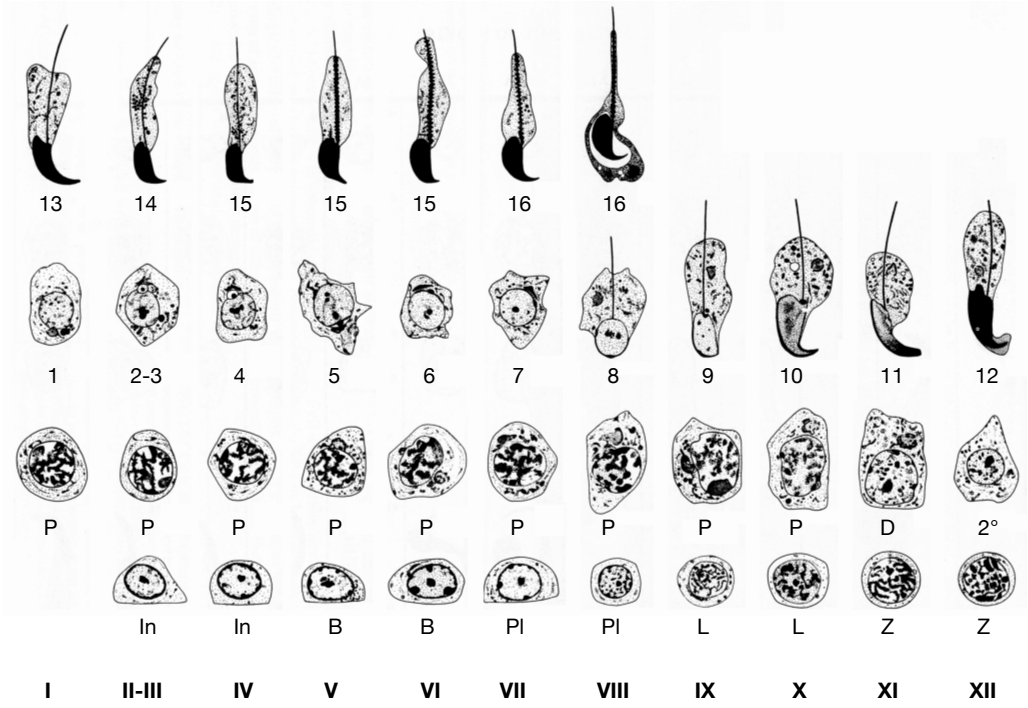

Figure I.6: Germ cell stages of the spermatogenic cycle of the mouse seminiferous epithelium
At any given cross section, one of the above displayed 12 stages (I-XII) can be observed; each characterized by a unique association of diploid and haploid cells, progressing from the lower to the upper part of the scheme. The developmental progression of one specific cell is followed horizontally until the right hand border and continues at the left of the cycle map one row up; the cycle map ends with the completion of spermiation. All stages originate from type A spermatogonia and approximately four cycles within a given region of the tubule occur before the spermatogonium is transformed into a spermatozoon. In = intermediate spermatogonium; B = type B spermatogonium; Pl = preleptotene spermatocyte; L = leptotene spermatocyte; Z = zygotene spermatocyte; P = pachytene spermatocyte; D = diplotene spermatocyte; 2° = secondary spermatocyte; 1-16 = stages 1-16 of spermiogenesis in haploid spermatids. Picture modified after Russell et al., 1990.

For the purpose of our study, germ cell associations in cross sections didn't need to be staged, but the developmental phase of germ cells of interest was determined according to their position in the specific cell association and their morphological appearance (figure 1.6 and figure I.7).

The next chapter will explain more specifically the different types of germ cells in the proliferative, meiotic and haploid phase and how to distinguish each of them under the light microscope.

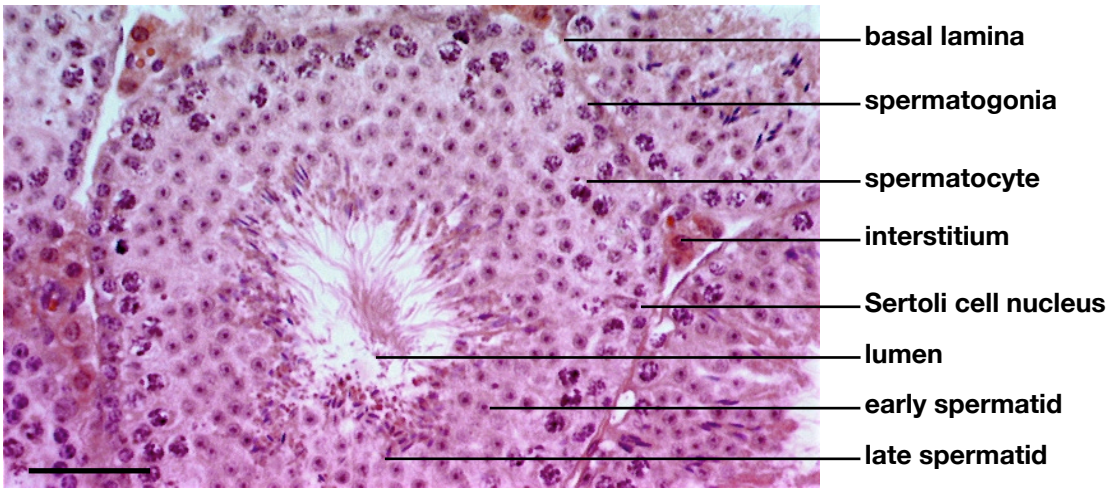

Figure I.7 Light microscopy image of a transverse section of mouse seminiferous tubule
The hematoxylin and eosin stained cross section of the testis shows a seminiferous tubule at stage V. Type B spermatogonia with an oval-shaped nucleus reside close to the basal lamina. Towards the lumen, large pachytene spermatocytes with chromatin patches and sometimes visible sex vesicle can be seen. Further towards the lumen, early (step 5) spermatids, sometimes with acrosomal vesicle spreading out over the nucleus, and late (step 15) spermatids with prominent middle piece, are detectable. Scale bar represents 50 µm. Picture taken during course of this study.

The next sections will explain more specifically the different types of germ cells in the proliferative, meiotic and haploid phase and how to distinguish each of them under the light microscope.

2.1.2.2 Proliferative phase: spermatogonial stem cells and spermatogonia

Spermatogenesis relies on spermatogonial stem cells (SSCs) and the homeostasis between their renewal and differentiation (de Rooij et al., 1998). The BTB creates the unique and essential microenvironment for SSCs in the basal compartment of the seminiferous tubule (the spermatogonial stem cell niche), where growth factors stimulate renewal and differentiation throughout life (de Rooij et al., 1998).

In the adult mouse, a heterogeneous population of spermatogonia can be found (Oakberg, 1971). A-single (A_s) spermatogonia are considered undifferentiated SSCs, able to renew themselves to maintain the stem cell pool or to divide and give rise to two interconnected and more differentiated daughter cells, called A-paired (A_{pr}) spermatogonia. A_{pr} spermatogonia continue to divide, thereby increasing their size while staying interconnected and building an increasingly large syncytia of germ cells, now named A-aligned (A_{al}) spermatogonia. A_{al} spermatogonia differentiate into A_1, followed by A_2, A_3 and A_4 spermatogonia cell stages and, after a total of 9-11 mitotic divisions, give rise to intermediate

spermatogonia (In) and finally type B spermatogonia (de Rooij et al., 1998). Type B spermatogonia enter meiosis and form spermatocytes.

In our study we detected the AIRE protein mainly in spermatogonia, a cell type that is also commonly affected by apoptosis during adulthood. Spermatogonia can be found at the basal lamina of the seminiferous tubule, generally one surface flattened along the basal lamina, and one rounded surface in contact with Sertoli cells. In most species, all type A spermatogonia appear morphologically relatively similar. Type A, intermediate and type B spermatogonia differ from each other structurally and can be distinguished by the amount of chromatin lying along the inner aspect of the nuclear envelope. Type A spermatogonia display none, intermediate spermatogonia have a moderate amount, and type B spermatogonia possess a large amount of chromatin, which can be seen as a more prominent nuclear boundary under the light microscope (figure I.6) (Russell et al., 1990).

2.1.2.3 Meiotic phase: spermatocytes

During the meiotic phase of spermatogenesis, diploid (primary) spermatocytes (2n) duplicate their DNA content and divide into secondary spermatocytes, which divide again during the second meiotic division (meiosis II), and differentiate into haploid, round spermatids (1n) (Russell et al., 1990).

Meiosis I starts with primary preleptotene spermatocytes, which developed from type B spermatogonia (de Kretser et al., 1998). The morphology (figure I.6) is similar to type B spermatogonia, though preleptotene spermatocytes are smaller and have more rounded nuclei (Russell et al., 1990). The preleptotene spermatocytes enter prophase I. Prophase I is subdivided based on the processes in the nucleus in leptotene, zygotene, pachytene and diplotene and lasts about 22 days in the mouse. This accounts for over 90% of the duration of meiosis (Cobb and Handel, 1998), and therefore, most of the spermatocytes in sections will be seen in this stage (Russell et al., 1990). In the one day transition from preleptotene to leptotene, spermatocytes migrate away from the base of the seminiferous tubule, thereby penetrating the BTB (Russell et al., 1990). The homologous chromosomes condense and start to pair, and genetic recombination and the formation of double strand breaks (DSBs) begins (Cobb and Handel, 1998). Morphologically (figure I.6), leptotene cells are round with round nuclei, and thin threads of chromatin, characteristic of those cells, can be seen in sections as numerous small spots under the light microscope (Russell et al., 1990). In the

subsequent zygotene, the synaptonemal complex begins to assemble, linking the axial cores of the homologs with transverse filaments, thereby closing the gap between the chromosomes (Page and Hawley, 2004). Under the light microscope, the paired chromosomes in zygotene primary spermatocytes appear thicker in comparison to leptotene, thereby forming crowded patches within the nucleus (figure I.6) (Russell et al., 1990). In the mouse, the chromosomes remain fully paired for nearly a week, during which homologous recombination (crossing over) occurs (Russell et al., 1990), a phase referred to as pachytene. In the beginning of this stage, large chromatin patches, leaving little interchromosomal clear spaces, can be seen, and cells and their nuclei are round. During the course of development, the pachytene cells become progressively larger. Furthermore, at stage VII of the cycle, the sex vesicle can be detected in most cells, and the nuclei become slightly oval with an irregular contour. Interchromosomal spaces increase due to chromosome separation, giving the impression of large clear areas within the nucleus; the chromatin stains lighter (figure I.6) (Russell et al., 1990). During the following diplotene the synaptonemal complex disassembles, allowing chromosomal pairs to separate, whereas the individual crossover events between the non-sister chromatids can be seen as chiasmata. These now play a crucial part in holding the chromosomes together (Petronczki et al., 2003). The diplotene phase in males is brief and difficult to recognize in histological sections; the cells are the largest primary spermatocytes and also the largest of any germ cell types, with a more ovoid nucleus and lightly stained chromatin (figure I.6) (Russell et al., 1990). Prophase I ends with diakinesis, the transition to metaphase I.

After the long prophase I, metaphase I, anaphase I and telophase I are completed rapidly. In metaphase I, the kinetochores of the two sister chromatids of a homolog attach to microtubules originating from the same spindle pole. In anaphase I, the chiasmata resolve, allowing the chromosomal homologues to separate, while the residual cohesion complexes at the centromeres keep the sister chromatids together (Gerton, 2005). In telophase I, the nucleus and cytoplasm start dividing, producing two secondary spermatocytes, each with a single set of chromosomes and 2n DNA content (Russell et al., 1990). Secondary spermatocytes (2°) are short-lived and lack prominent distinguishing features. They are often confused with newly formed spermatids, but their nuclei are larger with fuzzy heterochromatin, compared to distinct heterochromatin in early spermatids (figure I.6) (Russell et al., 1990).

Meiosis I is followed by meiosis II, which generates haploid, round spermatids. Unlike meiosis I, meiosis II occurs rapidly and closely resembles mitosis without prior DNA replication. In prophase II, the nuclear envelope breaks down and a new spindle starts to form. During metaphase II the kinetochores of each sister chromatid attach to microtubules originating from the opposite spindle pole, allowing the sister chromatids to separate in anaphase II (Kerrebrock et al., 1992). In telophase II, the cell divides, giving rise to two haploid spermatids with 1n DNA content and an unique arrangement of genetic material. Cells undergoing meiosis II can be differentiated from meiosis I cells based on their relatively smaller size; resulting spermatids (starting stage 1 of spermiogenesis) are small and show areas of condensed chromatin (figure I.6) (Russell et al., 1990).

2.1.2.4 Haploid phase: spermatozoa

After the meiotic phase, the haploid spermatids undergo substantial remodeling during stages 1-16 of spermiogenesis, as seen in figure I.6. During this process, which doesn't include any cell divisions, four major morphogenic modification steps occur: development of the flagellum, development of the acrosome, nuclear shaping and condensation, and elimination of the cytoplasm (de Kretser et al., 1998).

The flagellum, the motile force of the spermatozoon, evolves from one of the two centrioles, which grow the flagellar axoneme, first visible at stage 8 of spermiogenesis. At stage 15, mitochondria aggregate around the axoneme, forming the prominent mid-piece. The mitochondria generate ATP for dynein motor proteins, which convert the chemical energy into mechanical bending of the flagellum (Porter and Sale, 2000). Sperm released from the seminiferous epithelium, though equipped with the flagellum, are still immotile until they develop full motility in the epididymis.

The acrosome covers the anterior half of the nucleus, and is essential for fertilization. During the acrosomal reaction, hydrolytic enzymes help the spermatozoon to penetrate the *zona pellucida* of the oocyte (Moreno and Alvarado, 2006). The first proacrosomal vesicles can be seen in stage 2-3 of spermiogenesis, and from there on, the acrosomal vesicle gradually spreads over the nucleus.

At stage 8, the acrosomal region of the nucleus makes contact with the cell surface, causing asymmetry and reshaping as seen in stage 9. The reshaping of the nucleus, which evolves into a shape characteristic for each species (Russell et

al., 1990), is due to condensation of the nucleus into transcriptionally inactive DNA, assisted by DSBs and histone-to-protamine replacement (Govin et al., 2004). Protamines are found only in spermatids (Wouters-Tyrou et al., 1998) and as a consequence of their small size and charge, permit the packaging of sperm chromatin into an extremely small space, stabilizing the DNA and making it more resistant (Bennetts and Aitken, 2005).

Furthermore, spermatids need to eliminate cytoplasm, to be small, streamlined and highly motile. During elongation of the spermatid, starting stage 9, water is already eliminated from the nucleus and cytoplasm, which makes elongated spermatids appear to be more dense; further excess cytoplasm is discarded in residual bodies that contain packed RNA, organelles and inclusions, and are phagocytosed by Sertoli cells (Russell et al., 1990).

All this results in a mature spermatozoon (figure I.8), that will detach from the Sertoli cell and from its synchronously developed partners in a process called spermiation. Once released into the lumen of the seminiferous tubules, the spermatozoa travel immersed in testicular fluid produced by Sertoli cells through the *rete testis* to the epididymis (Russell et al., 1990).

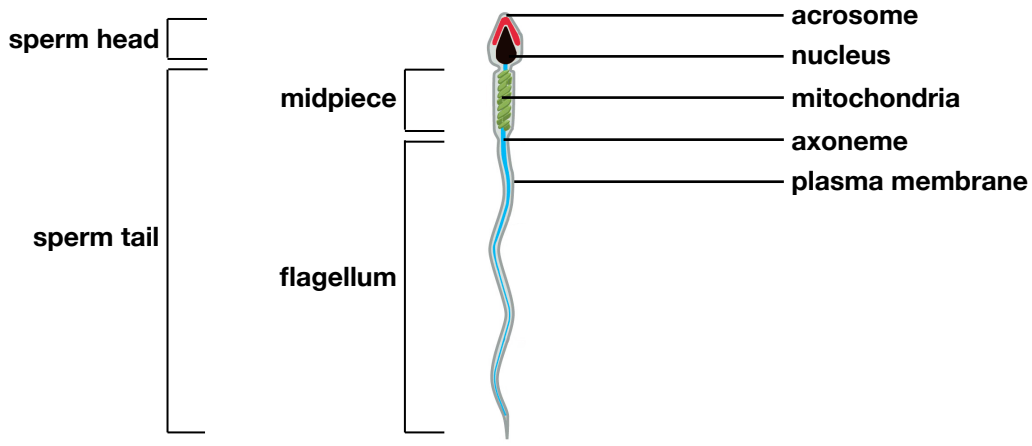

Figure I.8: Simplified scheme of a longitudinal section of a mature spermatozoon
The spermatozoon consists of two morphologically and functionally distinct regions: sperm head and tail, both surrounded by a single plasma membrane. At the anterior end of the sperm head the acrosome is positioned, containing hydrolytic enzymes required to penetrate the oocyte. The DNA in the nucleus is tightly packed with protamines and sperm-specific histones that permit the nucleus to be shaped into a compact, hydrodynamic form. The sperm head is deficient of ribosomes, endoplasmic reticulum and Golgi apparatus. The sperm flagellum is the motile force; the inner, central structure is the axoneme, that originates behind the nucleus and progresses to the distal end. The mid-piece is covered by the mitochondrial sheath, a helix of mitochondria that produce ATP to fuel the dynein motor proteins to provide sperm motility. Modified after Alberts et al., 2008.

2.1.3 Sperm maturation in the epididymis

In our study we investigated not only cross sections of testes, but also spermatozoa from the epididymis, in order to learn more about the observed infertility in *Aire*-deficient mice.

In the epididymis, post-testicular maturation of spermatozoa takes place. After release into the lumen of the seminiferous tubule, the spermatozoa are still immature and incompetent to fertilize an oocyte (Cooper, 1998). The spermatozoa must transit the epididymis, a single convoluted tube consisting of *caput*, *corpus* and *cauda* (figure I.4), on their way from the testis to the *vas deferens* (Russell et al., 1990). The lumen of the epididymis is secluded by the blood-epididymal barrier (Hinton and Palladino, 1995) and filled with fluid, containing various compounds secreted by principal cells via secretory organelles (Gatti et al., 2005). In the lumen, spermatozoa acquire new proteins by interacting with epididymosomes released from the principal cells. These proteins permit the spermatozoa to develop motility and the ability to fertilize an oocyte (Sullivan et al., 2007). An important factor secreted by the epididymosomes in many mammals is ubiquitin. The epididymal fluid contains all essential ubiquitin-system enzymes and it is proposed that defective spermatozoa are marked via ubiquitination and removed by the proteasome during a checkpoint for sperm quality (Baska et al., 2008).

Further modifications, like capacitation, occur in the special environment in the female reproductive tract. These greatly increase the motility of the flagellum and make the sperm capable to undergo the acrosomal reaction (de Lamirande and Gagnon, 1993). Only after all those modifications is the spermatozoon able to fertilize an oocyte.

2.1.4 Regulation of germ cell development

As described in the previous sections, the production of spermatozoa is a complex process requiring a precise program regulating the specific gene expression necessary for each stage of germ cell maturation (Eddy, 2002). Hundreds of genes are upregulated during development, many of which encode proteins for meiosis and spermiogenesis (Schlecht et al., 2004). Other genes are - as in the thymus - expressed promiscuously, but the role of those transcripts is unclear (Chalmel et al., 2007). Germ cell development and hence gene expression in the testis is regulated by a variety of factors. Though many are still unknown, extrinsic

hormonal influences as well as interactions with Sertoli cells have been identified to play a key role in germ cell maturation (Shima et al., 2004).

2.1.4.1 Hormonal regulation

Hormonal regulation of germ cell development in the context of *Aire*-deficiency is particularly interesting since APECED patients show autoantibodies against proteins in organs such as the pituitary and adrenal glands (Nagamine et al., 1997; Bensing et al., 2007). The pituitary gland plays an important role in spermatogenesis by releasing the two gonadotropins, follicle stimulating hormone (FSH) and luteinizing hormone (LH), which act on Sertoli and Leydig cells, respectively (McLachlan et al., 2002). Furthermore, Leydig cells are, beside the adrenal glands, the main producers of the important androgen testosterone and enzymes involved in the synthesis have been shown to be targeted by autoantibodies in APECED patients as well (Krohn et al., 1992; Winqvist et al., 1992).

Secretion of gonadotropin releasing hormone (GnRH) by the hypothalamus stimulates the secretion of the gonadotropins FSH and LH from the pituitary gland (hypophysis) (figure I.9) (McLachlan, 2000). In males the receptor for FSH is exclusively displayed on Sertoli cells (Rannikki et al., 1995), and the receptor for LH can be found primarily on Leydig cells, but also on spermatogenic cells (Heckert and Griswold,1991). The main function of FSH is to initiate spermatogenesis via stimulation of Sertoli cell proliferation during prepuberty (Heckert and Griswold, 2002). Furthermore, FSH plays a key role in spermatogonial development and homeostasis by controlling the paracrine growth factor GDNF (glial cell line-derived neurotrophic factor) (Meng et al., 2000). LH acts on Leydig cells in the interstitial space by stimulating them to synthesize the major androgen testosterone (Mendis-Handagama, 1997).

Cholesterol is the substrate for testosterone synthesis either via uptake or *de novo* synthesis by Leydig cells (Mendis-Handagama, 1997). The conversion of cholesterol to testosterone involves several steps catalyzed by enzymes (Payne and Youngblood, 1995), among them steroid hormone 17-α-hydroxylase (P450c17) and side-chain cleavage enzyme (P450scc), both antigens in APECED patients (Krohn et al., 1992; Winqvist et al., 1992). The released testosterone either diffuses into the tubule or is bound to a carrier that delivers it across the lymphatic space to the seminiferous tubule, leading to concentrations of testosterone in the

seminiferous tubule 10-100 times higher as in the serum (Turner et al., 1984). Testosterone assumes the lead role in morphological development of mammalian males and the onset and maintenance of spermatogenesis; withdrawal leads to acute regression of the seminiferous epithelium (Ghosh et al., 1991). In the testis, testosterone can be transformed into dihydrotestosterone (DHT) and estradiol (E2), which play as well roles in germ cell development and sexual differentiation in males (Holdcraft and Braun, 2004).

Receptors for testosterone are continuously found on Leydig cells, myoid cells and, depending on the differentiation stage of the tubule, in Sertoli cells (Holdcraft and Braun, 2004), as well as in the epididymis (Robaire, 2006). Since Sertoli cells are the cells that are in direct contact with the germ cells, they are considered to be important mediators and transducers for testosterone signals. The receptors for androgens regulate the testosterone levels via several feedback mechanisms: autocrine feedback to the Leydig cells, endocrine feedback to the hypothalamus influencing GnRH production, and endocrine feedback to the pituitary gland reducing LH release, all of which inhibit the production of testosterone (Amory and Bremner, 2001).

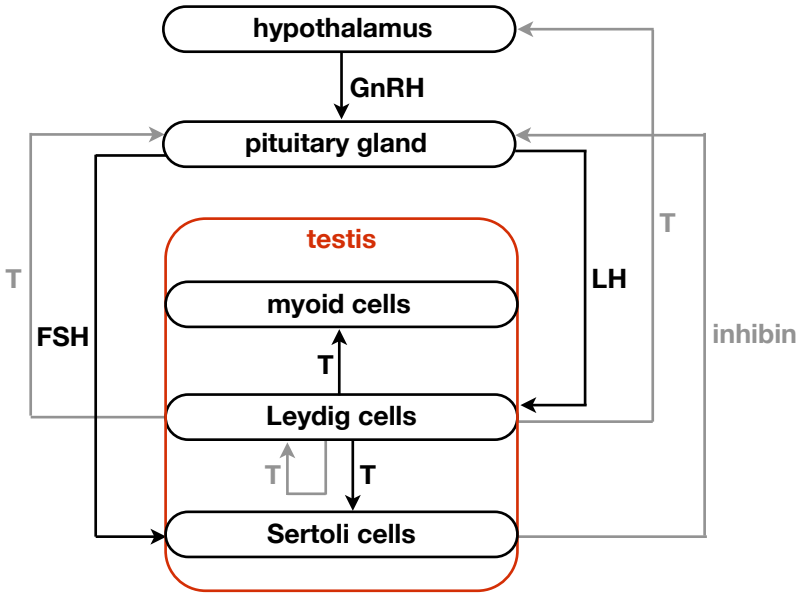

Figure I.9: Overview of hormonal regulation of mammalian spermatogenesis
GnRH (gonadotrophin releasing hormone) stimulates the pituitary gland to synthesize and secrete LH (luteinizing hormone) and FSH (follicle stimulating hormone), which stimulate Leydig and Sertoli cells, respectively. Stimulated Leydig cells synthesize and secrete T (testosterone), which acts on myoid and Sertoli cells in the seminiferous tubules. Inhibin, secreted by Sertoli cells, negatively regulates the pituitary gland, and testosterone levels are regulated via several negative feedback mechanisms (grey). Modified after Holdcraft and Braun, 2004.

2.1.4.2 Sertoli cells

The somatic Sertoli cells play an exceptional role in the development and survival of germ cells in the seminiferous epithelium; it is proposed that a certain ratio between germ cells and Sertoli cells is necessary for functional spermatogenesis (Rodriguez et al., 1997). With specific receptors for FSH and testosterone, Sertoli cells function as mediators between hormone signals and germ cells (Sanborn and Steinberger, 1977). The secretion of androgen-binding protein helps to concentrate testosterone in the seminiferous tubule. On the contrary, the release of inhibin suppresses synthesis of FSH in the pituitary gland (Sofikitis et al. 2008). During embryonic development, Sertoli cells produce anti-Muellerian hormone, promoting regression of the Muellerian duct in the male fetus (Muensterberg and Lovell-Badge, 1991). Later in development, synthesis of GDNF and c-KIT ligand critically influence spermatogonial stem cells (Meng et al., 2000; Oatley et al., 2007). Sertoli cells constitute the BTB and kill via FAS ligand infiltrating, auto-antigenic lymphocytes (Lee et al., 1997). Germ cells can also be induced to apoptose (Lizama et al., 2007). Dead cells are phagocytosed by the Sertoli cells, which also phagocytose during spermiogenesis discarded cytoplasm (Russell et al., 1990). Sertoli cells actively facilitate continued upward movement of germ cells toward the lumen, and additional secretion of fluid supports the transport of spermatozoa within the male duct system (Russell et al., 1990). Via gap junctions, Sertoli cells communicate with each other and with other cell types and synchronize the spermatogenic cycle and other events during spermatogenesis (Russell et al., 1990). By connecting the vascular and lymphatic system with the germ cells, Sertoli cells guarantee the exchange of metabolites and nutrients (Russell et al., 1990).

Though extending from the base of the tubule to the lumen, the outlines of Sertoli cells are hard to find in the light microscope. The elongated nucleus, which is often triangular in outline and possesses numerous foldings and a prominent nucleolus, makes it possible to distinguish them from germ cells (Russell et al., 1990).

2.2 Germ cell apoptosis

It is known that apoptosis plays an essential role in male germ cell development because disruption of the balance between survival and death results in spermatogenic dysfunction (Knudson et al., 1995; Rucker et al., 2000). However, the underlying reasons for apoptosis in the testis are mainly unknown (Blanco-Rodriguez, 1998). AIRE, which is responsible for promiscuous gene expression and

negative selection of self-reactive T cells in the thymus, might have an influence on apoptosis in the testis. This idea appears to be reasonable, since *Aire*-deficient male mice are less fertile, and our study found apoptotic rates in *Aire*-deficient mice differ from those in wild-type mice.

2.2.1 Apoptotic pathways

Apoptosis depends on intracellular proteolytic cascades, mediated by caspases. Initiator-caspases cleave downstream pro-caspases, and produce an amplifying chain reaction by activation of downstream effector-caspases. The caspases target specific proteins in the cell, leading to the classical cellular features of apoptosis like DNA fragmentation and the formation of apoptotic bodies (Los et al., 2001). The irreversible, self-amplifying caspase cascade can be induced by an extrinsic or intrinsic pathway (Boatright and Salvesen, 2003): the extrinsic pathway is activated through FAS receptor on the surface of the targeted cell and FAS ligand (Holler et al., 2003). Upon activation, FAS recruits FADD (Fas-associated protein with death domain) and the complex binds to certain pro-caspase. The death inducing signaling complex (DISC) forms and the proximity of the pro-caspases in the complex cleaves and activates them. The newly formed caspases start the caspase cascade leading to apoptosis (Danial and Korsmeyer, 2004). Additionally, FAS can trigger activation of procaspase 2, and its activity correlates with apoptosis in certain cell types like germ cells (Zheng et al., 2006). FAS ligand can be found on activated immune cells and Sertoli cells (French et al., 1996; Lee et al., 1997).

The intrinsic pathway depends on the release of mitochondrial cytochrome c into the cytosol and is regulated by the BCL2 protein family. Cytochrome c binds in the cytosol to pro-caspase-activating adaptor protein APAF-1 (apoptotic-protease activating-factor-1), causing APAF-1 to oligomerize into an apoptosome. The APAF-1 proteins in the apoptosome bind to pro-caspases 9, which are activated by their proximity to each other, and further activate downstream caspase to induce apoptosis (Newmeyer and Ferguson-Miller, 2003).

The regulating BCL2 family consists of three classes of subfamilies: the anti-apoptotic BCL2 proteins (e.g. BCL2, BCL-X_L), the pro-apoptotic BH123 proteins (e.g. BAX, BAK) and the pro-apoptotic BH3-only proteins (e.g. BAD, BIM, BID, PUMA, NOXA) (Galonek and Hardwick, 2006). Apoptotic stimuli activate pro-apoptotic BH123 proteins, which aggregate to oligomers in the outer mitochondrial

membrane and help to release cytochrome c into the cytosol. In absence of an apoptotic stimulus, the anti-apoptotic BCL2 proteins, located on the cytosolic surface of the outer mitochondrial membrane, inhibit apoptosis by binding and blocking pro-apoptotic BH123 proteins. This prevents them from oligomerizing and releasing cytochrome c (Galonek and Hardwick, 2006). The pro-apoptotic BH3-only proteins are capable of inhibiting the anti-apoptotic BCL2 proteins in response to an apoptotic stimulus by binding to the anti-apoptotic BCL2 proteins, thereby blocking any interactions with BH123 proteins. The BH123 proteins now become activated and promote the release of cytochrome c into the cytosol (Galonek and Hardwick, 2006).

2.2.2 Apoptosis in the testis

Apoptosis in the testis takes place during the fetal period (Coucouvanis et al., 1993), scheduled at the first wave of spermatogenesis during prepuberty (Rodriguez et al., 1997) and spontaneously throughout adult life (Blanco-Rodriguez and Martinez-Garcia, 1996). Furthermore, apoptosis in the mammalian testis can be induced be various conditions like hyperthermia (Hikim et al., 2003), hormonal withdrawal (Blanco-Rodriguez and Martinez-Garcia, 1996), radiation (Embree-Ku et al., 2002) and various drugs (Koji and Hishikawa, 2003).

2.2.2.1 Scheduled apoptosis during the first wave of spermatogenesis

A massive outburst of apoptosis among germ cells can be observed during the first round of spermatogenesis in the prepubertal mouse (figure I.10), when around 80% of germ cells are eliminated (Rodriguez et al., 1997). Apoptosis starts to increases around day 14 *post partum,* peaking around day 21, thereby reaching apoptotic rates seven times higher than observed in mature testis. Elevated apoptotic levels reach normal values again around day 30 *post partum* (Rodriguez et al., 1997). Spermatogonia and spermatocytes are mostly affected, the latter to a greater extent (Rodriguez et al., 1997; Zheng et al., 2006).

The underlying reasons for the prepubertal apoptotic wave are not known, but so far it was proposed that a critical ratio between germ cells and supporting Sertoli cells has to be established in a short time, resulting in death of the ‘surplus’ germ cells (Rodriguez et al., 1997). Additionally, it has also been suggested that mutated DNA, eventually caused by incorrect DNA rearrangements during crossing over in meiosis I, triggers the apoptotic wave (Mori et al., 1997; Rodriguez et al., 1997).

Several molecular factors influencing the balance of apoptosis and survival have been identified, among them the interaction between BAX, BCL2 and BCL-X_L (Korsmeyer, 1995). Transgenic mice expressing *Bcl2*, usually not significantly detectable in testis of all ages, or overexpressing *Bcl-X_L*, don't undergo the prepubertal wave of spermatogenesis and are sterile when mature, showing severely decreased numbers of spermatocytes, spermatids and spermatozoa (Rodriguez et al., 1997). Spermatogonia appear not to be affected and have - as observed in the testis of mature wild-type mice - normal sporadic apoptosis, not prevented by BCL2 or BCL-X_L (Rodriguez et al., 1997). *Bax*-deficiency results in a similar phenotype (Knudson et al., 1995): immature, *Bax*-deficient testes show decreased apoptosis during prepuberty, leading to increased numbers of spermatogonia and spermatocytes (Russell et al., 2002). Adult *Bax*-deficient male mice develop infertility, with atypical premeiotic germ cell accumulations, but no spermatocytes and haploid spermatozoa (Knudson et al., 1995). Besides its pro-apoptotic function, mature *Bax*-deficient testis display increased apoptosis but never establish normal spermatogenesis, suggesting that apoptosis might be triggered by overcrowded seminiferous tubules via a BAX-independent mechanism (Russell et al., 2002).

Besides the intrinsic also the extrinsic apoptotic pathway might play a role during the first wave of spermatogenesis. Caspase 8 is active in spermatocytes undergoing apoptosis as shown in rats, suggesting a possible FAS-mediated activation (Codelia et al., 2008). Sertoli cells ubiquitously express FAS ligand (Riccioli et al., 2000) and FAS can be detected upregulated on adjacent spermatocytes during the prepubertal wave of spermatogenesis (Lizama et al., 2007).

Hormones regulate and influence both apoptotic pathways during prepuberty and testosterone and FSH seems to act as survival factor during the meiotic phase of the first wave of spermatogenesis (Ruwanpura et al., 2008).

Many other factors might influence the apoptotic outburst during prepuberty. Gene expression microarray data identified 1667 genes that are regulated during the first wave of spermatogenesis, a high proportion of which uncharacterized (Clemente et al., 2006).

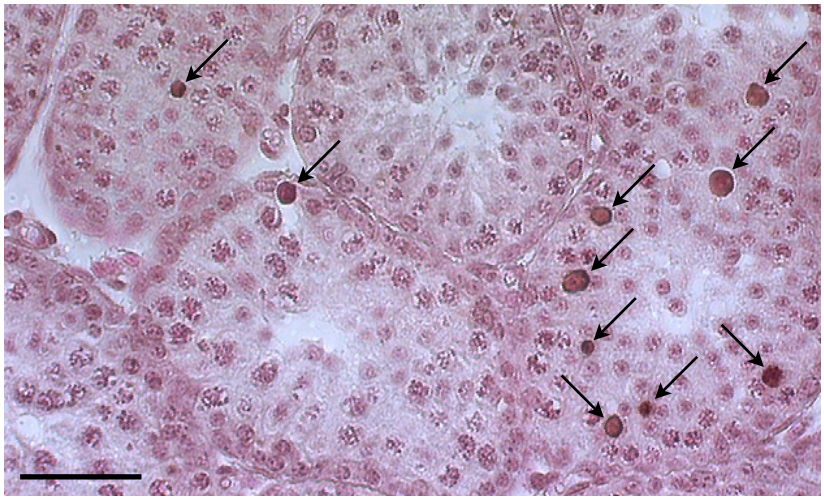

Figure I.10: Light microscopy image of a transverse section of 3-week-old mouse seminiferous tubules showing apoptotic germ cells
During prepuberty, massive apoptosis of germ cells can be observed. Apoptotic spermatogonia, spermatocytes and spermatids have been detected with the TUNEL-technique and appear brown (arrows). Scale bar represents 50 µm. Picture taken during course of this study.

2.2.2.2 Sporadic apoptosis during adulthood

Apoptosis is a constant feature of normal spermatogenesis (figure I.11) in many mammalian species and occurs spontaneously throughout adult life (Hikim et al., 2003). All germ cell types in the seminiferous tubule are prone to apoptosis (Blanco-Rodriguez and Martinez Garcia, 1996), with spermatogonia being mostly affected; in mice, spermatocytes apoptose frequently, as well (Rodriguez et al., 1997). The underlying reasons are unknown, but potential checkpoints during spermatogenesis could activate apoptosis in mutant and non-functional germ cells (de Rooij and de Baer, 2003).

Again, the BCL2 family-proteins play a crucial role: pro-apoptotic BAX is present in spermatogonia, spermatocytes and spermatids irrespectively of age and co-localizes with apoptosing cells (Krajewski et al., 1994); anti-apoptotic BCL-X_L and BCL-W can be detected in spermatogonia, early spermatocytes and spermatids (Beumer et al., 2000); BCL-W is essential during adulthood and deficient mice show numerous apoptotic testis cells, including Sertoli cells (Print et al., 1998).

The FAS-FAS ligand extrinsic system plays a minor role in apoptosis during adulthood (Print and Loveland, 2000). Sertoli cells express FAS ligand and can kill invading, FAS-bearing T cells. FAS is displayed on Sertoli cell-adjacent spermatogonia and spermatocytes (Lee et al., 1996), and FAS ligand was found on spermatozoa (Riccioli et al., 2003). Nevertheless, *Fas*-deficient mice and mice

lacking functional FAS ligand, are fertile with normal apoptotic rates (Lee et al., 1997). The FAS-FAS ligand system becomes important under certain conditions like Sertoli cell injury and hypothermia, when FAS production increases, leading to more apoptosis (Koji and Hishikawa, 2003).

The main upstream regulators of the extrinsic and intrinsic pathway during regular germ cells apoptosis are unclear. Hormones play a role in immature and adult mice by indirectly - via somatic cells - activating BCL2 family proteins. Testosterone, LH and FSH act as survival factors (Ruwanpura et al., 2008). The lower gonadotropin levels in immature mice compared to mature ones, lead to insufficient suppression of *Bax* transcription resulting in more apoptosis (Rodriguez et al., 1997).

Apoptosis is triggered by DNA lesions like DNA double strand breaks (DSBs), which can be induced by alkylating agents, oxidative stress (Agarwal et al., 2008), agents inducing bulkyl lesion such as cisplatin (Seaman et al., 2003) and ionizing radiation (Kaina, 2003). In response to DNA damage that cannot be repaired, the tumor suppressor protein p53 accumulates and activates the transcription of genes that encode several BH3-only proteins, whereas BCL2 declines, thereby triggering the intrinsic pathway and eliminating potentially dangerous cells that otherwise could become cancerous (Kaina, 2003).

Germ cells died of apoptosis are either sloughed into the tubule lumen or phagocytosed by Sertoli cells (Russell et al., 1990).

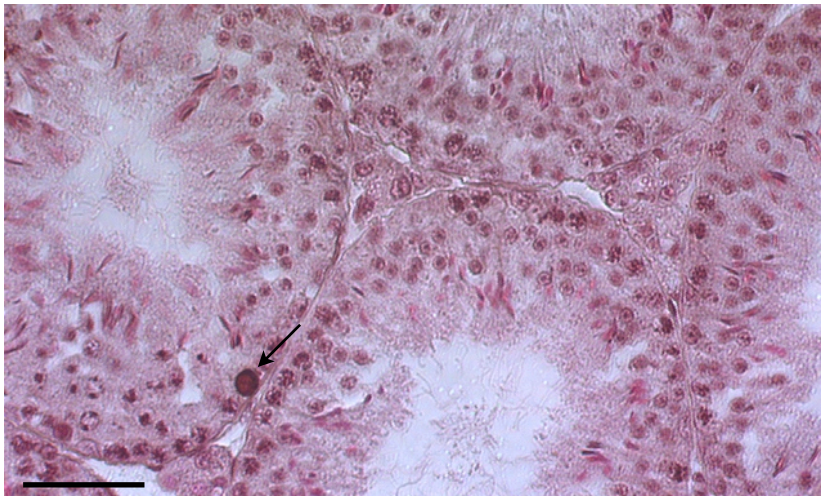

Figure I.11: Light microscopy image of a transverse section of 3-month-old mouse seminiferous tubules showing an apoptotic germ cell
Sporadic apoptosis in the testis occurs throughout adulthood. The apoptotic spermatogonium is detected with the TUNEL-technique and stains brown (arrow). Scale bar represents 50 µm. Picture taken during course of this study.

CHAPTER II: AIM OF STUDY

The aim of this study was to investigate the effect of AIRE on both scheduled and sporadic apoptosis in the testis. This included to verify and quantify *Aire* mRNA expression and AIRE protein in the testis as well as to assess if genes transcriptionally controlled by AIRE in the thymus are as well under AIRE control in the testis. For reproducibility, the influence of AIRE on apoptosis in the testis was studied in two *Aire*-knockout mouse models with different genetic backgrounds. An involvement of the adaptive immune system in apoptosis in the testis was excluded by further studies using mice with *Rag-1*-deficiency. To proof the hypothesis that the underlying reasons for the scheduled and sporadic apoptosis in germ cells is mutated DNA, the testis of mismatch-repair-deficient mice were examined. Furthermore, a potential role of AIRE in the ubiquitin pathway was addressed as well as its influence on fertility.

CHAPTER III: MATERIALS AND METHODS

1. Materials

1.1 Instruments

cell culture incubator	B5060-EK-CO2
	Heraeus/Kendro; Newtown, CT
centrifuge	Marathon 13
	Fischer Scientific; Pittsburgh, PA
electrophoresis power supply	Fisher Electrophoresis Systems
	Fischer Scientific; Pittsburgh, PA
gel imaging system	Bio-Rad Gel Doc 1000
	Bio-Rad; Hercules, CA
gel electrophoresis unit	Bio-Rad Wide Mini-Sub Cell
	Bio-Rad; Hercules, CA
Neubauer hemocytometer	American Optical Corporation
	Buffalo, NY
incubator	VWR 1530
	VWR Sci. Inc.; West Chester, PA
microcentrifuge	Eppendorf 5415D
	Eppendorf; Westbury, NY
microscope	Leica DM LB
	Mc Bain Instr.; Chatsworth, CA
microscope camera system	DEI-750
	Optronics; Goleta, CA
microwave	Panasonic
	Secaucus, NJ
PCR thermal cycler	PTC-100 Peltier Thermal Cycler
	PTC-200 Peltier Thermal Cycler
	Bio-Rad; Hercules, CA
ph meter	Oakton 510
	Fischer Scientific; Pittsburgh, PA
waterbath	Thelco PS
	Fischer Scientific; Pittsburgh, PA

1.2 Chemicals

Chemicals were purchased from the manufacturer with the most competitive pricing.

1.3 Buffers and solutions

Buffers and solutions, unless otherwise stated, were made with double-distilled water (ddH_2O). For tail lysis buffer and TE buffer autoclaved ddH_2O was used.

DNAseI buffer	50 mM Tris-HCl pH 7.5,
	10 mM $MgCl_2$ pH 7.5
IHC buffer	50 mM phosphate buffer pH 7.4,
	25 mM Tris-HCl pH 7.4,
	3% normal goat serum,
	1% BSA,
	0.3% Triton-X 100
PBS	10 mM phosphate buffer pH 7.4,
	0.15 M NaCl
sperm buffer	MEM (with Earle's salts, L-glutamine),
	0.075% Penicillin G,
	0.05% streptomycin sulfate,
	0.01 mM EDTA,
	3% BSA (w/v),
	5% FBS (v/v),
	0.23 M sodium pyruvate,
	non-essential amino acid solution (100 x) 1% (v/v)
tail lysis buffer	100 mM Tris-HCl pH 8.5,
	5 mM EDTA,
	200 mM NaCl,
	0.2% SDS,
	200 μg/ml Proteinase K
TBE	89 mM Tris base,
	89 mM boric acid,
	2 mM EDTA, pH 8.0

TE 10mM Tris-HCl pH 8.0
1 mM EDTA

1.4 Materials and frozen tissue preparation

Tissues were frozen in Tissue-Tek cryomolds with Tissue-Tek O.C.T. compound (Electron Microscopy Sciences; Hatfield, PA).

1.5 Fixatives

For Bouin's fixative, 2% picric acid powder (w/v) was dissolved in ddH_2O with gentle heat. Picric acid solution was diluted 4:1 with formaldehyde solution (37%), and a 95% solution with glacial acetic acid (v/v) was prepared.

The 10% buffered formalin fixative was made from a 37% stock solution of formaldehyde diluted with 0.2 M phosphate buffer pH 7.3.

1.6 Slides, cover glasses and mounting

For all tissue and cell preparations only Fisherbrand Superfrost microscope slides (Fisher Scientific; Pittsburgh, PA) were used. Tissue samples were mounted with Clarion Mounting Media (Biomeda; Foster City, CA) and covered with Microscope Cover Glasses (Fisher Scientific; Pittsburgh, PA).

1.7 Enzymes

Recombinant Taq DNA Polymerase and Proteinase K were purchased from Invitrogen (Carlsbad, CA). Proteinase K was diluted with autoclaved ddH_2O to a stock concentration of 10 mg/ml, aliquoted and stored at 4°C.

Gradel DNAseI was bought from Roche Diagnostics GmbH (Penzberg, Germany), diluted with DNAseI buffer to a stock concentration of 10 mg/ml, aliquoted and stored at -20°C.

1.8 Cell stains

Harris Hematoxylin and Eosin were purchased from Surgipath Medical Industries, Inc. (Richmond, IL), and Nuclear Fast Red from Vector Laboratories Inc. (Burlingame, CA).

1.9 Nucleotides

A 100 mM dNTP set was obtained from Invitrogen (Carlsbad, CA), diluted with autoclaved ddH_2O to a concentration of 10 mM, aliquoted and stored at -20°C.

1.10 Oligonucleotides

Oligonucleotides were synthesized by IDT (Integrated DNA Technologies, Inc., Coralville, IA). A stock solution of 100 μM was prepared by dissolving the lyophilized powder in TE buffer and subsequently stored at -20°C.

Morphogene genotyping

Name	Sequence	amplification
LongT7	5'-TAA TAC GAC TCA CTA TAG GGA GAC CCA AGC-3'	163 bp morphogene
Morpho	5'-CCA CCT GCC CAG AGC AAA TC-3'	

***Rag-1* genotyping**

Name	Sequence	amplification
IMR3104	5'-TAA TAC GAC TCA CTA TAG GGA GAC CCA AGC-3'	474 bp wt allele
IMR1746	5'-GAG GTT CCG CTA CGA CTC TG-3'	
IMR3104	5'-CCG GAC AAG TTT TTC ATC GT-3'	530 bp mutant allele
IMR0189	5'-TGG ATG TGG AAT GTG TGC GAG-3'	

HD-*Aire* genotyping

Name	Sequence	amplification
HD Aire wt fwd	5'-ATA GCA CCA CGA CAC CCA AG-3'	507 bp wt allele
HD Aire wt rev	5'-ATA TCA TTC TCC AAC TCC TGC CTC TTT-3'	
HD Aire fwd	5'-GTC ATG TTG ACG GAT CCA GGG TAG AAA GT-3'	1150 bp wt, 690 bp mutant allele
HD Aire rev	5'-AGA CTA GGT GTT CCC TCC CAA CCT CAG-3'	

LA-*Aire* genotyping

Name	Sequence	amplification
LA Aire wt fwd	5'-CAG TTC CTC TGT GTA GCT TTG GCT GTC GTG G-3'	438 bp wt allele
LA Aire wt rev	5'-GCT CGG ACC ACT GGC TTT AGG CTG CTA C-3'	
neo direct	5'-CGA CGG CGA GGA TCT CGTCGT GAC-3'	800 bp *neo* insert
LA Aire rev	5'-TCT TGG GAC TTA CCT GGT TAA CCT GGG GCT -3'	

1.11 Kits

DAB Substrate Kit for Peroxidase	Vector Laboratories Inc. Burlingame, CA
***In Situ* Cell Death Detection Kit, POD**	Roche Diagnostics GmbH Penzberg, Germany
Vectastain Elite ABC Kit	Vector Laboratories Inc. Burlingame, CA

1.12 Antibodies

Hamish Scott at the Walter and Eliza Hall Institute in Victoria, Australia, produced the monoclonal anti-AIRE antibody. The antibody was raised in rat against a mouse epitope of 21 amino acid peptides, corresponding to the 20 C-terminal amino acids of the mouse AIRE protein (LQWAIQSMSRPLAETPPFSS). The peptide with a C residue at the N-terminus was conjugated to keyhole limpet hemocyanin (KHL) and used to immunize rats. For our studies, clone 5H12 was used which belongs to the subclass IgG2c. The concentration of the antibody was 0.7 mg/ml and sodium azide with a final concentration of 0.1% was added.

The rabbit anti-GFP polyclonal serum (Cat. No.: A-6455) was purchased from Molecular Probes (Invitrogen; Carlsbad, CA), and the rabbit polyclonal anti-ubiquitin (Cat. No.: VP-U576) from Vector Laboratories (Burlingame, CA).

1.13 Secondary antibodies and reagents

As a secondary antibody for anti-AIRE, a biotinylated rabbit anti-rat IgG antibody (Cat. No.: BA-4001, Vector Laboratories; Burlingame, CA) was used. Further steps involved peroxidase-conjugated streptavidin, which was obtained from Jackson ImmunoResearch Laboratories (Cat. No.: 016-030-084, West Grove, PA).

To detect anti-GFP, a biotinylated goat anti-rabbit antibody (Cat. No.: 111-065-003, Jackson ImmunoResearch Laboratories Inc.; West Grove, PA) was applied.

For anti-ubiquitin a biotinylated goat anti-rabbit IgG antibody (Cat. No.: BA-1000, Vector Laboratories; Burlingame, CA) was used.

1.14 Mice strains

C57BL/6

The inbred strain was created in 1921, by crossing 20 consecutive generations of brothers and sisters. They are used in a wide variety of research areas, as well as for the generation of transgenic mice.

In this study, C57BL/6 mice were used for general purposes, e.g. morphological comparisons to *Aire*-deficient strains.

HD-*Aire*-deficient mouse model

The HD-*Aire*-knockout mouse model was made by Anderson and coworkers in 2002 at Harvard Medical School (hereafter designated as HD-*Aire* mice in our study). A targeting vector bearing a l*oxP* site-flanked Pgk-neo cassette was inserted into intron 2 and an additional single *loxP* site was placed in intron 1. The targeting construct was electroporated into 129S2/SvPas-derived D3 embryonic stem (ES) cells. Correctly targeted ES cells were injected into C57BL/6 blastocysts. The resulting chimeric mice were mated with CMV-cre transgenic mice on a C57BL/6 background and further backcrossed to C57BL/6 mice. The mice carry the mutant allele with a deletion of exon 2, as well as parts of the upstream and downstream introns. The absence of exon 2 causes a frame shift which results in premature truncation of the AIRE protein shortly after exon 1.

LA-*Aire*-deficient mouse model

The LA-*Aire*-knockout mice were generated by Ramsey and coworkers in 2002 at the University of California Los Angeles (hereafter designated as LA-*Aire* mice in this study). Via homologous recombination in ES cells, a *neo*-cassette in the beginning of exon 6 was inserted into the *Aire* gene. J129 embryonic stem (ES) cells were used and positive ES cells were injected into C57BL/6 blastocysts. Animals were backcrossed to the 129S1 agouti mouse strain. The mice carry a deletion starting from intron 5 and ending in intron 6 which causes interruption of *Aire* (mRNA) as well as early termination of all synthesized polypeptides.

Testes of 3-week- and 3-month-old homozygous and heterozygous *Aire*-deficient mice as well as homozygous *Aire*-sufficient littermates, were used for morphological and immunohistochemical studies as well as for evaluation of apoptosis.

Morphogene mice (mismatch-repair-deficient mouse model)

These mice - made by Morphotek Inc. (Exton, PA) - have a dominant negative mutant transgene of the mismatch repair protein *Pms2* (referred to as morphogene). Morphogene mice were crossed with HD-*Aire* and LA-*Aire* mice to create *Aire*-deficient offspring in combination with the dominant negative transgene.

Morphology and apoptosis in target tissue of 3-week- and 3-month-old mice were investigated.

***Aire*-driven *Igrp-Gfp* (*Adig*) transgenic mice**

This transgenic mouse model was created by Anderson and coworkers at University of California San Francisco. The construct consists of the gene for Islet-specific glucose-6-phosphatase-related protein (*Igrp*) fused to the gene for green fluorescent protein (*Gfp)* and a SV40 polyadenylation signal. The construct is flanked by exon 1, containing the *Aire* promoter, and exon 3 of the *Aire* gene and places the *Igrp-Gfp* gene under the *Aire* promoter and regulatory elements. To stabilize transgene expression, a β-globin splice donor and acceptor cassette were placed in the first exon of the *Aire* gene upstream of the ATG initiation site. The *Igrp-Gfp* fusion/SV40 sequence was inserted immediately downstream of the β-globin splice site.

Testes and thymi of *Aire*-driven *Igrp-Gfp* were used to confirm *Aire* expression with an anti-GFP antibody.

***Rag-1*-deficient mice**

Rag-1-deficient mice were obtained from 'The Jackson Laboratory' (Bar Harbor, ME). The mice, backcrossed to the C57BL/6 strain, have a 1356 bp deletion in the 5' end of the *Rag-1* coding sequence. *Rag-1*-deficiency results in a defect in VDJ-recombination, and the mice are therefore unable to produce mature T and B cells.

Rag-1-deficient mice were mated with HD-*Aire*-deficient mice, and testes were used to investigate morphological aspects and to evaluate apoptosis.

2. Methods

2.1 DNA isolation

For identification of transgenic and knockout mice the genotype was determined by analysis of DNA extracted from tail tissues. A 5 mm tail biopsy was excised with scissors and subsequently placed in 500 µl tail lysis buffer. The tubes were incubated at 55°C overnight. After complete lysis, the debris was spun down for 3 min at 15,000 g. The supernatant was transferred into a new tube, and genomic DNA was precipitated with an equal volume of 2-propanol under agitation. The precipitate was extracted with a sterile loop, washed in 500 µl of 70% ethanol and dried at 37°C overnight. The DNA was eluted in 100 µl TE buffer at 55°C for 3 hours.

2.2 Polymerase chain reaction (PCR)

Polymerase chain reaction (Saiki et al., 1985; Mullis et al., 1986; Mullis and Faloona, 1987) is a technique that repeatedly amplifies a specific region of DNA. Two oligonucleotides that flank the desired nucleotide sequence on the 5'-end and on the opposite strand on the 3'-end, are used as primers for *in vitro* DNA synthesis, catalyzed by the enzyme DNA polymerase. The template DNA is denatured by heating and then cooled to a temperature that allows the primers to hybridize to complementary sequences. The annealed primers are extended with DNA polymerase in the presence of the four deoxyribonucleotidetriphosphates (dNTPs), so that the favored DNA is synthesized. The cycles of denaturation, annealing and extension are repeated, and the newly synthesized fragments serve as templates, producing predominantly DNA that is identical to the sequence bracketed by and including the two primers in the original template.

Here, this method was used to genotype mice of different strains. The protocol is based on the recommendations of the recombinant Taq DNA polymerase manufacturer, Invitrogen, and a standard PCR mix consisting of the following components: 1 x PCR buffer, 1.5 mM $MgCl_2$, 0.5 µM of each primer, 0.2 mM of each dNTP, 0.5 ng of template DNA and 0.5 units of Taq DNA polymerase, wherein one unit incorporates 10 nmol of deoxyribonucleotide into acid-precipitable material within 30 min at 74°C.

For efficient amplification, the annealing temperature (T_A) of each primer pair was determined. First, the melting temperatures (T_M) of the primers were obtained by using the online Oligonucleotide Properties Calculator (http://www.basic.northwestern.edu/biotools/oligocalc.html) and then T_A was calculated

as followed: $T_A = T_M - 5°C$. T_A was also checked in a gradient PCR and adjusted for optimal results.

After an initial denaturation step at 94°C for 7 min, 35 cycles of PCR amplification were performed: denaturation for 30 sec to 1 min at 94°C, annealing for 30 sec to 1 min at the calculated temperature, extension for 45 sec to 2 min at 72°C. A final extension step for 7 min at 72°C was carried out, and the reaction maintained at 4°C. Specific annealing temperatures, times and extension times were empirically modified for ideal results.

Primer 1	HD Aire wt fwd	HD Aire fwd	LA Aire wt fwd	*Neo* direct	Long T7	IMR 3104	IMR 3104
Primer 2	HD Aire wt rev	HD Aire rev	LA Aire wt rev	LA Aire rev	Morpho	IMR 1746	IMR 0189
Initial denaturation	94°C, 7 min						
Denaturation	94°C, 1 min	94°C, 1 min	94°C, 1 min	94°C, 1 min	94°C, 1 min	94°C, 30 sec	94°C, 30 sec
Annealing	66°C, 1 min	67°C, 30 sec	65°C, 1 min	68°C, 30 sec	60°C, 1 min	58°C, 45 sec	58°C, 45 sec
Extension	72°C, 1 min	72°C, 90 sec	72°C, 1 min	72°C, 2 min	72°C, 1 min	72°C, 45 sec	72°C, 45 sec
Cycles	35 X						
Final extension	72°C, 7 min						

2.3 DNA agarose gel electrophoresis

Agarose gel electrophoresis is a standard method to separate, identify, and purify DNA fragments. Migration of the DNA is dependent upon four parameters: molecular size of the DNA (Helling et al., 1974), agarose concentration, DNA conformation (Thorne, 1966) and electric current. Bands within the gel are stained with the fluorescent intercalating dye ethidium bromide and detected in ultraviolet light. The technique was used to identify the length of specific, amplified DNA fragments in order to determine the genotype of the mouse DNA donor.

Gels were made with 1% Agarose (w/v) in Tris-borate-EDTA buffer (TBE) and a final concentration of 0.5 μg/ml ethidium bromide. DNA samples were mixed with 6x

DNA loading buffer consisting of 40% (w/v) sucrose and 0.25% (w/v) bromphenolblue, loaded onto the gel and run in a gel electrophoresis tank covered with TBE buffer. A 1 kb DNA ladder was included as a molecular weight marker. DNA fragments were separated with 5 volts/cm distance between the electrodes and detected with a UV transilluminator coupled to a gel imaging system.

2.4 Tissue fixation and preparation

To avoid tissue digestion by enzymes present within the cells (autolysis) or by bacteria, and to preserve the structure and molecular compositions, tissues were fixed or frozen immediately.

For histological analysis and *in situ* cell death detection, testes were fixed in freshly made Bouin's solution. Bouin's fixative is widely used for testes due to its excellent preservation of nuclear details. Fixation time varied according to the age of mice, and therefore testis size. Immature testes were immersed for 8 hours in 5 ml Bouin's solution at room temperature and mature testes for 10 hours. Testes were washed several times in 70% ethanol and embedded in paraffin according to standard procedures. Embedded testes were transverse sectioned (4 μm) using Fisherbrand Superfrost microscope slides. For the *in situ* cell death detection, sections were cut at five tissue levels with approximately 500 μm between each level. Slides were stored at room temperature in the dark until further processing.

For immunohistochemical methods, testes were fixed in freshly made 10% neutral buffered formalin overnight at 4°C, washed several times in PBS, embedded in paraffin, and cut and stored as described above.

Frozen sections were also prepared for immunohistochemical staining. Dissected testes and thymi were carefully patted dry and immediately frozen in Tissue-Tek O.C.T. compound using crushed dry ice covered with 2-methylbutane. Frozen sections were cut (4 μm) at five tissue levels, mounted on Fisherbrand Superfrost microscope slides and stored at -80°C until further processing.

2.5 Histology

Histology is described as the study of tissues and how these tissues are arranged to constitute organs. Here, histological techniques were used to examine morphological differences in testes of mice with various genetic backgrounds. Harris Hematoxylin in combination with Eosin (H&E) was used for blue staining of

the nuclei and pink staining of the cytoplasm, respectively. The procedure was done according to the manufacturer's guidelines.

For *in situ* cell death detection assays and immunohistochemical procedures, a counterstain was used to visualize tissue components. Either Harris Hematoxylin or a one step staining method with Nuclear Fast Red, resulting in light red nuclei, was applied.

2.6 Immunohistochemistry

Immunohistochemistry is a method that allows detection of proteins in tissue sections through specific binding of antibodies and visualization with fluorescent chemicals or enzymes capable of converting a substrate into a visible dye.

Detection of AIRE

To detect AIRE protein in mouse testes and to verify the appearance in thymic tissue, an indirect immunohistochemical method aiming at signal enhancement was applied. The rat monoclonal anti-AIRE antibody was detected with a biotinylated anti-rat IgG antibody. Streptavidin – in this case conjugated to peroxidase - binds with a strong non-covalent interaction to biotin. Peroxidase catalyzes the oxidation of the substrate 3,3'-diaminobenzidine (DAB) in presence of hydrogen peroxide, resulting in an insoluble brown-colored product. Metal salts like nickel intensify the color.

Frozen testis and thymus sections were air-dried for 30 min, fixed in ice-cold acetone for 10 min and air-dried again. Samples were washed in PBS for 2 min, followed by immersion in 0.5% H_2O_2 in PBS for 10 min at room temperature to inactivate endogenous peroxidase activity. After thorough washing, the tissue was blocked in 10% (v/v) normal rabbit serum in PBS for 30 min at room temperature. Subsequently, the tissue was incubated with monoclonal rat anti-AIRE in 1:100 dilution in PBS with 3% BSA for 60 min. After washing in PBS, mouse Ig-absorbed, biotinylated rabbit anti-rat secondary antibody, diluted 1:100 in PBS with 3% BSA, was applied for 45 min. Following immersion in PBS, the tissue was incubated with a 1:50 dilution of streptavidin-HRP in PBS for 30 min. The substrate 3,3'-diaminobenzidine (DAB) was applied according to the manufacturer's recommendations. The slides were counterstained with Nuclear Fast Red for 5 min and mounted with coverslips.

All incubations were done at room temperature in a humidified chamber. Final volumes of diluted reagents were 30 μl per section. A hydrophobic barrier pen was used to keep the staining reagents localized on the tissue sections.

Detection of *Aire*-driven IGRP-GFP

To verify *Aire* expression, testes and thymi of transgenic mice carrying an *Aire*-driven *Igrp-Gfp* construct, were stained with an anti-GFP polyclonal antibody.

After removal of paraffin in fresh xylene, slides were rehydrated in graded series of ethanol diluted in double-distilled water. Samples were immersed in PBS, followed by 3% H_2O_2 in methanol for 15 min at room temperature to inactivate endogenous peroxidase activity. After being washed in IHC buffer for 5 min, sections were incubated with diluted Normal Blocking Serum from the Vectastain Elite ABC Kit, which was used according to the manufacturer's guidelines. After excess serum was blotted from the sections, rabbit anti-GFP polyclonal serum, diluted 1:250 in IHC buffer, was applied, covered with cover glasses and incubated overnight at 4°C in a humidified chamber. The next day, slides were washed for 5 min in IHC buffer under light agitation and the 1:100 diluted biotinylated goat anti-rabbit antibody was applied for 30 min at room temperature. Next, the slides were washed twice in PBS and incubated for 30 min with Vectastain Elite ABC reagent. The substrate 3,3'-diaminobenzidine (DAB) was applied according to the manufacturer's recommendations. The slides were counterstained with Harris Hematoxylin for 1 min, dehydrated in ethanol, cleared in xylene, then mounted with coverslips.

Detection of ubiquitin

To localize ubiquitin, testes of *Aire*-deficient and *Aire*-sufficient mice were stained with anti-ubiquitin polyclonal antibody.

After adequate removal of paraffin in fresh xylene, slides were rehydrated in graded series of ethanol diluted in double-distilled water. Samples were immersed in methanol with 3% H_2O_2 for 15 min at room temperature to inactivate endogenous peroxidase activity. After rinsing in double-distilled water, slides were washed in PBS containing 0.2% Tween 20 (PBS-T) for 10 min on a rotating table. Then the sections were incubated with 10% goat serum diluted in PBS-T for 30 min. After blotting excess serum from the sections, rabbit polyclonal anti-ubiquitin, diluted 1:250 in PBS-T containing 10% goat serum, was applied, covered with cover glasses and incubated overnight at 4°C in a humidified chamber. The next day, the

slides were washed in two changes of PBS-T for 3 min each. Biotinylated goat anti-rabbit antibody (diluted 1:100 in PBS-T with 10% goat serum), was applied for 30 min at room temperature. Next, the slides were washed twice in PBS-T, and incubated for 30 min with Vectastain Elite ABC Reagent. The buffer for the ABC reagents was made of PBS with 0.2 M methyl-alpha-D-mannopyranoside and 1 M sodium chloride. Sections were washed twice with PBS for 3 min each, quickly rinsed in double-distilled water and developed with 3,3'-diaminobenzidine (DAB) according to the manufacturer's recommendations. The slides were counterstained with Harris Hematoxylin for 20 sec, dehydrated in ethanol, cleared in xylene, then mounted with coverslips.

2.7 *In situ* cell death detection with terminal deoxynucleotidyl transferase-mediated dUTP-biotin nick end labeling (TUNEL)

Apoptotic cells display a characteristic pattern of structural changes in the nucleus and cytoplasm. One of them is the activation of DNAse in the nucleus, resulting in DNA fragmentation. DNA strand breaks can be enzymatically labeled using terminal deoxynucleotidyl transferase (TDT), which catalyzes polymerization of labeled nucleotides to free 3'-OH ends.

For detection and localization of apoptotic cells and in testes of mice with various genetic backgrounds and ages, the Roche *In Situ* Cell Death Detection Kit, POD, was used and modified as described.

After adequate removal of paraffin in fresh xylene, slides were rehydrated in a graded series of ethanol diluted in double-distilled water. Samples were immersed in PBS followed by 3% H_2O_2 in methanol for 10 min at room temperature to inactivate endogenous peroxidase activity. After washing in PBS, the tissue was permeabilized in 0.1 M citrate buffer, pH 6.0, with microwave irradiation at 500 W for 70 sec, and subsequently transferred into PBS. Sections were blocked in 3% BSA in PBS for 25 min at room temperature. The reaction mixture, containing Label Solution with nucleotide mixture and Enzyme Solution with terminal deoxynucleotidyl transferase (TdT), was prepared according to the manufacturer's guidelines and then applied to the samples. The slides were incubated at 37°C for 60 min in a humidified chamber. After washing in PBS, Converter POD, containing anti-fluorescein antibody conjugated with horseradish peroxidase (POD), was applied for 30 min at 37°C in a humidified chamber. 3,3'-diaminobenzidine (DAB) was used as a peroxidase substrate intensified with Ni^{2+} to obtain dark-brown

staining. Sections were counterstained with Nuclear Fast Red for 10 min, dehydrated in ethanol, cleared in xylene, then mounted with coverslips.

For positive labeling control, sections were treated with DNaseI, grade I (1500 U/ml, 1 mg/ml BSA in DNAseI buffer) for 30 min at 37°C in a humidified chamber to induce DNA strand breaks. Negative labeling control sections were incubated in Label Solution only.

2.8 Fertility assay

Sperm count, motility and morphology are essential parameters to evaluate fertility. These parameters were examined in *Aire*-deficient and *Aire*-sufficient male mice.

Sperm buffer was incubated at 37°C, 5% CO_2 for 1h. One entire epididymis containing *caput*, *corpus* and *cauda* was used for sperm count and one caudal part to examine sperm motility. Tissue parts were excised and transferred into 1 ml of preheated buffer, minced with scissors and incubated at 37°C, 5% CO_2. After one hour in the media, released sperm were counted using a hemocytometer and progressive, non-progressive and immobile sperm were distinguished.

To examine head and tail morphology of the sperm, a cell smear was prepared. 30 µl of the caudal epididymis cell preparation was distributed on a microscope slide, dried for 1 hour at room temperature and stained with Harris Hematoxylin for 3 min. After being rinsed in tap water for 2 min, the slides were dried and mounted with coverslips.

2.9 Microscopy and quantitative evaluation

The slides were viewed using light microscopy (Leica DM LB) with a 10x (aperture 0.30), 20x (aperture 0.50) or 40x magnification (aperture 0.70) objective. Pictures were recorded with a microscope camera system (DEI-750, Optronics) and digitized with Scion Image Software (Scion Corporation).

Percentage of apoptotic cells

A germ cell was considered apoptotic when it showed dark-brown and intense nuclear staining. Apoptotic germ cells in 20 randomly selected seminiferous tubules per level (100 tubules per testis) were counted and divided by the total number of all germ cells in all evaluated seminiferous tubules multiplied by 100. Germ cell stages of apoptotic cells were identified according to their morphology and position in the seminiferous tubule.

Percentage of AIRE-positive cells

AIRE-positive cells were counted in 20 randomly selected seminiferous tubules per level (100 tubules per testis) and divided by the total, average number of germ cells obtained from the apoptotic study, multiplied by 100.

Percentage of ubiquitin-positive cells

Ubiquitin-positive cells were counted in 80 randomly focused seminiferous tubules. This number was divided by the total number of germ cells in the specific tubules and multiplied by 100 to obtain the ubiquitin index.

2.10 Statistics

The quantitative results in this study are shown as means ± StDev. Statistical significance was assessed by the student's t-test. P-values below 0.05 were considered as statistically significant.

2.11 Mice

Mice were kept in a rodent barrier facility under sterile conditions and had *ad libitum* access to food and water. Animals were killed by CO_2 overexposure with controlled inflow, using a flow rate of 1-2 liter per minute, followed by cervical dislocation.

All procedures were performed in accordance with the guidelines of the University of California San Francisco Institutional Animal Care Committee (IACUC) and in compliance with guidelines established by the National Institute of Health (NIH).

CHAPTER IV: RESULTS

1. AIRE protein detection and *Aire* mRNA expression in the testis

1.1 AIRE protein detection

Before our study, it had been shown that AIRE protein is predominantly present in medullary thymic epithelial cells (mTECs) (Heino et al., 2000; Anderson et al., 2002). Results regarding AIRE in peripheral lymphoid and non-lymphoid organs were discordant (Blechschmidt et al., 1999; Ruan et al., 1999; Heino et al., 2000; Zuklys et al., 2000; Derbinski et al., 2001; Halonen et al., 2001; Anderson et al., 2002; Ramsey et al., 2002; Adamson et al., 2004). *Aire* mRNA was detected in the testis, but presence of a functional protein remained to be demonstrated (Blechschmidt et al., 1999; Ruan et al., 1999; Heino et al., 2000; Halonen et al., 2001). Subsequent research documented AIRE protein in spermatocytes and spermatids with use of a polyclonal antibody against mouse AIRE peptide (amino acids 160-176) (Halonen et al., 2001). A polyclonal antibody against a human AIRE peptide (amino acids 147-165) found AIRE protein to be present in the seminiferous tubules, located in spermatocytes but not in spermatids (Adamson et al., 2004). None of the two studies quantified the amount of AIRE protein.

To clarify the presence of AIRE protein excluding any unspecific detection caused by polyclonal antibodies, we used a monoclonal rat α-mouse AIRE antibody for our studies (see Materials and Methods: 1.12 and 2.6).

First, we confirmed AIRE protein in mTECs of 3-month-old *Aire*-sufficient mice (figure IV.1 A and B), which served as a positive control. In homozygous *Aire*-deficient littermates, no AIRE protein was detected in the thymus (figure IV.1 C). The isotype control was negative (figure IV.1 D).

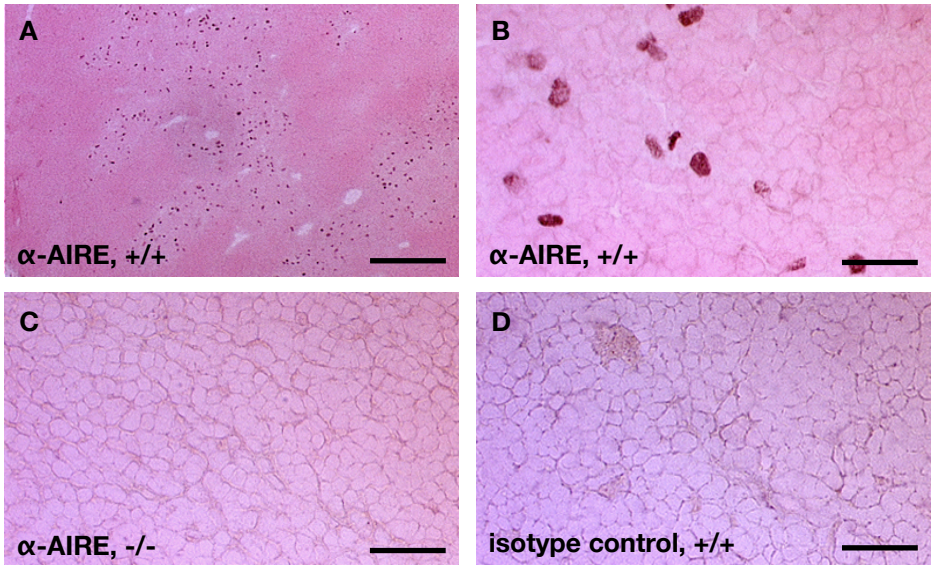

Figure IV.1: AIRE protein detection in thymic medullary epithelial cells
Staining of mice thymic frozen sections with monoclonal rat α-mouse AIRE antibody detects AIRE (brown staining) in medullary thymic epithelial cells (A, B). The littermate's *Aire*-deficient thymus shows no staining (C), as well as the section treated with an irrelevant antibody (D). Scale bar in picture A represents 60 µm, in picture B, C and D 40 µm.

The subsequent staining with the monoclonal rat α-mouse AIRE antibody of testes sections of 3-month-old wild-type mice detected AIRE protein in spermatogonia and spermatocytes (figure IV.2 A and B). The germ cells were staged according to their position in the seminiferous tubule and their morphological appearance. Spermatids, Sertoli cells and interstitial cells were not stained. In addition, no signal showed up in the testes of *Aire*-deficient littermates (figure IV.2 C) or in the isotype control (figure IV.2 D).

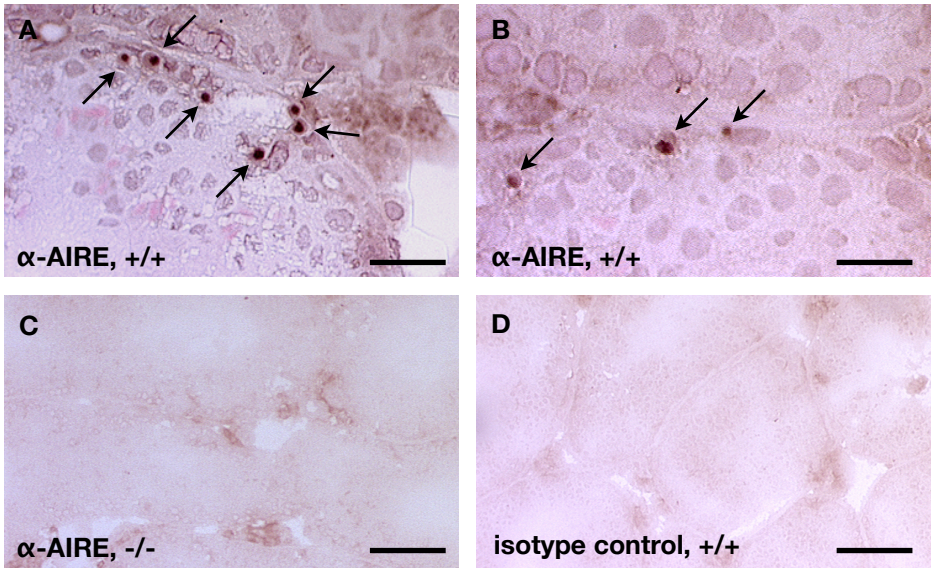

Figure IV.2: AIRE protein detection in germ cells of the testis
Staining of mice seminiferous tubules frozen sections with monoclonal rat α-mouse AIRE antibody detects AIRE (brown staining) in spermatogonia and spermatocytes (arrows) (A, B). The testis section of an *Aire*-deficient littermate shows no staining (C), as well as the section treated with an irrelevant antibody (D). Scale bar in picture A represents 50 µm, in picture B 40 µm, and in picture C and D 60 µm.

During the course of is study, we verified *Aire* expression in frozen testis sections of *Aire*-driven *Igrp-Gfp* (*Adig*) transgenic mice (Gardner et al., 2008), independent of the monoclonal rat α-mouse AIRE antibody. In the *Adig* mouse model the gene for *Igrp* (islet-specific glucose-6-phosphatase-related protein) was fused to the *Gfp* (green fluorescent protein) gene and placed under control of the *Aire* promoter and regulatory elements (see Materials and Methods 1.14). Staining with a polyclonal α-GFP antibody (see Materials and Methods 2.6) detected the presence of *Aire*-regulated GFP protein in spermatogonia and spermatocytes, as well as in the interstitium (figure IV.3 A and B). Thymic sections served as positive control with staining in mTECs (figure IV.3 C); the wild-type testis section showed no signal (figure IV.3 D) as did transgenic testis sections treated with secondary antibody only (not shown).

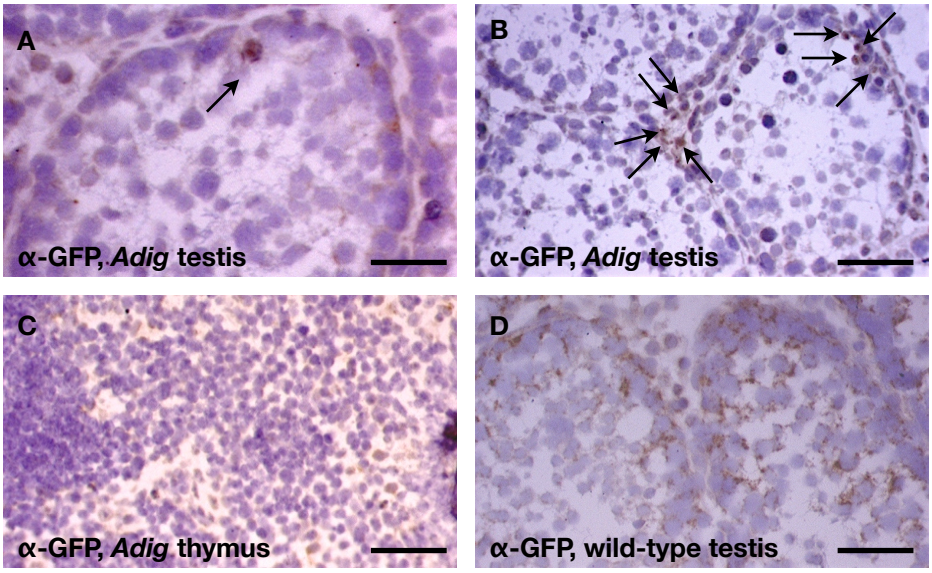

Figure IV.3: Detection of GFP protein in *Aire*-driven *Igrp-Gfp* (*Adig*) transgenic mice testis and thymus
Frozen sections of seminiferous tubules of transgenic mice with IGRP-GFP fusion protein, controlled by the *Aire* promoter, show brown-colored staining in spermatogonia, spermatocytes and the interstitium after application of α-GFP antibody (arrows) (A, B). The presence of GFP, and therefore *Aire* expression, was found as well in thymic epithelial cells (C) of transgenic mice. No staining was detected in wild-type testis (D). Scale bar in picture A and C represents 40 µm, in picture B and D 50 µm.

1.2. Quantification of AIRE protein and *Aire* mRNA

After confirming AIRE's presence in the testis we quantified the amount of the protein in prepubertal 3-week- and adult 3-month-old mice. We used two different *Aire*-deficient mice strains (see Introduction 1.2.5 and Materials and Methods 1.14), one of which was designated as LA-*Aire* -/- (Ramsey et al., 2002) and the other one as HD-*Aire* -/- (Anderson et al., 2002). By using two different mice strains we reduced potential founder effects that occur in colonies founded by a few members and were able to compare the effects caused by *Aire*-deficiency in mice on two different genetic backgrounds.

Frozen testis cross sections were prepared from five *Aire*-sufficient littermates of 3-week-old HD-*Aire* -/- and LA-*Aire* -/- as well as from 3-month-old HD-*Aire* -/- animals. The tissue sections were incubated with the monoclonal rat α-mouse AIRE antibody (see Materials and Methods 2.6) and the number of AIRE-positive cells was quantified; 100 seminiferous tubules per cross section were evaluated. In 3-week-old HD-*Aire*-sufficient mice, 0.44% of cells in cross sections of the seminiferous tubules were AIRE positive; in LA-*Aire*-sufficient mice 0.43% (figure IV.4 A).

The cross sections in the prepubertal mice had on average 7,548 cells per 100 seminiferous tubules, resulting in 1 of every 240 germ cells being positive for AIRE. In 3-month-old HD-*Aire*-sufficient mice, 0.15% of cells stained positive for AIRE (figure IV.4 A). The adult seminiferous tubules have on average 13,247 cells per 100 tubules, and therefore 1 out of every 670 cells contains a detectable level of AIRE protein.

The staining of the germ cells in the 3-week- and 3-month-old testis is intense (figure IV.4 B and C), suggesting that a significant amount of AIRE protein is present. This is consistent with the results from quantitative RT-PCR done in collaboration with Clifford L. Wang: the ratio of *Aire* to β-actin expression was between 0.8×10^{-4} in 3-week-old and 2.2×10^{-4} in 3-month-old mice. To obtain a range of the *Aire* to β-actin ratio per cell, the relative expression of *Aire* to β-actin values were multiplied by 240 and 670, which yielded an estimate of a 10- to 35-fold lower abundance of *Aire* mRNA compared with that of β-actin. The actual value might be even higher, since the number of Sertoli cells were disregarded in the quantification.

In the analyzed testis sections, no defined stage in which all the germ cells produce AIRE was found (figure IV.2 A and B; IV.3 A and B; IV.4 B and C), suggesting a sporadic expression pattern. Because the testis is characterized by promiscuous gene expression (see Introduction 2.1.4) many expressed sequence tags for numerous genes with specific functions in other tissues can be found. Thus, *Aire* mRNA and the translated product might be without function.

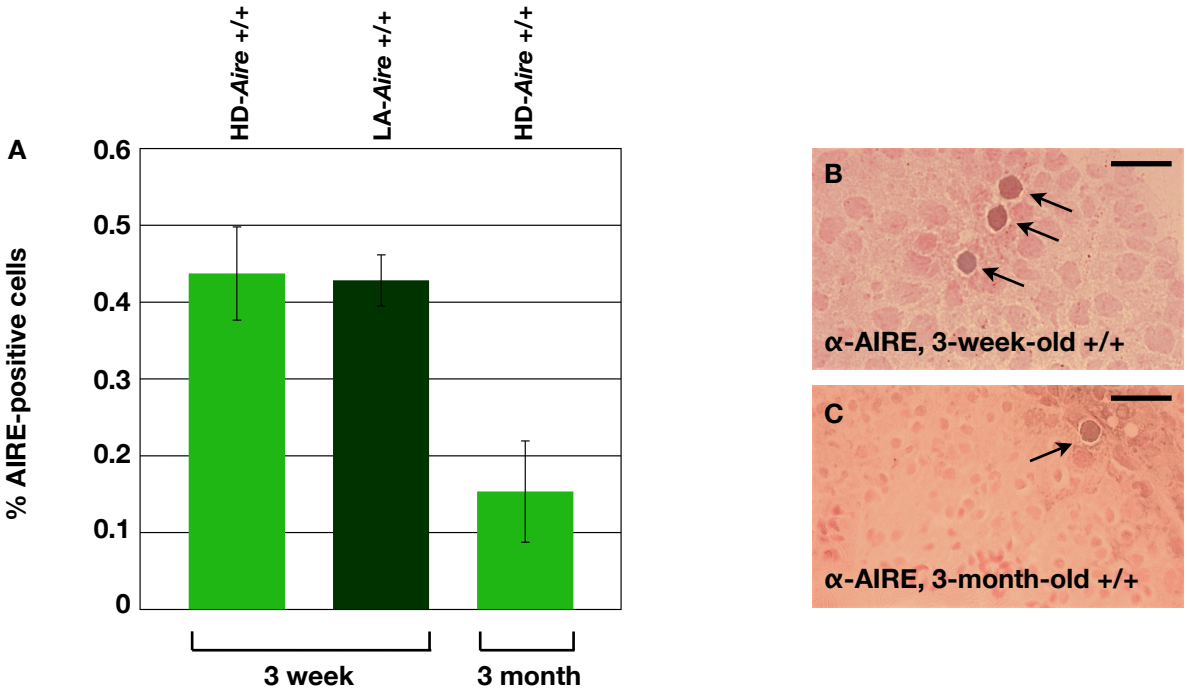

Figure IV.4: Percentage of AIRE-positive germ cells in testis
The percentage of AIRE-positive cells (A) was evaluated in testis cross sections of 3-week-old (B) and 3-month-old (C) *Aire*-sufficient littermates of HD-*Aire* -/- and LA-*Aire* -/- animals. For each data set, frozen sections stained with α-AIRE antibody of five animals were investigated, whereas 100 seminiferous tubules per section were quantified. Scale bar in picture B represents 40 µm, in picture C 50 µm.

2. AIRE and gene regulation in thymus and testis

The thymus is an additional organ with promiscuous gene expression (see Introduction 2.1.4). AIRE also controls the expression of many genes in the thymus (see Introduction 1.2.4) and therefore it is of interest to see whether those genes are regulated by AIRE in the testis, as well. This hypothesis was tested by quantitative RT-PCR done in collaboration with Clifford L. Wang.

Five genes, known to be under AIRE control in the thymus, were selected: *Irbp* (interphotoreceptor retinoid binding protein), *Fabp* (fatty acid binding protein), Proinsulin, *Ptdgs* (prostaglandin-D2-synthase) and *Spt1* (salivary protein 1). The ratio of expression in *Aire*-heterozygous over *Aire*-deficient testes of 23-day-old mice was measured. As control, the expression levels of those genes were evaluated in the thymus retrieved from the same animal as the testis. The results showed that *Fabp*, Proinsulin, *Ptdgs* and *Spt1* are highly upregulated in the heterozygous thymus, even though whole thymic cell lysates were used, resulting in signal dilution due to the fact that the vast majority of thymic cells do not produce AIRE (figure IV.5 A). In addition, a gene dosage effect of AIRE was

observed in heterozygous mice (Liston et al., 2005). *Irbp* remained undetected. Because there are even fewer AIRE-producing cells in the testis, an even higher signal dilution can be expected. Yet it seems clear that in 23-day-old testis higher expression levels of *Irbp*, Proinsulin, *Ptdgs* and *Spt1* were not detected (figure IV.5 B), suggesting that expression of those genes is not regulated by AIRE; *Fabp* was not detected at all. In adult testis additional genes were tested: *Hbb-y* (hemoglobin Y β-like embryonic chain), *Npy* (neuropeptide Y) and *Spt2* (salivary protein 2), but there was no indication of *Aire*-regulated expression (figure IV.5 C); instead all genes, with exception of *Spt2*, were slightly suppressed. *Spt2*, which was not studied in the 23-day-old testis, was measured to be somewhat upregulated. In conclusion, none of the tested genes, though promiscuously expressed in testis and thymus, were expressed at higher levels in *Aire*-sufficient testis and are therefore under different transcriptional control.

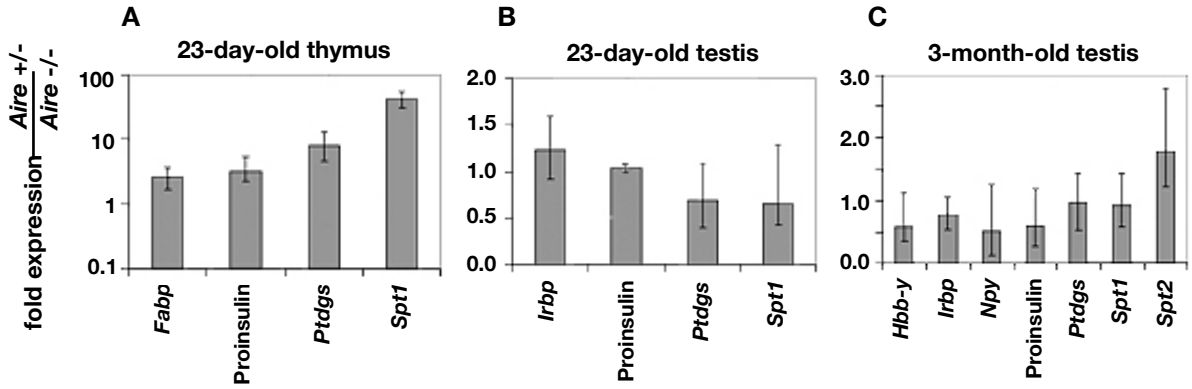

Figure IV.5: Dependance of gene expression on AIRE
AIRE dependance is represented as the quotient of gene expression levels in *Aire*-heterozygous and *Aire*-deficient mice. A 23-day-old thymus (A), 23-day-old testis from the same animal (B) and testis of 3-months age (C) were used. *Fabp* = fatty acid binding protein 2 intestinal; *Ptdgs* = prostaglandin-D2 synthase; *Spt1* = salivary protein 1; *Irbp* = interphotoreceptor retinoid binding protein; *Hbb-y* = hemoglobin Y β-like embryonic chain; *Npy* = neuropeptide Y; Spt2 = salivary protein 2. *Fabp* was undetected in the 23-day testes, and *Irbp* was undetected in the thymus. Tests on their expression were performed but there was no interpretable signal in these after 40 cycles.

3. Apoptosis in the testis

Though we couldn't identify promiscuously expressed genes under AIRE control in the thymus and testis, we kept searching for a possible function of AIRE during germ cell development. The promiscuous gene expression in the thymus is necessary for negative selection of self-reactive thymocytes and to establish central tolerance (see Introduction 1.1.2); during the selection processes, around

95% of T cells undergo apoptosis, and only a small fraction of efficient and harmless T cells leaves the thymus (Huesmann et al., 1991).

The testis is another location with promiscuous gene expression and vivid apoptotic activity (see Introduction 2.2). Scheduled apoptosis during prepuberty and sporadic apoptosis throughout adult life are essential for functional spermatogenesis and lead to substantial loss of germ cells (Rodriguez et al., 1997; Hikim et al., 2003). The hypothesis that promiscuous gene expression - as in the thymus - is followed by a negative selection process leading to apoptosis of mutant germ cells motivated us to have a closer look at apoptosis in *Aire*-sufficient and *Aire*-deficient prepubertal (3-week-old) and adult (3-month-old) mice.

3.1 Scheduled and sporadic apoptosis in *Aire*-deficient mice

For this experiment, testes of five *Aire*-sufficient (+/- or +/+) and five *Aire*-deficient mice of the HD-*Aire* and LA-*Aire* strains (see Introduction 1.2.5 and Materials and Methods: 1.14), aged 3-weeks and 3-months, were used. For improved histological quality, the testes were fixed in Bouin's solution and embedded in paraffin. Sections were cut out of five levels of the organ and apoptotic germ cells were detected using the TUNEL-technique, which enzymatically labels the apoptosis induced DNA strand breaks (figure IV.6) (see Materials and Methods 2.7). The TUNEL-positive, apoptotic germ cells were quantified in 20 seminiferous tubules per level section, equaling 100 seminiferous tubules per testis, and the percentage of apoptotic germ cells determined.

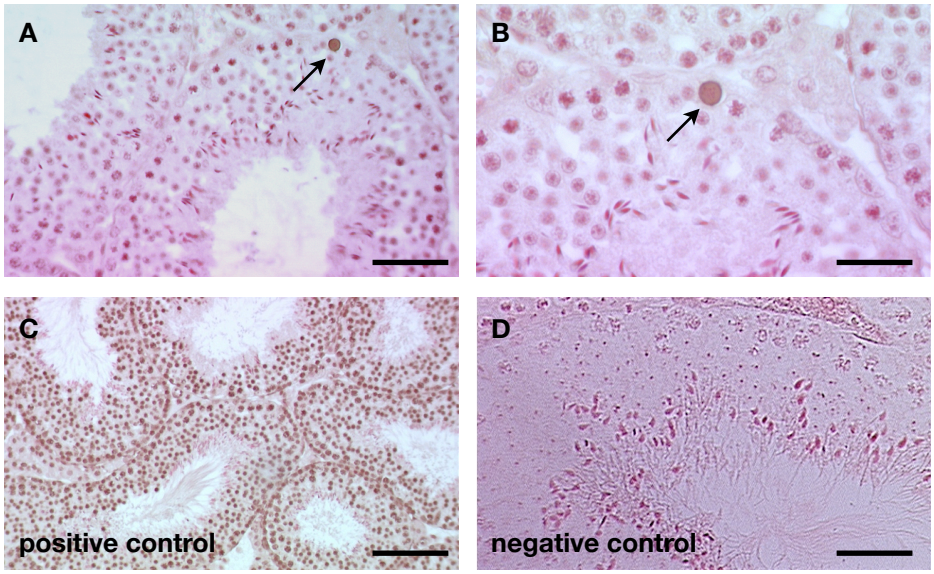

Figure IV.6: Detection of apoptotic germ cells with the TUNEL-technique
Apoptotic germ cells in the seminiferous tubules of HD-*Aire*-sufficient, LA-*Aire*-sufficient and *Aire*-deficient littermates were detected in Bouin's fixed paraffin sections with the TUNEL-technique. A cell was considered as TUNEL-positive when the nuclear staining is dark-brown, intense and homogeneous (arrows). The percentage of apoptotic cells was evaluated and the differentiation stage of the specific cell identified. A: lower magnification of a seminiferous tubule as used for quantification of apoptotic germ cells; scale bar represents 50 µm. B: higher magnification used to determine the differentiation stage of the specific germ cell; scale bar represents 40 µm. C: DNAase treated testis section used as positive control in the TUNEL experiment; scale bar represents 60 µm. D: negative control; scale bar represents 50 µm.

We then compared the percentages of apoptosed germ cells over all germ cells between the *Aire*-sufficient and the *Aire*-knockout mice (figure IV.7, table IV.10). Three-week-old LA-*Aire*-sufficient mice showed on average 1.67% apoptotic cells, with a standard deviation of 0.14. Values for 3-week-old HD-*Aire*-sufficient mice were comparable, with 1.59% of apoptotic cells and a standard deviation of 0.1. Both values are in good agreement with the average 1.4% reported previously (Rodriguez et al., 1997), in which apoptotic cells were measured with the TUNEL-technique as well. On the contrary, *Aire*-deficient mice of 3-week age show a substantial reduction of apoptotic cells: LA-*Aire* -/- testis have apoptotic rates of 1.23% (StDev 0.14) and HD-*Aire* -/- testis of 1.24% (StDev 0.1), which represents a 25% reduction when compared to the values of the *Aire*-sufficient littermates (p = 0.001 for LA-*Aire* mice; p = 0.0005 for HD-*Aire* mice). No anatomic abnormalities were detected in the seminiferous tubules and the interstitium of the testis of *Aire*-deficient 3-week-old mice.

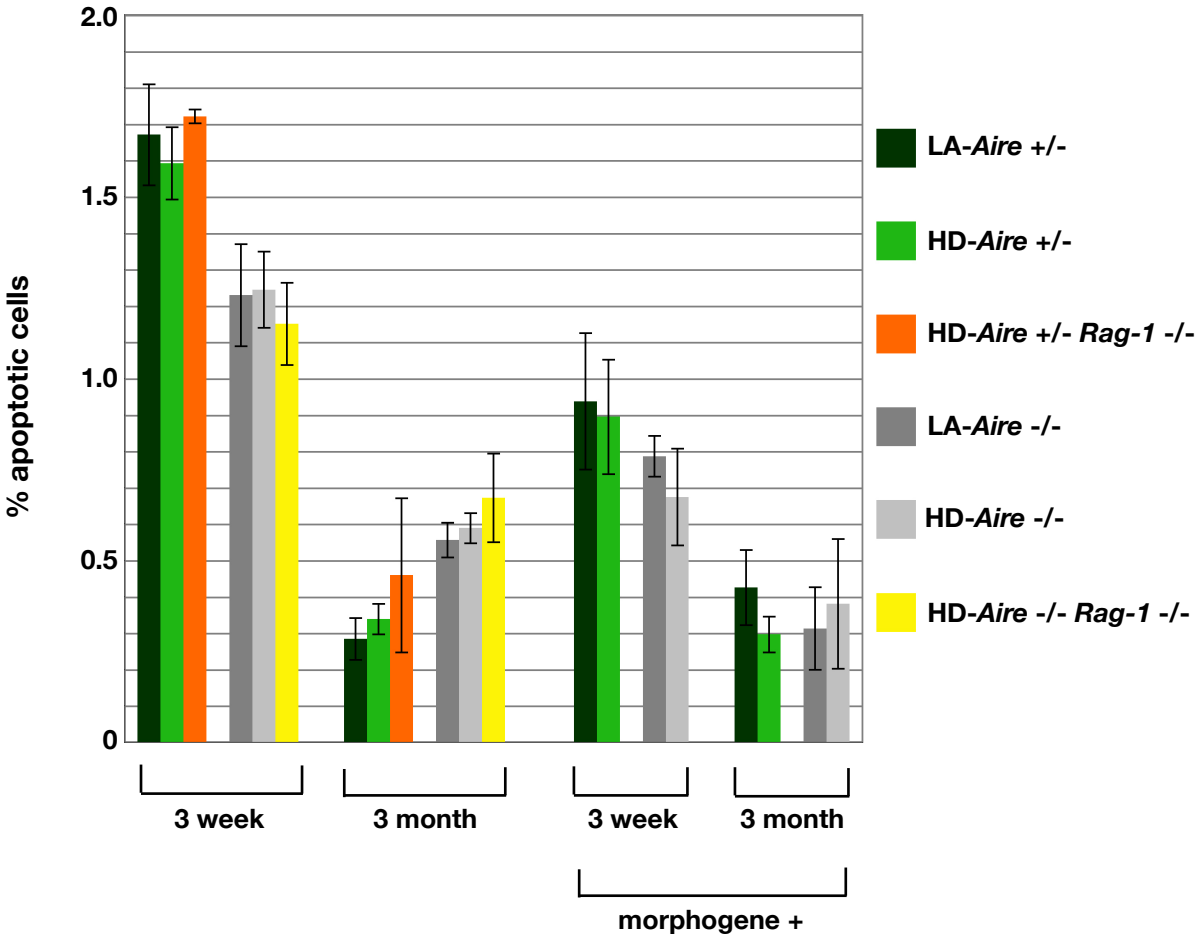

Figure IV.7: Percentage of apoptotic (TUNEL-positive) germ cells
Percentage of apoptotic germ cells of 3-week-old and 3-month-old LA-*Aire*-sufficient and HD-*Aire*-sufficient (dark-green and bright-green bars) as well as LA-*Aire*-deficient and HD-*Aire*-deficient mice (dark-gray and bright-grey bars). *Aire*-sufficient mice were mostly heterozygous, but also a small number of homozygous animals was included showing similar apoptotic values. Orange and yellow bars present HD-*Aire* +/- *Rag-1* -/- and HD-*Aire* -/- *Rag-1* -/- mice, respectively. Morphogene + are mice with the dominant negative mutant transgene of the mismatch-repair protein *Pms2*. Bars represent the arithmetic mean with standard deviation. Each data set was obtained from five mice (except for three HD-*Aire* +/+, *Rag-1* -/-); 100 seminiferous tubules each were evaluated. For exact values see table IV.10.

To exclude an involvement of the adaptive immune system, we generated HD-*Aire* *Rag-1*-/- mice (see Materials and Methods 1.14). RAG-1 is involved in VDJ-recombination of lymphocytes (see Introduction 1.1.2.1), and deficiency causes T cell and B cell loss. This absence assures that the observed effects in the testes are not caused by an attack of lymphocytes or autoantibodies, which are potentially able to penetrate the blood-testis barrier (see Introduction 2.1.1.2).

The percentage of apoptotic cells in prepubertal HD-*Aire*-deficient and HD-*Aire*-sufficient mice were similar to the one obtained in HD-*Aire*-deficient and HD-*Aire*-

sufficient mice on a *Rag-1-/-* background, which excludes an involvement of the adaptive immune system in the observed phenotype (figure IV.7, table IV.10).

We also had a closer look at what specific germ cell subtypes were affected (figure IV.8). Spermatocytes from late pachytene stages onward (here labeled spermatocytes II) were mostly affected by apoptosis in 3-week-old LA-*Aire*- and HD-*Aire*-sufficient testis. In the LA-*Aire*- (p = 0.08) and HD-*Aire*-deficient (p = 0.0003) littermates, a pronounced reduction was observed, with only half as many apoptotic late spermatocytes. In spermatogonia, early spermatocytes and spermatids the difference was less noticeable.

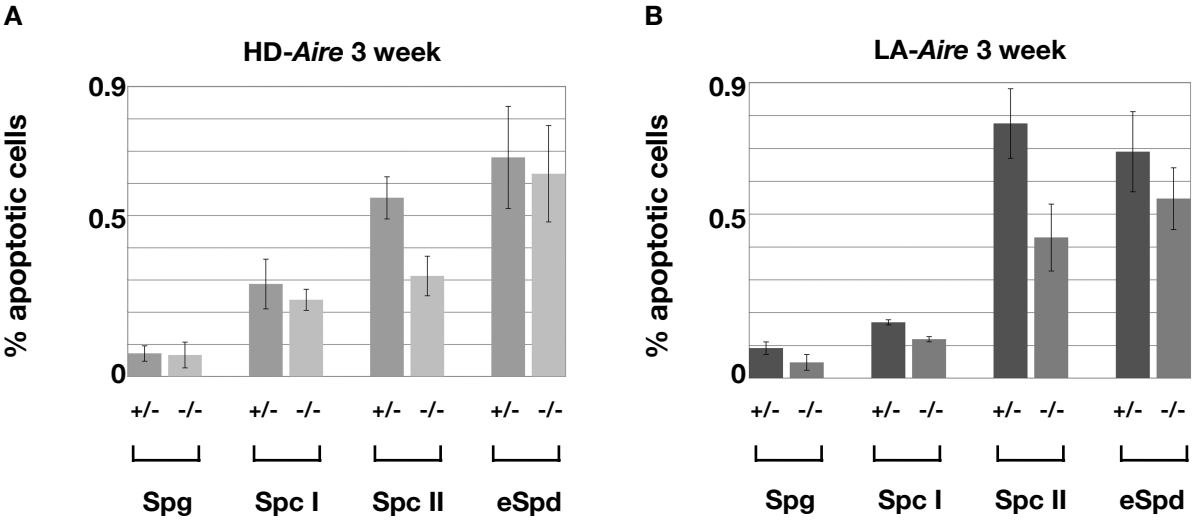

Figure IV.8: Percentage of apoptotic germ cells, stratified according to cell differentiation stage
Bars represent the arithmetic mean with standard deviation of the percentage of apoptotic germ cells in 3-week-old HD-*Aire*- and LA-*Aire*-sufficient (+/- and +/+) as well as in HD-*Aire*- and LA-*Aire*-deficient mice. Each data set was obtained from five mice and 100 seminiferous tubules each were evaluated. Spg = spermatogonia; Spc I = early spermatocytes; Spc II = spermatocytes from late pachytene stages onward; eSpd = early spermatids.

We also had a look at the apoptotic values of germ cells in 3-month-old *Aire*-sufficient mice and their *Aire*-deficient littermates (figure IV.7, table IV.10). The causes and/or pathways of the scheduled apoptosis in adult mice seem to differ from those in prepubertal mice, in which apoptosis occurs spontaneously (see Introduction 2.2.2.1 and 2.2.2.2). This can be observed in transgenic mice expressing *Bcl2*, or over-expressing *Bcl-X*$_L$, which don't undergo the prepubertal wave of spermatogenesis but show normal sporadic apoptosis later in life (Rodriguez et al., 1997).

Our study found, as reported previously (Rodriguez et al., 1997), substantially dropped apoptotic rates in 3-month-old *Aire*-sufficient testis: 0.28% apoptotic cells were detected in LA-*Aire*-sufficient (StDev 0.06) and 0.34% in HD-*Aire*-sufficient mice (StDev of 0.04), which is around one fifth of the 3-week level. However, in 3-month-old *Aire*-deficient mice, we discovered apoptotic values increased by factor two. In LA-*Aire*-deficient testis 0.56% of cells apoptose (StDev 0.05) and in HD-*Aire*-deficient mice 0.59% (StDev 0.04) (p = 0.00005 for LA-*Aire* mice; p = 0.00001 for HD-*Aire* mice). As in the 3-week-old *Aire*-deficient tubules, no anatomic abnormalities were seen.

As in the testis of 3-week-old mice, the apoptotic values in 3-month-old HD-*Aire* +/-, *Rag-1* -/- and HD-*Aire* -/-, *Rag-1* -/- testis were similar to the value in HD-*Aire* +/- and HD-*Aire* -/- testis only, excluding an involvement of the adaptive immune system (figure IV.7, table IV.10).

In 3-month-old testis, all germ cell subtypes in *Aire*-deficient testis - spermatogonia, spermatocytes and spermatids - seem to be affected by the increase in apoptosis, though the highest increase was in spermatocytes from pachytene stages onward (SpcII), as seen in figure IV.9.

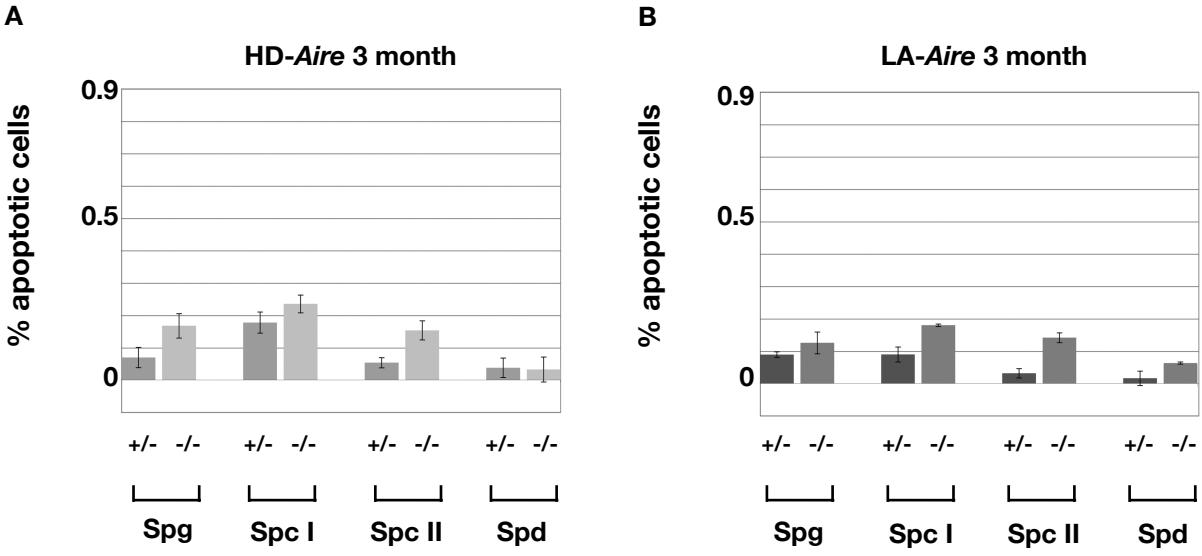

Figure IV.9: Percentage of apoptotic germ cells, stratified according to cell differentiation stage
Bars represent the arithmetic mean with standard deviation of the percentage of apoptotic germ cells in 3-month-old HD-*Aire*- and LA-*Aire*-sufficient (+/- and +/+) as well as in HD-*Aire*- and LA-*Aire*-deficient mice. Each data set was obtained from five mice and 100 seminiferous tubules each were evaluated. Spg = spermatogonia; Spc I = early spermatocytes; Spc II = spermatocytes from late pachytene stages onward; Spd = spermatids.

3.2 Scheduled apoptosis in mismatch-repair-deficient mice

The observation that *Aire*-deficiency leads to around 25% reduced apoptosis in 3-week-old testis but to twice as much apoptosis in 3-month-old testis, raised the question regarding the underlying reasons for apoptosis in *Aire*-sufficient mice. Two hypotheses are reasonable: the first is that the apoptotic wave in prepubertal mice establishes a critical ratio of germ cells to their supporting Sertoli cells (Rodriguez et al., 1997). The second proposes that mutated DNA, which was generated during meiosis I, triggers the cell death (Rodriguez et al., 1997; Mori et al., 1997). According to the first 'homeostasis' hypothesis, almost any substantial reduction in apoptosis - regardless of the cause - would disturb the strict stoichiometry, leading to dysfunction of spermatogenesis. However, according to the second hypothesis, a reduction in apoptosis would increase the amount of cells with mutations, but would not severely affect spermatogenesis per se.

To test those hypotheses, we studied the effect of a dominant negative mutant transgene of the mismatch-repair protein *Pms2*, referred to as morphogene (Nicolaides et al., 2005). Inheritance of a compromised version of this gene predisposes humans to hereditary nonpolyposis colon cancer (HNPCC) (Nicolaides et al., 1998) and, if introduced into cells of bacteria, yeasts, plants and mammals, increases the rate of genome-wide mutagenesis (Nicolaides et al., 2005). *Pms2* is best known as the *E.coli MutL* homologue and functions in DNA mismatch-repair, thereby contributing to genomic integrity. But *Pms2* is also a link to apoptosis of cells damaged beyond repair, thereby reducing the mutational load; it stabilizes the apoptosis-inducing protein p73 (Shimodaira et al., 2003; Ramadan et al., 2005) and is a direct target of p53 (Chen and Sadowski, 2005), which triggers the intrinsic apoptotic pathway (see Introduction 2.2.2.2).

Pms2-deficient somatic mouse cells apoptose less in response to DNA damage (Zeng et al., 2000) and so we investigated the apoptotic rates in transgenic morphogene germ cells. Indeed, in 3-week-old mice testis we found the percentage of apoptotic cells reduced by almost half (figure IV.7, table IV.10). LA-*Aire*-sufficient morphogene testes had 0.94 % and HD-*Aire*-sufficient morphogene testis 0.89% apoptotic cells, whereas the non-morphogene testis showed values around 1.6%. Also, in *Aire*-deficient 3-week-old mice a reduction was observed: in that 0.78% of germ cells apoptose in LA-*Aire*-deficient morphogene and 0.67% in HD-*Aire*-deficient morphogene mice (around 1.2% of germ cells are apoptotic in non-morphogene *Aire*-deficient testis). In 3-month-old transgenic morphogene

mice, no significant difference was noticeable. In all mice, the seminiferous tubules appeared normal, without any anatomic abnormalities.

The results showed that the morphogene can reduce the levels of scheduled apoptosis in germ cells, and thus can interfere with the critical ratio of germ cells to Sertoli cells. Because this does not affect adult spermatogenesis, but increases the mutational load, this might be an evidence for a contribution postulated by the second hypothesis, which interprets the prepubertal apoptotic wave as a consequence of mutated DNA. If this is correct, then up to 80% of germ cells in 3-week-old *Aire*-sufficient mice could contain mutations. Because over 80% of cells are deleted during this prepubertal time (Rodriguez et al., 1997), this translates into the 1.6% steady-state level of apoptotic cells scored in the evaluated tissue sections.

Mice	Age	Mean	StDev
LA-*Aire* +/- or LA-*Aire* +/+	3-week	1.67	0.14
HD-*Aire* +/- or HD-*Aire* +/+	3-week	1.59	0.10
HD-*Aire* +/+ *Rag-1* -/-	3-week	1.72	0.02
LA-*Aire* -/-	3-week	1.23	0.14
HD-*Aire* -/-	3-week	1.24	0.10
HD-*Aire* -/- *Rag-1* -/-	3-week	1.15	0.11
LA-*Aire* +/- or LA-*Aire* +/+	3-month	0.28	0.06
HD-*Aire* +/- or HD-*Aire* +/+	3-month	0.34	0.04
HD-*Aire* +/+ *Rag-1* -/-	3-month	0.46	0.21
LA-*Aire* -/-	3-month	0.56	0.05
HD-*Aire* -/-	3-month	0.59	0.04
HD-*Aire* -/- *Rag-1* -/-	3-month	0.67	0.12
LA-*Aire* +/- morpho or LA-*Aire* +/+ morpho	3-week	0.94	0.19
HD-*Aire* +/- morpho or HD-*Aire* +/+ morpho	3-week	0.89	0.16
LA-*Aire* -/- morpho	3-week	0.79	0.06
HD-*Aire* -/- morpho	3-week	0.67	0.13
LA-*Aire* +/- morpho or LA-*Aire* +/+ morpho	3-month	0.43	0.10
HD-*Aire* +/- morpho or HD-*Aire* +/+ morpho	3-month	0.30	0.05
LA-*Aire* -/- morpho	3-month	0.31	0.11
HD-*Aire* -/- morpho	3-month	0.38	0.18

Table IV.10: Apoptotic values
The table shows the arithmetic mean and the standard deviation of the percentage of apoptotic germ cells for each data set. Each data set was obtained from five mice (except for three HD-*Aire* +/+ *Rag-1* -/-) and 100 seminiferous tubules each were evaluated.

4. Ubiquitin protein quantification in testes of *Aire*-deficient mice

The first PHD zinc finger of the AIRE protein has been shown to have E3 ubiquitin ligase activity (see Introduction 1.2.3 and 1.2.6) (Uchida et al., 2004), suggesting a possible physiological role of AIRE in the ubiquitin proteasome pathway.

The ubiquitin proteasome pathway plays an essential role in a variety of cellular processes, such as cell cycle progression, degradation of intracellular proteins, membrane receptor endocytosis and apoptosis (Hershko and Ciechanover, 1998). In spermatogenesis, the ubiquitin-proteasome system is required for apoptosis and the degradation of numerous proteins throughout the proliferative, meiotic and haploid phase as well as in the epididymis (see Introduction 2.1.3) (Baarends et al., 2000). E3 ubiquitin ligases catalyze the attachment of ubiquitin to the amino group of the substrates lysine residue, thereby forming an isopeptide bond. Several attached ubiquitin molecules form a polyubiquitin chain that serves as a recognition marker for degradation by the 26S proteasome (Dahlmann, 2005).

The importance for the ubiquitin proteasome pathway in spermatogenesis was demonstrated in mice lacking *Uchl-1* (ubiquitin C-terminal hydrolase L-1) (gad mice), a molecule controlling the cellular ubiquitin balance by releasing conjugated ubiquitin from unfolded proteins (Wing, 2003). Prepubertal testis of gad mice show significantly fewer apoptotic cells, and adult mice have reduced sperm counts in the epididymis as well as defective spermatozoa (Kwon et al., 2005). *Aire*-deficient testis also show reduced apoptotic levels during prepuberty and reduced sperm counts in adulthood. If AIRE functions as an E3 ubiquitin ligase, attaching ubiquitin to misfolded proteins, then *Aire*-deficiency might be detectable as higher free monoubiquitin levels in the seminiferous tubules.

We stained paraffin testes sections of three adult HD-*Aire*-sufficient mice and three HD-*Aire*-deficient littermates with an α-ubiquitin antibody (see Materials and Methods 1.12 and 2.6). Positively stained germ cells were quantified in 80 seminiferous tubules: ubiquitin was clearly detectable (figure IV.11 A and B), but no significant difference between *Aire*-sufficient and *Aire*-deficient mice was evident. Ubiquitin was detectable in 28.1% of the germ cells in *Aire*-sufficient testis and in 25.4% in *Aire*-deficient testis (figure IV.11 E). Germ cells close to the basal lamina stained more frequently. Ubiquitin was as well detected in the epididymis and in epididymial spermatozoa in *Aire*-sufficient (not shown) and *Aire*-deficient mice (figure IV.11 D), though no quantification was carried out.

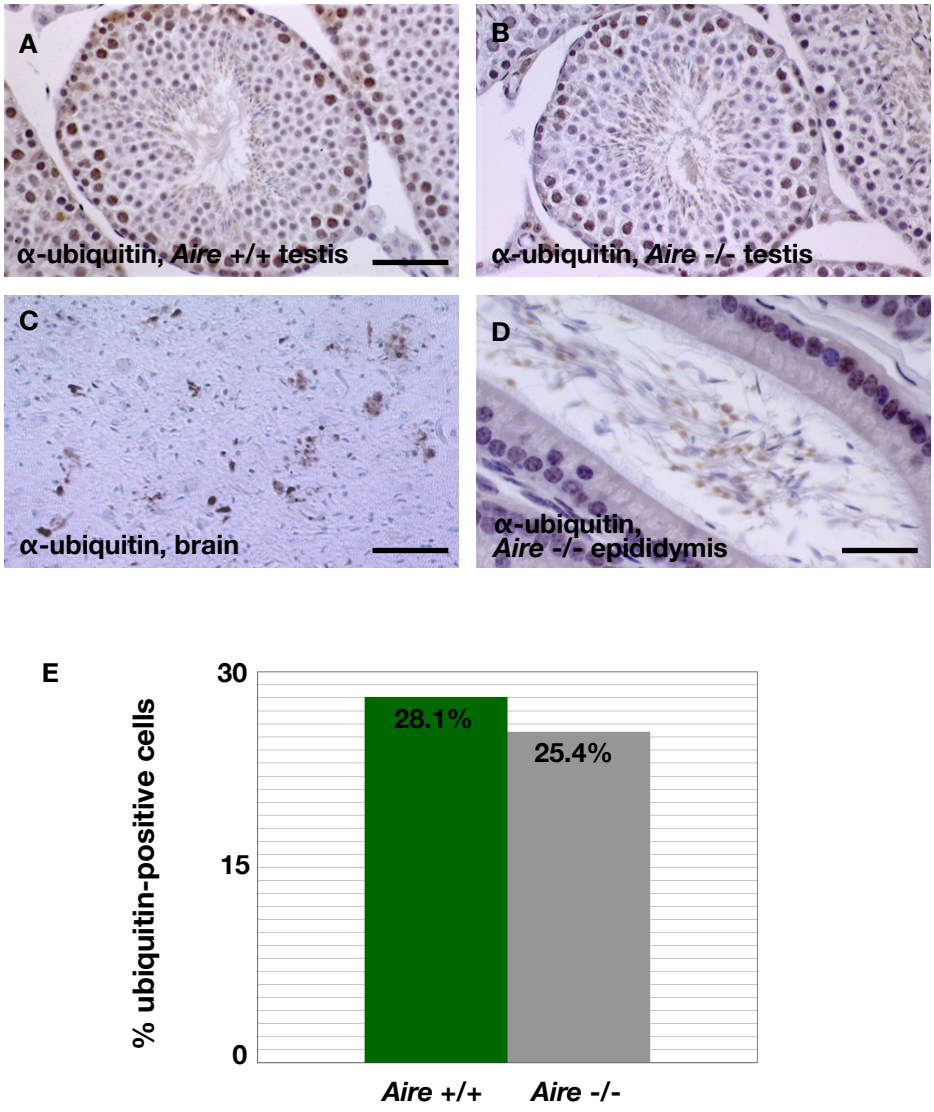

Figure IV.11: Ubiquitin protein detection in testis and epididymis and percentage of ubiquitin-positive germ cells in seminiferous tubules
Paraffin sections of seminiferous tubules of *Aire*-sufficient (A) and *Aire*-deficient (B) testis stained with α-ubiquitin antibody. Ubiquitin-positive cells (brown staining) were detected in germ cell close to the basal lamina. C: positive control showing neurons with staining threads and tangles in the entorhinal cortex of a Alzheimer patient. D: strong ubiquitin staining was as well detectable in the epididymis of *Aire*-deficient (D) mice. The graph (E) shows the arithmetic mean of the percentage of ubiquitin-positive germ cells for *Aire*-sufficient (+/+) and *Aire*-deficient (-/-) testis. Each data set was obtained from three mice and 80 seminiferous tubules each were evaluated. Scale bar in picture A, B and C represents 50 µm, in picture D 40 µm.

5. Fertility assay with *Aire*-deficient mice

Male and female APECED patients suffer from gonadal dysfunction. The testicular failure, which can be heterogenous, is observed in 14% of the patients and leads to reduced fertility or complete infertility (Perheentupa, 2006) (see Introduction 1.2.1.2). In APECED patients, autoantibodies against key enzymes involved in the

hormonal regulation of spermatogenesis, which might be one of the possible reasons for the observed infertility, can be found (see Introduction 2.1.4.1). LA-*Aire*-deficient mice show a substantial drop in fertility as well (Ramsey et al., 2002) (see Introduction 1.2.5). We already found an unusual pattern of apoptosis in 3-week- and 3-months old *Aire*-deficient mice that is independent of the adaptive immune system. Therefore we investigated whether the observed apoptotic pattern translates into abnormal mature spermatozoa in the epididymis. In the epididymis, post-testicular maturation takes place and spermatozoa gain full motility and the potential to fertilize an oocyte (see Introduction 2.1.3).

The testis, epididymis and the epididymial spermatozoa in *Aire*-deficient mice show no anatomic abnormalities (figure IV.12 A and B), but a sperm count with spermatozoa of the whole epididymis (*caput*, *corpus* and *cauda*) of *Aire*-deficient mice showed a significant decline when compared to *Aire*-sufficient littermates (figure IV.13 A, table IV.14). We counted half as many spermatozoa in *Aire*-deficient mice, with a mean of 13.5 x 10^6 spermatozoa in *Aire*-sufficient mice and a mean of 7.7 x 10^6 spermatozoa in *Aire*-deficient mice (p = 0.049). In one *Aire*-deficient mouse we observed values 10 times lower. The data were obtained from five mice each. Two of the *Aire*-deficient males were infertile and had no offspring after mating with young C57BL/6 females for six months. The remaining three *Aire*-deficient males were subfertile and didn't produce as frequent offspring when compared to C57BL/6 mice.

After assessing the morphology and concentration of epididymial spermatozoa, we looked at the quality in terms of motility and compared the number of progressive (motile), twitching and immobile spermatozoa between the two sets of mice (figure IV.13 B, table IV.14). For fertilization, progressive motile spermatozoa are essential and their optimal concentration differs between species. Though we didn't detect a significant difference between *Aire*-sufficient and *Aire*-deficient mice (figure IV.13 B), we found the number of progressing spermatozoa in all *Aire*-deficient mice lowered when compared to their *Aire*-sufficient littermates. The two infertile mice had on average only 5.4% progressing spermatozoa, their *Aire*-sufficient littermates twice and four times as many. Nevertheless, those experiments showed that *Aire*-deficiency mainly affects the quantity and to a lesser degree the quality in terms of motility of epididymial spermatozoa.

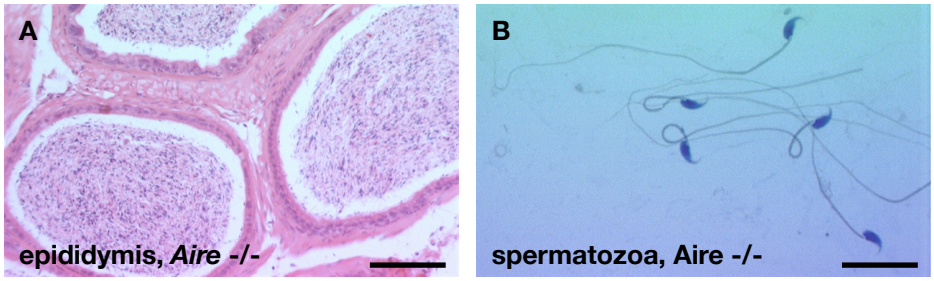

Figure IV.12: Morphology of epididymis and epididymial spermatozoa
A: H&E stain of *Aire*-deficient epididymis with no detectable anatomic abnormality. B: Spermatozoa of *Aire*-deficient mice showing no anatomic abnormalities. Epididymial tissue and spermatozoa were investigated in five *Aire*-sufficient and five *Aire*-deficient littermates. Scale bar in picture A represents 60 µm, in picture B 40 µm.

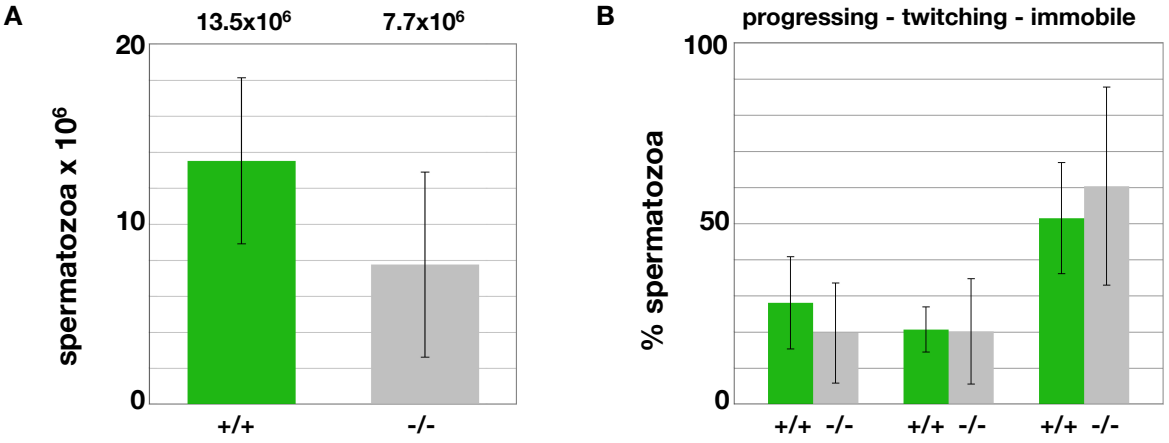

Figure IV.13: Fertility assay evaluating the number and motility of epididymial spermatozoa
Graph A shows the arithmetic mean of the amount of spermatozoa in *Aire*-sufficient and *Aire*-deficient epididymides. Graph B shows the arithmetic mean of the percentage of progressing, twitching and immobile spermatozoa in *Aire*-sufficient and *Aire*-deficient epididymides. All data sets were obtained from five mice each.

Mice	**HD *Aire* +/-**	**HD *Aire* -/- (infertile)**
Sperm count	7 x 10^6	8 x 10^5
Progressing sperm	20.10%	5.35%
Twitching sperm	29.10%	5.35%
Immotile sperm	50.80%	89.30%
Mice	**HD *Aire* +/+**	**HD *Aire* -/- (infertile)**
Sperm count	1.8 x 10^7	1.1 x 10^7
Progressing sperm	11%	5.50%
Twitching sperm	12.50%	4%
Immotile sperm	76.50%	90.50%
Mice	**HD *Aire* +/-**	**HD *Aire* -/- (subfertile)**
Sperm count	1.75 x 10^7	1.4 x 10^7
Progressing sperm	43.50%	37%
Twitching sperm	22.20%	26.60%
Immotile sperm	34.30%	36.40%
Mice	**HD *Aire* +/-**	**HD *Aire* -/- (subfertile)**
Sperm count	1.4 x 10^7	5 x 10^6
Progressing sperm	30%	24%
Twitching sperm	22.10%	28%
Immotile sperm	47.90%	48%
Mice	**HD *Aire* +/-**	**HD *Aire* -/- (subfertile)**
Sperm count	1.1 x 10^7	7.9 x 10^6
Progressing sperm	35.30%	26.30%
Twitching sperm	17.10%	36.50%
Immotile sperm	47.60%	37.20%

Table IV.14: Fertility assay evaluating the number and motility of epididymial spermatozoa
Table shows the exact values for the amount of spermatozoa in *Aire*-sufficient and *Aire*-deficient epididymides as well as of the percentage of progressing, twitching and immobile spermatozoa in *Aire*-sufficient and *Aire*-deficient epididymides.

CHAPTER V: DISCUSSION

1 The early wave of apoptosis in spermatogenesis: establishment of homeostasis between germ cells and Sertoli cells or triggered by a quality checkpoint for genomic health?

In our study we investigated the influence of *Aire*-deficiency and mismatch-repair-deficiency on the early wave of apoptosis during the first round of spermatogenesis and the long range effects on sporadic apoptosis during adulthood. In agreement with previous studies (Rodriguez et al., 1997) we found on average 1.65 % of germ cells apoptotic during the first round of spermatogenesis and around 0.3% during adulthood (see Results 3.1).

The underlying reasons for the prepubertal, scheduled wave of apoptosis were previously unknown. Our results question the proposed hypothesis that a critical ratio between germ cells and the supporting Sertoli cells had to be established in a short time frame, resulting in apoptosis of the 'surplus' germ cells (homeostasis hypothesis) (Rodriguez et al., 1997). Additionally, it had been suggested that mutated DNA, caused eventually by DNA rearrangements during meiosis, triggers the apoptotic wave (checkpoint hypothesis) (Mori et al., 1997; Rodriguez et al., 1997). According to the homeostasis hypothesis, a substantial reduction of apoptosis during prepuberty influences the strict stoichiometry between germ cells and Sertoli cells and might disrupt normal spermatogenesis later in life. Rodriguez et al. (1997) established that a complete disruption of the scheduled apoptotic wave, as observed in transgenic *Bcl2* mice, or mice that overexpress *Bcl-X*$_L$, results in sterility and severely reduced numbers of spermatocytes, spermatids and spermatozoa during adulthood. In our study we showed that mice carrying the morphogene (Nicolaides et al., 2005), a dominant negative mutant transgene of the mismatch-repair protein PMS2, have substantially reduced apoptosis at three weeks of age. The percentage of apoptotic cells dropped by almost half resulting in around 0.92% of apoptotic germ cells versus 1.65% in non-morphogene testis (see Results 3.2). The decline in apoptosis was expected because PMS2 stabilizes the apoptosis activating protein p73 (Shimodaira et at., 2003) and is a direct target of p53 (Chen and Sadowskyt, 2005), thereby contributing to genomic integrity through DNA repair and promoting apoptosis of cells damaged beyond repair. But the substantially reduced wave of apoptosis in 3-week-old morphogene mice had no obvious effect later in life. The morphology and the apoptotic values in 3-month-old morphogene testes are similar to those in wild-type mice (see Results 3.2).

This leads to the conclusion that the scheduled wave of apoptosis during the first round of spermatogenesis in 3-week-old mice seems not to be a developmental necessity to establish a distinct ratio between germ cells and Sertoli cells. Certainly, Sertoli cells are crucial for germ cell development (see Introduction 2.1.4.2) and their ideal supportive capacity is limited to a particular number of germ cells. However, this number might be somewhat flexible, rather than fixed. One important function of Sertoli cells is to transduce hormonal signals to germ cells, since germ cells lack receptors for FSH and testosterone, the two major hormones regulating spermatogenesis (see Introduction 2.1.4.1). Mice with missing receptors on Sertoli cells for both hormones, thereby mimicking Sertoli cell deficiency, show highly reduced germ cell numbers due to failure to progress beyond early meiosis later in life (Abel et al., 2008). On the other hand, a higher number of Sertoli cells, which can be induced by FSH or by perinatal induction of hypothyroidism, increases the spermatogenic output of the testis (de Kretser, 2007). These data suggest that a certain ratio of Sertoli cells and germ cells is needed for optimized spermatogenesis, but that unless the number of Sertoli cells is not significantly diminished, spermatogenesis is not impaired.

Rather than establishing a strict homeostasis between the supporting Sertoli cells and the germ cells, we propose that the scheduled outburst of apoptosis in the prepubertal mouse might be instead a checkpoint for genomic health. As discussed in the introduction, the development of haploid spermatozoa is a complex process. All three major phases, the proliferative, meiotic and haploid, are prone to errors and DNA damage that eventually jeopardize the genomic health of the offspring. So far, several checkpoints are known to be monitoring specific developmental steps. This becomes apparent as many mutations affecting various cellular processes induce spermatogenic arrest and apoptosis at specific developmental stages (de Rooij and de Boer, 2003).

The proliferative phase (see Introduction 2.1.2.2) is particularly important for spermatogenesis: spermatogonial stem cells must replicate themselves error-free or go through multiple mitotic divisions to become type B spermatogonia. The multiple mitotic cell divisions in conjunction with the lifelong continuous spermatogonial stem cell renewal after puberty (de Rooij et al., 1998) generate spontaneous point mutations, leading from two (Bohossian et al., 2000) to six times higher mutational rates in the male than in female germline (Hurst and Ellegren, 1998). This mutation rate highlights the need for mitotic checkpoints during this developmental phase to keep the germline stable. In somatic cells three

mitotic checkpoints are known: the start checkpoint, at which the cell commits to enter the cell cycle, the G_2/M checkpoint that triggers chromosome alignment on the spindle in metaphase, and the spindle assembly checkpoint (SAC) that stimulates sister chromatid separation leading to completion of mitosis. The start as well as the G_2/M checkpoint are able to detect DNA damage and, if not repaired, subsequent higher levels of p53 cause cell cycle arrest and/or apoptosis (Harrison and Haber, 2006). Not much is found in the literature about specific differences in mitotic checkpoints for germ cells when compared to somatic cells. Previous results suggest that similar checkpoints are involved, but the checkpoint proteins differ between somatic and germ cells (Jeganathan and van Deursen, 2006).

The meiotic phase (see Introduction 2.1.2.3) is especially prone to error: in the long prophase of meiosis I, the duplicated homologous chromosomes pair during leptotene and the sister chromatids have to be held together via the cohesin complex. At zygotene, the chromosomes synapse with help of the synaptonemal complex. At pachytene, DNA double-strand breaks occur at several locations in each sister chromatid, resulting in large numbers of DNA recombination events between the homologues. Failure in any of those three processes leads to apoptosis of spermatocytes during pachytene (Yuan et al., 2000; Revenkova et al., 2004; Barchi et al., 2005), though different opinions have been discussed with regard to the existence of one or two different checkpoints for synapsis and unrepaired DNA damage due to failed recombination (Hamer et al., 2008; Li and Schimenti, 2007). After diplotene, in which the synaptonemal complex disassembles and the chromosomal pairs segregate, the cells enter metaphase I. At this time, the sister chromatids attach to the same pole (monopolar attachment), whereas the homologues attach to the opposite spindle pole (bipolar attachment) and segregate apart from each other (reductional segregation) during anaphase I. In contrast, at metaphase of meiosis II, the sister chromatids attach to the opposite poles and then segregate apart from each other (equational segregation) during anaphase II, a process that closely resembles mitosis. These distinct types of chromosome segregation depend on distinct types of spindle attachment of the chromosomes. The spindle assembly checkpoint (SAC), which plays as well an important role during mitosis, seems to control the proper attachment during metaphase I and metaphase II (Yamamoto et al., 2008), though the specific mechanisms might differ in mitosis and meiosis (Jeganathan and van Deursen, 2006).

During the haploid or spermiogenic phase (see Introduction 2.1.2.4) intensive cytoplasmatic and nuclear reorganization takes place. The development of the acrosomal vesicle is accompanied by major morphological changes depending on many genes and controlled by a checkpoint (de Rooij and de Boer, 2003). The existence of checkpoints was confirmed in several knockout mouse models in which virtually all spermatids underwent apoptosis at a specific developmental stage (Kang-Decker et al., 2001; Martianov et al., 2002). Almost in synchrony with the development of the acrosome, the nucleus condenses into transcriptionally inactive DNA. This is due to the replacement of the majority of histones first by transition proteins and then by protamines (Meistrich et al., 2003). Though protamine packed DNA is more resistant to DNA damage, it has been shown that the chromatin of spermatozoa often contains double- or single-strand breaks that may have been induced either by the protamine replacement, by reactive oxygen species (ROS) or by mutagens (Shaman et al., 2006). The presence of DNA strand breaks may often results in apoptosis (Sakkas et al., 2003), suggesting postmeiotic checkpoints during the haploid phase (Clemente et al., 2006). Further possible checkpoints during the proliferative, meiotic and spermiogenic phase can be reviewed by de Rooij and de Baer (2003).

The necessity for checkpoints that monitor the complex and lifelong processes of spermatogenesis and result in eventual apoptosis of non-functional germ cells, is apparent. Still, this doesn't explain why one or several checkpoints during the initial round of spermatogenesis might trigger such an apoptotic wave. The possible explanation might be found in the developmental processes that occur in the pre- and neonatal testis. The foundation of spermatogenesis starts in the mouse at day 7.25 *post coitum* (*pc*) (Ginsburg et al., 1990) with only a few founder cells (primordial germ cells) (Clark and Eddy, 1975). After migration to the genital ridge and differentiation, the cells, now termed gonocytes (McLaren, 2003), undergo a prenatal wave of apoptosis (Wang et al., 1998). The surviving cells undergo two or three rounds of mitosis, and male gonocytes subsequently enter mitotic arrest in the G0/G1 phase of the cell cycle between day 12.5 *pc* and 15.5 *pc*, now referred to as prospermatogonia (McLaren, 2003). After birth, those few prospermatogonia establish the spermatogonial stem cell niche and reinitiate mitosis at day 1.5 *post partum* (*pp*) (Vergouwen et al., 1991). During this neonatal phase, the number of prospermatogonia increases dramatically (Shinohara et al., 2000). Until puberty several doublings occur resulting in 2-3 x 10^4 spermatogonial

stem cells which are the source for life-long and continuous spermatogenesis (Tegelenbosch and de Rooij, 1993).

Besides the extensive cell proliferation in the spermatogonial stem cell pool, another important process, epigenetic reprogramming, takes places during the pre- and neonatal development of the testis. Epigenetic reprogramming regulates via DNA modifications like methylation, tissue-specific gene expression, imprinting of genes and silencing of transposable elements (Goll and Bestor, 2005). Upon fertilization and at the blastocyst stage, the male genome is actively and passively demethylated (Santos et al., 2002), whereas parentally methylated imprinted genes are excluded (Lane et al., 2003; Morgan et al., 2005). With the differentiation of the first two cell lineages - the inner cell mass and the trophectoderm, *de novo* methylation occurs (Santos et al., 2002). At gametogenesis another round of reprogramming happens. The genome in the gonocytes is extensively demethylated between day 11.5 and 12.5 *pc*, including imprinted genes (Yamazaki et al., 2003). This wave of demethylation controls the expression of several genes required for gametogenesis by abolishing the silencing effect of methylation (Maatouk et al., 2006). *De novo* methylation in the male germline starts day 15.5 *pc* in the entire cohort of mitotically quiescent prospermatogonia, thereby silencing and imprinting parts of the genome (Bourc'his and Viegas-Pequignot, 2001; Trasler, 2006). Methylation is completed by day 17.5 *pc* in repetitive elements (Lees-Murdock and Walsh, 2003), but is only finished after birth at differentially methylated regions (DMRs) of imprinted loci (Li et al., 2004). Failure can contribute to male infertility and other conditions including cancer, neurological and immunological disorders and aging (Rodenhiser and Mann, 2006; Egger et al., 2004). Not only is epigenetic reprogramming a complex process with several cycles of methylation and demethylation, *de novo* methylation of CpG sites also has a high potential of inducing mutations. 5-methylcytosine often spontaneously deaminates to thymine, giving rise to C to T transition mutations (Bestor and Coxon, 1993). Furthermore, spermatogonia must maintain the methylation patterns for a large number of mitotic divisions prior to meiosis which increases the load of C to T mutations (Schaefer et al., 2007).

The intense proliferation of prospermatogonia together with epigenetic reprogramming during the pre- and postnatal period might require additional surveillance. The prepubertal round of spermatogenesis might be an initial test run with specific screening checkpoints of the developing germ cells for mutations and epigenetic defects. Affected spermatogonial stem cells and their descents undergo

apoptosis, thereby establishing a more pristine pool which builds the foundation for lifelong spermatogenesis. In addition, the above mentioned meiotic checkpoints might control the germ cells “meiotic competence”. Cells with meiotic errors or protein defects in the meiotic machinery are subject to apoptosis as well, which can explain why our study found germ cells in 3-week-old mice from late pachytene stages onward mostly affected (see Results 3.1). Noteworthy in this context is that p53 is present in large amounts in pachytene spermatocytes of prepubertal testis, whereas its level decreases dramatically in adult germ cells (Rodriguez et al., 1997).

Taken together, we favor that the prepubertal outburst of apoptosis is not a way to establish homeostasis between germ cells and Sertoli cells, but is triggered by a checkpoint for genomic health. The two hypotheses are not mutually exclusive, but the second hypothesis provides a potential connection to the sporadic apoptosis that occurs during adulthood. Our study found a substantial reduction of apoptosis in 3-week-old *Aire*-deficient mice (see Results 3.1). Compared to *Aire*-sufficient littermates around 25% less germ cells apoptose during the early wave of spermatogenesis. This effect translates into a significant increase in apoptosis later in life. In adult, 3-month-old *Aire*-deficient testis we found on average 0.58% of germ cells apoptotic, almost twice as many as in *Aire*-sufficient littermates. The general underlying cause of adult sporadic apoptosis in not well understood, but mostly spermatogonia undergo apoptosis during the latter part of the proliferative phase, suggesting a checkpoint at this developmental stage (Eddy, 2002). We propose that the in our study observed long-range effect of increased apoptosis in *Aire*-deficient mice might be caused by an ineffective prepubertal checkpoint. Spermatogonial stem cells with mutations and/or epigenetic defects can survive the prepubertal surveillance and give rise to spermatogonia and spermatocytes which apoptose at a higher rate, as seen in our experiments, during adulthood as a consequence of deleterious mutations. Germ cells that can’t apoptose, as seen in the morphogene mouse, would carry a higher mutational load.

Aire-deficiency clearly seems to have an influence on the early wave of apoptosis during the first round of spermatogenesis which correlates with increased apoptotic values later in life. Its specific role in spermatogenesis though is unclear. The next sections discuss how AIRE, based on its structure and features, could potentially influence spermatogenesis and cause the above discussed effects on apoptosis in the testis.

2. Potential role of AIRE during spermatogenesis

2.1 AIRE as transcriptional activator for gene expression

AIRE's role in the immune system is well established. In the thymus, AIRE is found in medullary thymic epithelial cells (mTECs), promoting the transcription of around 1500 (Derbinski et al., 2005) peripheral tissue antigen (PTA)-encoding genes (Anderson et al., 2002; Liston et al., 2003; Anderson et al., 2005; Kont et al., 2008), which represent nearly all organs in the body (Derbinski et al., 2001) (see Introduction 1.2.4). In our study we tested whether some of these genes controlled by AIRE in the thymus are also under AIRE control in the testis, another location with promiscuous gene expression (Chalmel et al., 2007). But the results showed that the subset of genes we examined are under different transcriptional regulation in the two tissues (see Results 2.). Recent results found AIRE to be responsible for transcription of PTA-encoding genes in peripheral lymphoid organs, where extrathymic *Aire*-producing cells (eTACs) were detected (Gardner et al., 2008). Around 150 genes were shown to be under AIRE control, representing a complementary pool of self-antigens. Hence, AIRE might be in charge in controlling the transcription of a different subset of genes in the testis than in the thymus. Furthermore, as in the thymus, where not all PTA-encoding genes are dependent on AIRE, also the transcripts found in the testis are most likely transcribed by many different factors. The fact that male germ cells express a diverse group of transcription factors (Eddy, 2002), supports this hypothesis.

The answer to the question of how AIRE promotes the expression of PTA-genes is still unclear. AIRE, based on its domains (see Introduction 1.2.3) is a multifunctional protein. Its core domains, the CARD, SAND and two PHD zinc fingers, suggest a function as a transcriptional activator and therefore regulator of gene expression. PHD zinc fingers are known to interact with histones (Mellor, 2006), the structural core units of chromatin. Recently, AIRE has been shown to interact with chromatin *in vivo*. Its first PhD zinc finger binds to the aminoterminal tail of unmethylated histone H3K4 (H3K4me0), a recognition code for silenced genes (Koh et al., 2008; Org et al., 2008), suggesting a role for AIRE as an epigenetic regulator. In mTECS, the PTA-encoding genes are usually not highly expressed and therefore unmethylated or monomethylated at H3K4 (Org et al., 2006). By binding to H3K4me0 and the DNA-dependent protein kinase (DNA-PK) complex, AIRE could function as an transcriptional activator, possibly via the activation of RNA polymerase II, and initiate gene expression. The binding properties of AIRE's first PHD zinc finger to H3K4me0 are very similar in DNMT3L (DNA (cytosine-5)

methyltransferase 3-like), an important epigenetic regulator in germ cells (Koh et al., 2007). As a neighboring gene of *Aire*, the potential influence of the *Aire*-knockout mouse models on *Dnmt3l*'s function will be discussed in the last section of this chapter.

In the testis, a similar mechanism of transcriptional regulation might be possible. The previous section discussed the necessity for a prepubertal checkpoint in spermatogonial stem cells and their descendants. By scanning the genome for mutations or epigenetic defects resulting from pre- and postnatal development, germ cells damaged beyond repair would die, resulting in the prepubertal wave of apoptosis during the first round of spermatogenesis. The prepubertal quality checkpoint and the expression of numerous genes might be closely connected. In general, testis development and spermatogenesis require well-ordered and sequential changes in gene expression. Microarray studies revealed almost 10,000 transcripts expressed differentially in a significant manner (Shima et al., 2004). The role these transcripts play is unclear and many genes from which these transcripts originate are undefined (Schulz et al., 2008). Gene cluster analysis found several distinct expression patterns within a time course of testis development (Shima et al., 2004): a major increase in expression occurs the first few days after birth and around day 10 *post partum* (*pp*). The most significant change can be observed in two gene clusters starting day 14 to day 30 *pp*, when numerous transcripts are about to get expressed (Shima et al., 2004). Interestingly, many of those transcripts starting to be expressed around day 14 *pp* are spermatid specific transcripts, though at this time, only spermatocytes can be observed in the testis. The expression of those numerous transcripts in the testis during the prepubertal period might be supported by AIRE. In our studies we detected a high amount of AIRE protein in 3-week-old *Aire*-sufficient testis, where 0.44% of the germs cells were AIRE positive (see Results 1.2). In comparison, in 3-month-old mice 0.15% of germs cells stained positive for AIRE. This equals a 10- to 35-fold lower abundance of AIRE compared with that of β-actin per cell. Similar as in mTECs, AIRE could bind to unmethylated histone H3K4 of silenced genes, opening the chromatin structure, permitting further activators to operate. The observed gene clustering of PTA-encoding genes (Johnnidis et al., 2005) and germ cell specific genes supports this mechanism (Shima et al., 2004). Assuming AIRE contributes to the numerous expression of transcripts during prepuberty, this still doesn't answer if the AIRE-dependent expression is part of a prepubertal checkpoint for genomic health. The early expression of spermatid specific transcripts might be an indicator

that genes are tested before finally translated into a functional protein at a later developmental stage. Our observation that *Aire*-deficiency alters the apoptotic rates in germ cells during prepuberty and adulthood, might be another sign (see Results 3.1). In *Aire*-sufficient 3-week-old mice on average 1.63% of all germ cells apoptose, in *Aire*-deficient mice this value substantially drops to 1.23%, which represents a 25% reduction. But later in life, *Aire*-deficiency is accompanied with an increase in apoptosis. *Aire*-sufficient 3-month-old mice show on average 0.31% apoptotic germ cells, whereas in *Aire*-deficient mice twice as many germ cells die. In general, germ cell apoptosis can be driven by different mechanisms and can be caspase-dependent or -independent (Lockshin and Zakeri, 2004). The scheduled wave of apoptosis during prepuberty and the sporadic apoptosis throughout lifetime seem to have different underlying causes and apoptotic pathways. This can be seen in transgenic mice expressing *Bcl2*, which is usually not significantly expressed in testis, or overexpressing *Bcl-X*$_L$, both anti-apoptotic proteins. The two mouse models don't undergo the prepubertal wave of apoptosis and are sterile when mature (Rodriguez et al., 1997; Russell et al., 2001). Though the number of spermatocytes, spermatids and spermatozoa is severely decreased, spermatogonia are unaffected and have normal sporadic apoptosis (Rodriguez et al., 1997). The reasons causing sporadic apoptosis throughout adulthood are not known. As mentioned earlier, our results suggest a hypothesis in which the adult sporadic apoptosis and the prepubertal scheduled wave of apoptosis are linked due to a prepubertal checkpoint for genomic health. And AIRE, based on its protein structure and its function in the immune system, could potentially contribute to this process. During the prepubertal phase of intense gene expression, AIRE is highly abundant and might function as a transcriptional activator for different subsets of clustered genes. The promiscuous gene expression of silenced meiosis- and/or spermatid-specific or other spermatogenesis related genes permits screening for mutations during a prepubertal checkpoint. The mutations might have been introduced during the critical phase of neonatal spermatogonial stem cell proliferation or during pre- and neonatal epigenetic reprogramming. Affected spermatogonia and their descendants apoptose, explaining why we found almost four times more apoptotic spermatocytes and spermatids than spermatogonia in 3-week-old testis (see Results 3.1). The apoptosis itself might be a consequence of the unfolded protein response, activated by the translation of mutated transcripts. In case of *Aire*-deficiency, promiscuous gene expression of certain genes and therefore counterselection of germ cells with mutant genes might not take place, as

observed in the testis of 3-week-old mice which show far less apoptosis. Though our results mostly found a reduction in spermatocytes, spermatogonia and spermatids also died at a lower rate. As a consequence, in 3-month-old *Aire*-deficient testis, spermatogonia with mutations were not counterselected during prepuberty and had passed on their mutations to spermatocytes and spermatids, resulting in twice as much apoptosis in 3-month-old *Aire*-deficient mice when compared to *Aire*-sufficient littermates. Also, all three major germ cell types apoptose in 3-month-old *Aire*-deficient mice at a higher rate, as seen in our results. The regular, sporadic apoptosis in *Aire*-sufficient mice might be caused by other quality checkpoints that monitor mutations throughout adulthood. However, AIRE's involvement in apoptosis in adult mice remains questionable.

Interestingly both, the reduction in apoptosis in 3-week-old mice and the increase in 3-month-old mice were highly reproducible (see Results 3.1). The data sets were obtained from five mice each and for each group the standard deviation proofed a low variability. Even when we used mice with different genetic backgrounds, as the HD-*Aire* and LA-*Aire*-knockout strains, we observed comparable apoptotic values. The gene dosage effect described by Liston et al (2004) was not noticeable and the for our apoptotic evaluation used heterozygous and homozygous testes didn't show different values. Furthermore, the increase and reduction were also seen in HD-*Aire*-sufficient and HD-*Aire*-deficient mice on a *Rag-1* -/- background (see Results 3.1). By using mice with *Rag-1*-deficiency, we excluded the genetic involvement of the adaptive immune system. In healthy mice, intratubular lymphocytes are rare (Naito and Itoh, 2008), because the blood-testis barrier (see Introduction 2.1.1.2) shelters parts of the seminiferous tubules from the immune system, creating in immunologically privileged site. However, under certain pathological conditions (Naito and Itoh, 2008), lymphocytes are able to penetrate the blood-testis barrier. Also, in young mice, the blood-testis barrier only begins to close around day 12 *post partum*, at the time when the first wave of spermatogenesis is about to start (de Kretser et al., 1998). *Rag-1*-deficiency causes combined B cell and T cell deficiency and assures that in *Aire*-knockout mice, which show lymphocyte infiltration in several organs (see Introduction 1.2.5), apoptosis in the testis is not induced by penetrating lymphocytes. This might be possible because invading, FAS ligand-bearing lymphocytes are able to induce cell death in Fas-presenting spermatogonia and spermatocytes (Lee et al., 1997).

Taken together, AIRE, based on its protein structure and function in the thymus, might act as a transcriptional activator in the testis. The promiscuous gene

expression, AIRE-dependent or not, might be an essential part of a prepubertal checkpoint for quality control of germ cells to assure functional lifelong spermatogenesis and genomic health.

2.2 AIRE as E3 ubiquitin ligase

Based on its protein domains, AIRE appears to be a multifunctional protein (see Introduction 1.2.3 and 1.2.6). Besides its proposed function as a transcriptional regulator, it has been shown that AIRE's first PHD zinc finger has E3 ubiquitin ligase activity (Uchida et al., 2004). Though this has not been confirmed (Bottomley et al., 2005), we quantified in our study the amount of ubiquitin protein in testis sections of *Aire*-deficient and *Aire*-sufficient mice (see Results 4.). In both, ubiquitin is highly abundant in more than one fourth of the germ cells, but no significant difference in the percentage of ubiquitin-positive germ cells between *Aire*-deficient and *Aire*-sufficient mice was evident. Our data are preliminary and require more research, but AIRE's potential function in the ubiquitin pathway will still be discussed in this section.

The ubiquitin-proteasome pathway plays an essential role in cell cycle progression, signal transduction, cell differentiation, DNA repair and apoptosis (Pickart, 2001). In the ATP-dependent pathway, ubiquitin, which is conserved in evolution, is activated by ubiquitin-activating-enzyme E1 and transferred to an ubiquitin-carrier-protein E2. This complex is attached to the target protein, a step catalyzed by a variety of substrate-specific E3 ubiquitin ligases. Polyubiquitination leads to degradation of the targeted protein into peptides by the 26S proteasome. The ubiquitin pathway and the unfolded-protein response (UPR) are closely connected: an improper folding of newly translated proteins in the endoplasmatic reticulum activates the UPR. Translocation of the misfolded protein back to the cytosol results in ubiquitination and degradation by the proteasome. If the accumulation of the misfolded proteins causes to much cell stress, the cell dies of apoptosis (Kaufman, 2002).

The ubiquitin system and the proteasomal subunits are present at all stages in the male germline (Wojcik et al., 2000). During the spermiogenic phase of spermatogenesis the ubiquitin system seems to be particularly important and removal of ubiquitin enzymes at this stage results in male infertility (Baarends et al., 2003; Kwon et al., 2003). Gad mice which lack *Uchl-1* (ubiquitin C-terminal hydrolase L-1), a molecule controlling the cellular ubiquitin balance by releasing

conjugated ubiquitin from unfolded proteins (Wing, 2003), show significantly lower apoptotic values in prepubertal testis and lower sperm counts and defective spermatozoa during adulthood (Kwon et al., 2005).

Potentially, AIRE's function as a transcriptional activator and E3 ubiquitin ligase can coexist (Villasenor et al., 2005). After activation of the expression of promiscuous genes, translated and due to mutations misfolded proteins would be tagged by ubiquitin, a step catalyzed by AIRE, and degraded. In case of to much cell stress, the germ cells die by apoptosis during the prepubertal checkpoint. However, a potential function for AIRE as E3 ubiquitin ligase attaching ubiquitin to misfolded proteins might be detectable as higher levels of free monoubiquitin in germ cells of *Aire*-deficient mice. But our experiments didn't detect a difference in ubiquitin levels between *Aire*-sufficient and *Aire*-deficient testis (see Results 4.). Also, a direct involvement of AIRE in marking cells with deleterious mutations can not explain the decline in apoptosis as seen in our results in 3-week-old *Aire*-deficient testis (see Results 3.1). Misfolded proteins, if not tagged by ubiquitin and degraded, would accumulate and induce more apoptosis in comparison with *Aire*-sufficient mice. But instead of marking misfolded proteins, AIRE could catalyze the tagging of members of the BCL2 family and caspases which have been shown to be direct targets for ubiquitination (Yang and Yu, 2003), suggesting a regulation of apoptosis by ubiquitination in the testis (Kwon et al., 2007). The balance of pro- and anti-apoptotic proteins regulated by ubiquitination has been shown to be important for the scheduled prepubertal wave of apoptosis as well as for sporadic apoptosis during adulthood (Kwon et al., 2007; Wright et al., 2007).

However, AIRE's ubiquitin ligase activity could play a more indirect role at the level of transcriptional regulation. A correlation between ubiquitination and transcriptional regulation of transcription factors or other nuclear factors is well established (Conaway et al., 2002), and this can lead either to proteasomal degradation or indirect enhancement of those factors (Mathis and Benoist, 2007). Thus there may be a variety of pathways by which AIRE could influence not only the promiscuous gene expression in thymus and testis, but also functionality of the prepubertal checkpoint and apoptosis *per se*. The production of checkpoint proteins could be dependent on the degradation of transcriptional inhibitors, similar to the inhibitor of NFκB (IκB) whose ubiquitination and degradation allows NFκB to enter the nucleus (Palombella et al., 1994). A nonfunctional prepubertal checkpoint results in reduction of apoptosis in germ cells of 3-week-old *Aire*-

deficient mice, but ultimately increases apoptosis during adulthood, as seen in our experiments.

2.3. AIRE and a direct involvement in apoptosis?

The recent finding that AIRE's homogeneously staining region (HSR) corresponds to a caspase recruitment domain (CARD) (see Introduction 1.2.3) suggests a direct involvement of AIRE in apoptosis. The CARD in AIRE is similar to that of the apoptosis-procaspase-activating-factor-1 (APAF-1), a molecule involved in the intrinsic apoptotic pathway that depends on the release of cytochrome c into the cytosol and is regulated by the BCL2 protein family. APAF-1 molecules oligomerize into an apoptosome, and each of the APAF-1 molecules binds to procaspase 9 molecules, which are activated by their proximity to each other and further activate downstream caspases to induce apoptosis (Newmeyer and Ferguson-Miller, 2003). CARD only interact with other CARD which thins the field of potential interaction partners for AIRE. Like APAF-1, AIRE's CARD therefore might be involved in the oligomerization of AIRE proteins and the formation of protein complexes that function in inflammation and apoptosis (Park et al., 2007).

In the thymus, AIRE seems to be directly involved in inducing apoptosis. AIRE-positive mTECs are short lived cells and survive only for a few days before dying by apoptosis. Also, *Aire* transfection of a thymic epithelial cell line results in apoptosis after a short time (Gray et al., 2007). It is proposed that the death of mTECs and therefore the high turnover rate of those cells helps to maximize the presentation of peripheral tissue-restricted antigens to T cells (Ferguson et al., 2008).

We can only speculate whether AIRE's cytotoxicity plays a role during spermatogenesis. In 3-week-old testis we detected AIRE protein in around 0.44% of germ cells (see Results 1.2). No germ cell stage in which all cells are AIRE-positive was identified, suggesting a sporadic presence for the protein. At the same time, almost four times more germ cells, around 1.65%, die by apoptosis (see Results 3.1). If AIRE is, as proposed in the previous sections, involved in the promiscuous gene expression in the testis as part of a checkpoint for mutations and epigenetic errors, the immediate death of AIRE-positive germ cells would be counterproductive by affecting healthy germ cells as well. Still, a mechanism, in which AIRE, regardless of whether it might be responsible for the promiscuous gene expression, only accumulates in germ cells with mutations, might be feasible.

Consequentially, the CARDs could oligomerize several AIRE proteins and the formation of protein complexes would trigger apoptosis. As shown in our study, *Aire*-deficiency results in a substantial drop in apoptosis in 3-week-old mice, but still around 1.2% of germ cells die. This could be due to a different apoptotic mechanism. In 3-month-old mice around 0.15% of germ cells are AIRE-positive and twice as many germ cells die. The pathways and reasons for sporadic apoptosis in adult mice and scheduled apoptosis in prepubertal mice seem to differ, but AIRE still could be directly involved in the apoptosis of certain germ cells that had accumulated mutations during their development. On the other hand, the increased levels of apoptosis in *Aire*-deficient adult mice might be caused by a different apoptotic pathway; one that induces germ cells to die if they have mutations which haven't been deleted during puberty due to a nonfunctional checkpoint.

3. Subfertility in *Aire*-deficient mice

Aire-deficiency is accompanied by reduced fertility (subfertility). In humans, male and female APECED patients suffer from gonadal dysfunction and therefore reduced fertility (Perheentupa, 2006) (see Introduction 1.2.1.2). In HD- and LA-*Aire*-deficient mice, we observed a significant drop in fertility, as well. In our study we evaluated morphology, concentration and motility of epididymial spermatozoa in five *Aire*-deficient and *Aire*-sufficient mice (see Results 5.). Though those traditional parameters provide only limited information, they are still widely used as a first line tool in the assessment of male fertility (deJonge and Barratt, 2006). The morphology of spermatozoa seemed to be unaffected by *Aire*-deficiency. Overall, no significant difference in the number of progressive spermatozoa was detectable, but two of the five *Aire*-deficient mice were infertile and showed severely diminished numbers of progressive spermatozoa in comparison to their *Aire*-sufficient littermates. Most strikingly, the concentration of spermatozoa in all five *Aire*-deficient mice was reduced on average by almost half compared to their *Aire*-sufficient littermates.

The decline in fertility and spermatozoa concentration might have several causes. As discussed in the previous sections, AIRE, based on its structure and function in the immune system, might be involved in the promiscuous gene expression in the testis. This may permit screening of certain genes for mutations or epigenetic errors during a prepubertal checkpoint. Consequently, *Aire*-deficiency might cause a reduction in apoptosis in germ cells of 3-week-old mice but higher rates in 3-month-

old germ cells, which eventually die more frequently as a result of accumulated mutations. The higher apoptotic rates in adult testis might directly influence the amount of epididymial spermatozoa. The epididymis is a location not only for storage and post-testicular maturation, but also for sperm quality control (Baska et al., 2008) (see Introduction 2.1.3). Our study only focused on apoptosis in the testis and we didn't consider an additional sperm quality checkpoint in the epididymis, but it is possible that defective spermatozoa in the epididymis, which are a result of the non-functional prepubertal checkpoint, are eliminated. This and the higher apoptotic values in the testis might be responsible for the low sperm counts observed in *Aire*-deficient mice.

But if the higher mutational load doesn't trigger apoptosis in the testis or nonfunctional spermatozoa ubiquitination in the epididymis, affected spermatozoa would survive and might be less competent to fertilize an oocyte. In sub- or infertile men, it has been shown that spermatozoa often carry chromosomal and/or genetic abnormalities (deJonge and Barratt, 2006). Also, several structural and functional abnormalities have been observed including an abnormal capacity to achieve capacitation, inability to bind to the *zona pellucida* and/or undergo acrosomal exocytosis (deJonge and Barratt, 2006). Knockout mouse models revealed numerous autosomal and X- or Y-chromosomal genes that - if affected - cause infertility (Cooke and Saunders, 2002; Matzuk and Lamb 2008). Besides mutations, epigenetic errors leading to defective methylation are as well connected with subfertility (Ludwig et al., 2005). The hypomethylation of certain imprinted genes seems to influence the quantity of spermatozoa, since many affected men show moderate to severe oligospermia (Marques et al., 2004). Abnormal genomic imprinting and other epigenetic errors might be linked to a lower activity of DNMT3L (DNA (cytosine-5) methyltransferase 3-like), which will be discussed in more detail in the next section.

In APECED patients, the gonadal dysfunction and reduced fertility might have an additional cause. Autoantibodies against proteins of the pituitary gland are a common diagnosis. The pituitary gland plays an important role in spermiogenesis by releasing the hormones FSH and LH, which act on Sertoli cells and Leydig cells, respectively (see Introduction 2.1.4.1). Furthermore, in many patients, autoantibodies against 17-α-hydroxylase (P450c17), 21-hydroxylase (P450c21) and side-chain cleaving enzyme (P450scc) have been detected, all of which are involved in steroid synthesis (see Introduction 1.2.1.2). P450scc and P450c17 play important roles in the conversion of cholesterol to testosterone. During the meiotic

phase, testosterone acts as a survival factor and inhibits apoptosis; during the spermiogenic phase, testosterone controls the detachment of spermatids from Sertoli cells (Erkkila et al., 1997; de Kretser, 2007). Lower testosterone levels therefore increase apoptosis and lower the number of spermatids. Both might contribute to lower sperm numbers resulting in subfertility (de Kretser, 2007). The tudor-domain-containing-protein 6 (TDRD6) has been recently identified as a major autoantigen in APECED patients (Bensing et al., 2007). In testis of 3-week-old mice, *Tdrd6* mRNA is highly abundant and a knockout mouse model revealed a block in spermiogenesis, resulting in twice as much apoptosis in *Tdrd6*-deficient mice and subsequent sterility (Vasileva et al., 2009). The function of TDRD6 is still elusive, but in humans a connection between AIRE and TDRD6 might help explain the observed infertility in APECED patients. However, in *Aire*-deficient mice, a different set of autoantigens exist, and autoantibodies against P450c17, P450c21 and P450scc have not been detected (see Introduction 1.2.5). No research yet investigated TDRD6 autoantibodies in *Aire*-deficient mice, but a potential link between the two proteins might reveal information on AIRE's influence on spermatogenesis and apoptosis.

4. *Aire* and *Dnmt3l*

In the last sections we discussed how AIRE potentially could play a role during spermatogenesis and how its deficiency influences the apoptotic pattern. Here we discuss whether the design of the HD- and LA-*Aire*-knockout strains has an influence on the function of the DNMT3L (DNA (cytosine-5) methyltransferase 3-like) gene, causing the effects observed in our results.

In the mouse, the *Aire* locus is tightly linked and partially overlaps with the *Dnmt3l* gene (see Introduction 1.2.2). *Dnmt3l* consists of 13 exons, spanning around 13 kb, and is positioned downstream of *Aire*, but transcribed in the opposite direction from telomere to centromere (Aapola et al., 2000; Deplus et al., 2002; Shovlin et al., 2007). In mouse testis, different transcripts from different promoters can be found (Shovlin et al., 2007). In pre- and neonatal prospermatogonia, as well as in embryonic stem cells, a transcript encoding the full-length version with all 13 exons of *Dnmt3l* exists. The promoter driving this expression is only 5 kb from the *Aire* promoter. Transcription is highest until day 17.5 *pc* and declines as prospermatogonia mature and ceases as the germ cells progress through the proliferative and meiotic phase (Bourc'his and Bestor, 2004; La Salle et al., 2004). From pachytene stage onward, an alternative promoter located in intron 9 of the

Dnmt3l gene is activated. This promoter produces three short transcripts in spermatocytes and spermatids, all of which lack significant open reading frames and are unlikely to produce functional proteins. The adult *Dnmt3l* testis transcripts are highly conserved between humans an mice, which suggests that these non-coding transcripts have important functions (Kleene, 2001). In mouse oocytes, a third promoter is active. Located upstream in the beginning of exon 1b and only used in the female germline, it is located between exon 3 and 4 of the *Aire* gene. As in prospermatogonia, this transcript produces a full-length protein containing all conserved motifs.

The DNMT3L protein belongs to the family of DNA (cytosine-5) methyltransferases (DNMTs). This conserved family of proteins plays an important role during spermatogenesis by mediating cytosine methylation via transfer of a methyl group to the 5-positioned carbon of a cytosine within a CpG dinucleotide (Nakao, 2001; Aapola et al., 2004). DNA methylation is important for various processes: methylation of CpG sites within promoter sequences of genes almost invariably silences transcription (Iguchi-Ariga and Schaffner, 1989). In addition to transcriptional control, most transposable elements, which comprise 37% of the mouse genome (Deininger et al., 2003), have to be - if not irreversibly deactivated - maintained in a predominantly methylated state. Their movement in the genome can cause gene activation or inactivation, chromosome breakage, improper recombination and genome rearrangement with possible mutagenic outcome (Yoder et al., 1997; Deininger et al., 2003). Also, their movement leads to DNA double-strand breaks which eventually trigger apoptosis (Haoudi et al., 2004). Furthermore, cytosine methylation at differentially methylated regions (DMRs) is required for the mono-allelic expression of imprinted genes. Paternally imprinted genes are methylated and silenced in male germ cells causing expression from the maternal gene locus. Failure to establish or maintain the methylation pattern at certain imprinted loci is responsible for a number of human disorders (Paulsen and Ferguson-Smith, 2001). So far only three paternally imprinted regions, *h19-Igf2*, *Rasgrf* and *Dlk-Gtl2*, have been identified and most imprinted genes undergo *de novo* methylation in oogenesis (Reik and Walter, 2001). X chromosome inactivation, in which transcription of genes on one of the two X chromosomes in females is silenced as a mean of dosage compensation, also depends on cytosine methylation (Panning and Jaenisch, 1998).
Besides DNMT3L, other DNMT family members have been found. All of them have important functions during development: DNMT1 is considered to be the major

methyltransferase (Bestor et al., 1988) and functions in maintaining existing methylation patterns (Stein et al., 1982). Deficiency causes genome wide demethylation, biallelic expression of imprinted genes (Li et al., 1993), ectopic X chromosome inactivation (Panning and Jaenisch, 1996), reactivation of normally silent IAP sequences (Walsh et al., 1998) and increased levels of apoptosis resulting in developmental arrest at day 8.5 *pc*. DNMT2 is the most conserved and widely distributed of the cytosine methyltransferases. Knockout mice appear normal and the specific function of DNMT2 is so far unknown (Yoder and Bestor, 1998). DNMT3A and DNMT3B are two *de novo* methyltransferases and both are highly abundant in embryonic stem cells, early embryos and developing germ cells (Okano et al., 1999). *Dnmt3a*-deficient mice die around four weeks of age and show defects in spermatogenesis (Okano et al., 1999). Germ-cell specific inactivation effects imprinting and disrupting of spermatogenesis (Kaneda et al., 2004). *Dnmt3b*-deficiency causes embryonic lethality (Okano et al., 1999), but germ-cell specific inactivation does not affect spermatogenesis (Kaneda et al., 2004). In humans, mutations in *DNMT3B* cause the ICF syndrome characterized by immunodeficiency, centromere instability and facial anomalies (Hansen et al., 1999). Both proteins, DNMT3A and DNMT3B, interact with DNMT3L (Chedin et al., 2002; Gowher et al., 2005; Suetake et al., 2006). All show strong homology, but DNMT3L lacks crucial catalytic motifs which are responsible for its catalytic inactivity (Aapola et al., 2000). DNMT3L is the only methyltransferase specifically found in germ cells (Aapola et al., 2000) where it regulates the activity of other methyltransferases (Gowher et al., 2005; Suetake et al., 2006) and induces *de novo* methylation by activation or recruitment of DNMT3A2 (Suetake et al., 2006; Ooi et al., 2007), a germ cell specific isoform of DNMT3A (Hata et al., 2002). DNMT3L-mediated methylation is needed for meiotic cells to progress through spermatogenesis (Zamudio et al. 2008). If knocked out, male and female mice are viable, but infertile (Bourc'his and Bestor, 2004). After birth, the testes appear histologically normal but show lower germ cell count (LaSalle et al., 2007). In young adult mice, only spermatogonia and leptotene and zygotene spermatocytes exist and adult mice are completely azoospermic (Hata et al., 2002; Webster et al., 2005). The *Dnmt3l*-deficient leptotene and zygotene spermatocytes show 'meiotic catastrophe' with failure to form synaptonemal complexes leaving nearly all chromosomal regions unpaired or engaged in non-homologous synapsis (Bourc'his and Bestor, 2004). As a consequence, the germ cells die by apoptosis at the pachytene stage (Webster et al., 2005). The observed meiotic catastrophe is most likely caused by failure to methylate retrotransposons, DMRs of imprinted

genes and other genomic sequences. Several retrotransposons are unmethylated in *Dnmt3l*-deficient mice (Bourc'his and Bestor, 2004), causing possibly activation or inactivation of nearby genes (Gwynn et al., 1998). Paternally imprinted genes, like *h19* loose DNA methylation (LaSalle et al., 2007) and interspersed repeats are hypomethylated (Webster et al., 2005). Furthermore, *Dnmt3l*-deficient testes show downregulation of various gonad-specific and/or sex chromosome linked genes, suggesting a role in germ cell specific gene expression via methylation (Hata et al., 2006). This all might lead to changes in gene expression, unwanted interactions between dispersed repeated sequences and single- or double-strand breaks produced during replicative retroposition, resulting in 'meiotic catastrophe' and apoptosis in *Dnmt3l*-deficient testis (Bourc'his and Bestor, 2004).

The design of the two *Aire*-knockout mouse models (see Introduction 1.2.5) used in our experiments might influence the function of the *Dnmt3l* gene. Although in the male HD- and LA-*Aire*-deficient mouse models, all exons of the *Dnmt3l* gene are untouched, the regions upstream of the two promoters active in the testis are affected. In HD-*Aire*-deficient mice, exon 2 of the *Aire* gene was deleted by *lox/cre*-mediated recombination. This deletion affects the surrounding intronic sequences and therefore a small DNA segment of intron 1 of the oocyte-specific *Dnmt3l* transcript. However, in testis, the prospermatogonia and the three spermatocyte and spermatid specific transcripts of *Dnmt3l* are untouched. In the LA-*Aire* mouse, a *neo*-cassette was inserted at the beginning of exon 6 leading to its targeted disruption. The insertion is approximately 1.7 kb upstream from the *Dnmt3l* oocyte promoter and 6.7 kb upstream from the prospermatogonia promoter. In both the HD- and LA-*Aire* mouse models, the disruption of sequence elements upstream of the *Dnmt3l* promoters could eventually lead to hypomorph phenotypes. Neither azoospermia nor 'meiotic catastrophe' or any visible disturbances in meiosis in 3-month-old HD- and LA-*Aire*-deficient mice were detectable in our studies. Still, our results detected the most significant increase in apoptosis in spermatocytes from pachytene stages onward, when compared to *Aire*-sufficient littermates (see Results 3.1). *Aire*-deficient mice also show significantly decreased fertility (see Results 5.). This was as well observed in a study with hypomorphic *Dnmt3l* male mice in which the offspring showed also high rates of aneuploidy due to loss of the paternal X or Y chromosome during spermatogenesis (Chong et al., 2007). The observed subfertility might also be connected to significantly lower sperm counts, as seen in our studies. Abnormal methylation in imprinted genes were observed in infertile men with oligospermia

(Marques et al., 2004; Kobayashi et al., 2007), suggesting a connection between failure of imprinting and infertility (Zamudio et al. 2008). If a hypomorph *Dnmt3l* phenotype influences meiosis, an increase in apoptosis might become only apparent during adulthood, and not in *Aire*-deficient mice at 3-weeks of age. But the decline in apoptosis in 3-week-old *Aire*-deficient mice, as seen in our result, is not in agreement with this hypothesis. Still, it cannot be excluded that hypomethylation in spermatogonia leads to changes in germ cell specific gene expression (Hata et al., 2002) and/or even activation of retrotransposons (La Salle et al., 2007). Even in the context of a checkpoint for mutations and epigenetic defects during prepuberty, a hypomorph *Dnmt3l* phenotype could influence the expression of silenced checkpoint proteins, debilitating the checkpoint and decreasing apoptosis. At 3-months of age, the accumulated mutations, together with the impaired meiosis, would cause significantly increased apoptotic values.

Whether AIRE or DNMT3L, or maybe a combined effect of both, are important factors for the scheduled wave of apoptosis during the first round of spermatogenesis remains open. Future research has to reveal AIRE's specific role during spermatogenesis and whether it functions as a transcriptional activator, ubiquitin ligase, as a direct inducer of apoptosis or even has an yet unknown role. However, our data suggest the presence of an important checkpoint during prepuberty for counterselection of germ cells with mutant genes. The observed promiscuous gene expression in the testis, *Aire*-dependent or not, might be an essential part of this checkpoint for quality control, which assures functional lifelong spermatogenesis and genomic health of the offspring.

CHAPTER VI: SUMMARY

The autoimmune regulator (AIRE) protein has been found in medullary epithelial cells (mTECs) and monocyte-dendritic cells of the thymus. There it mediates expression and presentation of a large variety of proteins, including peripheral organ-specific proteins. Self-reactive T cells recognizing the self-antigens are deleted during negative selection in the thymus in order to establish central tolerance. Furthermore, AIRE has been found in extrathymic AIRE-producing cells (eTACs) in peripheral lymphoid organs where it expresses a complementary set of antigens, suggesting a role in peripheral deletion of autoreactive T cells.

Found in the testis - another tissue with promiscuous gene expression - AIRE protein was determined to be sporadically present only in spermatogonia and spermatocytes, and the levels of protein are around three times higher in 3-week-old mice than in mice of 3-month age. Several genes that are under AIRE control in the thymus are not controlled by AIRE in the testis. However, in mice with a disrupted *Aire* gene, the scheduled apoptotic wave during the first round of spermatogenesis is reduced, and sporadic apoptosis during adulthood is increased. In mice deficient for *Rag-1*, which excludes an involvement of the adaptive immune system, the results are the same. We doubt that the scheduled wave of apoptosis has to establish a strict stoichiometry between germ cells and Sertoli cells (homeostasis hypothesis) because mismatch-repair-deficient mice show a substantial reduction of apoptosis during prepuberty with no obvious effect on spermatogenesis later in life. Alternatively, the scheduled wave of apoptosis might provide a counterselection mechanism during a prepubertal checkpoint for germ cells with mutant genes and/or epigenetic errors (checkpoint hypothesis). This second hypothesis provides a link between the scheduled and the sporadic apoptotic processes. Reduced apoptosis during prepuberty, as caused by *Aire*-deficiency, results in higher apoptotic rates during adulthood because defective germ cells were not efficiently counterselected during the early wave of apoptosis and therefore apoptose at a higher frequency during adulthood due to the accumulation of germ cells carrying disruptive mutations.

Based on its domains, AIRE is a multifunctional protein. The question of whether the AIRE protein functions as an transcriptional activator in the testis remains open. But regardless of its mode of involvement, the promiscuous gene expression in the testis might be an essential part of the proposed prepubertal quality control

checkpoint, which assures functional spermatogenesis and genomic health. Though AIRE's direct involvement in apoptosis or in the ubiquitin pathway and its influence on fertility need to be investigated in future research programs, the results of the research described here suggest several potentially fruitful research approaches.

CHAPTER VII: ABBREVIATIONS

aa	amino acids
ABC	avidin-biotin-enzyme complex
Aire	autoimmune regulator; *mus musculus* gene
AIRE	autoimmune regulator; *homo sapiens* gene
AIRE	autoimmune regulator; *mus musculus*, *homo sapiens* protein
Apaf-1	apoptosis-procaspase-activating-factor-1
APC	antigen presenting cell
APECED	autoimmune polyendocrinopathy-candidiasis-ectodermal dystrophy
APS-1	autoimmune polyendocrine syndrome type-1
B cells	B lymphocyte
BSA	bovine serum albumin
CARD	caspase recruitment domain
CD	cytoplasmatic domain
CREB	CRE-binding protein
cTEC	cortical thymic epithelial cell
DAB	3,3'-diaminobenzidine
DC	dendritic cell
Dnmt3l	DNA methyltransferase 3-like; *mus musculus* gene
DNMT3L	DNA methyltransferase 3-like; *homo sapiens* gene
DNMT3L	DNA methyltransferase 3-like; *mus musculus*, *homo sapiens* protein
dNTP	deoxyribonucleotide triphosphates
eTAC	extrathymic Aire-producing cell
ES cell	embryonic stem cell
FBS	fetal bovine serum
fwd	forward
GAD	glutamic acid decarboxylase
GFP	green fluorescent protein
H3K4me0	histone H3 non-methylated at lysine 4

HD-*Aire* knockout	*Aire*-knockout mouse model made by Anderson et al., 2002
H&E	hematoxylin and eosin
HLA	human leukocyte antigen
HRP	horseradish peroxidase
HSR	homogeneously staining region
IDDM	insulin-dependent diabetes mellitus
Ig	immunoglobulin
IHC	immunohistochemistry
IL	interleukin
IRBP	interphotoreceptor retinoid binding protein
ko	knockout
LA-*Aire* knockout	*Aire*-knockout mouse model made by Ramsey et al., 2002
MEM	minimal essential medium
MHC	major histocompatibility complex
mTEC	medullary thymic epithelial cell
NLS	nuclear localization signal
OMIM	online mendelian inheritance in men
PBS	phosphate buffered saline
PCR	polymerase chain reaction
pGE	promiscuous gene expression
PHD	plant homeodomain
POD	peroxidase
PRR	proline-rich-region
PTA	peripheral-tissue antigens
P-TEFb	positive transcription elongation factor b
Rag-1	recombination activating gene-1; *mus musculus* gene
RAG-1	recombination activating gene-1; *mus musculus*, *homo sapiens* protein
rev	reverse
rpm	rounds per minute
SAND	SP100, Aire-1, NucP41/P75, DEAF-1 domain

Sp100	speckled protein 100 kDa
StDev	standard deviation
T_A	annealing temperature
TBA	tris-borate-EDTA buffer
T cell	T lymphocyte, thymocyte
TCR	T cell receptor
TDT	terminal deoxynucleotidyl transferase
TE	Tris-HCl/EDTA buffer
T_H	T-helper cell
T_M	melting temperature
TRA	tissue-restricted antigens
Treg	regulatory T cells
p	percentile
wt	wild-type

CHAPTER VIII: LITERATURE

Aaltonen, J., P. Bjorses, L. Sandkuijl, J. Perheentupa, and L. Peltonen. **1994**. An autosomal locus causing autoimmune disease: autoimmune polyglandular disease type I assigned to chromosome 21. *Nat Genet* 8:83-87.

Aapola, U., K. Kawasaki, H. S. Scott, J. Ollila, M. Vihinen, M. Heino, A. Shintani, K. Kawasaki, S. Minoshima, K. Krohn, S. E. Antonarakis, N. Shimizu, J. Kudoh, and P. Peterson. **2000**. Isolation and initial characterization of a novel zinc finger gene, DNMT3L, on 21q22.3, related to the cytosine-5-methyltransferase 3 gene family. *Genomics* 65:293-298.

Aapola, U., K. Maenpaa, A. Kaipia, and P. Peterson. **2004**. Epigenetic modifications affect Dnmt3L expression. *Biochem J* 380:705-713.

Aasland, R., T. J. Gibson, and A. F. Stewart. **1995**. The PHD finger: implications for chromatin-mediated transcriptional regulation. *Trends Biochem Sci* 20:56-59.

Abel, M. H., P. J. Baker, H. M. Charlton, A. Monteiro, G. Verhoeven, K. De Gendt, F. Guillou, and P. J. O'Shaughnessy. **2008**. Spermatogenesis and sertoli cell activity in mice lacking sertoli cell receptors for follicle-stimulating hormone and androgen. *Endocrinology* 149:3279-3285.

Adamson, K. A., S. H. Pearce, J. R. Lamb, J. R. Seckl, and S. E. Howie. **2004**. A comparative study of mRNA and protein expression of the autoimmune regulator gene (Aire) in embryonic and adult murine tissues. *J Pathol* 202:180-187.

Agarwal, A., K. Makker, and R. Sharma. **2008**. Clinical relevance of oxidative stress in male factor infertility: an update. *Am J Reprod Immunol* 59:2-11.

Ahonen, P. **1985**. Autoimmune polyendocrinopathy--candidosis--ectodermal dystrophy (APECED): autosomal recessive inheritance. *Clin Genet* 27:535-542.

Ahonen, P., S. Myllarniemi, I. Sipila, and J. Perheentupa. **1990**. Clinical variation of autoimmune polyendocrinopathy-candidiasis-ectodermal dystrophy (APECED) in a series of 68 patients. *N Engl J Med* 322:1829-1836.

Akiyoshi, H., S. Hatakeyama, J. Pitkanen, Y. Mouri, V. Doucas, J. Kudoh, K. Tsurugaya, D. Uchida, A. Matsushima, K. Oshikawa, K. I. Nakayama, N. Shimizu, P. Peterson, and M. Matsumoto. **2004**. Subcellular expression of autoimmune regulator is organized in a spatiotemporal manner. *J Biol Chem* 279:33984-33991.

Alberts, B., A. Johnson, J. Lewis, M. Raff, K. Roberts, P. Walter. **2008**. *Molecular Biology of the Cell*. Garland Science.

Amory, J. K., and W. Bremner. **2001**. Endocrine regulation of testicular function in men: implications for contraceptive development. *Mol Cell Endocrinol* 182:175-179.

Anderson, M. S., E. S. Venanzi, Z. Chen, S. P. Berzins, C. Benoist, and D. Mathis. **2005**. The cellular mechanism of Aire control of T cell tolerance. *Immunity* 23:227-239.

Anderson, M. S., E. S. Venanzi, L. Klein, Z. Chen, S. P. Berzins, S. J. Turley, H. von Boehmer, R. Bronson, A. Dierich, C. Benoist, and D. Mathis. **2002**. Projection of an immunological self shadow within the thymus by the aire protein. *Science* 298:1395-1401.

Aschenbrenner, K., L. M. D'Cruz, E. H. Vollmann, M. Hinterberger, J. Emmerich, L. K. Swee, A. Rolink, and L. Klein. **2007**. Selection of Foxp3+ regulatory T cells specific for self antigen expressed and presented by Aire+ medullary thymic epithelial cells. *Nat Immunol* 8:351-358.

Atassi, M. Z., and P. Casali. **2008**. Molecular mechanisms of autoimmunity. *Autoimmunity* 41:123-132.

Baarends, W. M., R. van der Laan, and J. A. Grootegoed. **2000**. Specific aspects of the ubiquitin system in spermatogenesis. *J Endocrinol Invest* 23:597-604.

Barchi, M., S. Mahadevaiah, M. Di Giacomo, F. Baudat, D. G. de Rooij, P. S. Burgoyne, M. Jasin, and S. Keeney. **2005**. Surveillance of different recombination defects in mouse spermatocytes yields distinct responses despite elimination at an identical developmental stage. *Mol Cell Biol* 25:7203-7215.

Barry, M., and R. C. Bleackley. **2002**. Cytotoxic T lymphocytes: all roads lead to death. *Nat Rev Immunol* 2:401-409.

Baska, K. M., G. Manandhar, D. Feng, Y. Agca, M. W. Tengowski, M. Sutovsky, Y. J. Yi, and P. Sutovsky. **2008**. Mechanism of extracellular ubiquitination in the mammalian epididymis. *J Cell Physiol* 215:684-696.
Bennetts, L. E., and R. J. Aitken. **2005**. A comparative study of oxidative DNA damage in mammalian spermatozoa. *Mol Reprod Dev* 71:77-87.
Bensing, S., S. O. Fetissov, J. Mulder, J. Perheentupa, J. Gustafsson, E. S. Husebye, M. Oscarson, O. Ekwall, P. A. Crock, T. Hokfelt, A. L. Hulting, and O. Kampe. **2007**. Pituitary autoantibodies in autoimmune polyendocrine syndrome type 1. *Proc Natl Acad Sci U S A* 104:949-954.
Bestor, T. H. **1988**. Cloning of a mammalian DNA methyltransferase. *Gene* 74:9-12.
Bestor, T. H., and A. Coxon. **1993**. Cytosine methylation: the pros and cons of DNA methylation. *Curr Biol* 3:384-386.
Betterle, C., N. A. Greggio, and M. Volpato. **1998**. Clinical review 93: Autoimmune polyglandular syndrome type 1. *J Clin Endocrinol Metab* 83:1049-1055.
Beumer, T. L., H. L. Roepers-Gajadien, I. S. Gademan, T. M. Lock, H. B. Kal, and D. G. De Rooij. **2000**. Apoptosis regulation in the testis: involvement of Bcl-2 family members. *Mol Reprod Dev* 56:353-359.
Bjorses, P., J. Aaltonen, N. Horelli-Kuitunen, M. L. Yaspo, and L. Peltonen. **1998**. Gene defect behind APECED: a new clue to autoimmunity. *Hum Mol Genet* 7:1547-1553.
Bjorses, P., M. Halonen, J. J. Palvimo, M. Kolmer, J. Aaltonen, P. Ellonen, J. Perheentupa, I. Ulmanen, and L. Peltonen. **2000**. Mutations in the AIRE gene: effects on subcellular location and transactivation function of the autoimmune polyendocrinopathy-candidiasis-ectodermal dystrophy protein. *Am J Hum Genet* 66:378-392.
Bjorses, P., M. Pelto-Huikko, J. Kaukonen, J. Aaltonen, L. Peltonen, and I. Ulmanen. **1999**. Localization of the APECED protein in distinct nuclear structures. *Hum Mol Genet* 8:259-266.
Blanco-Rodriguez, J. **1998**. A matter of death and life: the significance of germ cell death during spermatogenesis. *Int J Androl* 21:236-248.
Blanco-Rodriguez, J., and C. Martinez-Garcia. **1996**. Spontaneous germ cell death in the testis of the adult rat takes the form of apoptosis: re-evaluation of cell types that exhibit the ability to die during spermatogenesis. *Cell Prolif* 29:13-31.
Blanco-Rodriguez, J., and C. Martinez-Garcia. **1996**. Induction of apoptotic cell death in the seminiferous tubule of the adult rat testis: assessment of the germ cell types that exhibit the ability to enter apoptosis after hormone suppression by oestradiol treatment. *Int J Androl* 19:237-247.
Blechschmidt, K., M. Schweiger, K. Wertz, R. Poulson, H. M. Christensen, A. Rosenthal, H. Lehrach, and M. L. Yaspo. **1999**. The mouse Aire gene: comparative genomic sequencing, gene organization, and expression. *Genome Res* 9:158-166.
Bloch, D. B., A. Nakajima, T. Gulick, J. D. Chiche, D. Orth, S. M. de La Monte, and K. D. Bloch. **2000**. Sp110 localizes to the PML-Sp100 nuclear body and may function as a nuclear hormone receptor transcriptional coactivator. *Mol Cell Biol* 20:6138-6146.
Boatright, K. M., and G. S. Salvesen. **2003**. Mechanisms of caspase activation. *Curr Opin Cell Biol* 15:725-731.
Boehm, T. **2008**. Thymus development and function. *Curr Opin Immunol* 20:178-184.
Boehm, T., and C. C. Bleul. **2007**. The evolutionary history of lymphoid organs. *Nat Immunol* 8:131-135.
Bohossian, H. B., H. Skaletsky, and D. C. Page. **2000**. Unexpectedly similar rates of nucleotide substitution found in male and female hominids. *Nature* 406:622-625.
Bottomley, M. J., M. W. Collard, J. I. Huggenvik, Z. Liu, T. J. Gibson, and M. Sattler. **2001**. The SAND domain structure defines a novel DNA-binding fold in transcriptional regulation. *Nat Struct Biol* 8:626-633.
Bouillet, P., and A. Strasser. **2002**. BH3-only proteins - evolutionarily conserved proapoptotic Bcl-2 family members essential for initiating programmed cell death. *J Cell Sci* 115:1567-1574.
Bourc'his, D., and T. H. Bestor. **2004**. Meiotic catastrophe and retrotransposon reactivation in male germ cells lacking Dnmt3L. *Nature* 431:96-99.
Bourc'his, D., and E. Viegas-Pequignot. **2001**. Direct analysis of chromosome methylation. *Methods Mol Biol* 181:229-242.
Brusko, T. M., A. L. Putnam, and J. A. Bluestone. **2008**. Human regulatory T cells: role in autoimmune disease and therapeutic opportunities. *Immunol Rev* 223:371-390.

Chalmel, F., A. Lardenois, and M. Primig. **2007**. Toward understanding the core meiotic transcriptome in mammals and its implications for somatic cancer. *Ann N Y Acad Sci* 1120:1-15.
Chedin, F., M. R. Lieber, and C. L. Hsieh. **2002**. The DNA methyltransferase-like protein DNMT3L stimulates de novo methylation by Dnmt3a. *Proc Natl Acad Sci U S A* 99:16916-16921.
Chen, J., and I. Sadowski. **2005**. Identification of the mismatch repair genes PMS2 and MLH1 as p53 target genes by using serial analysis of binding elements. *Proc Natl Acad Sci U S A* 102:4813-4818.
Chong, S., N. Vickaryous, A. Ashe, N. Zamudio, N. Youngson, S. Hemley, T. Stopka, A. Skoultchi, J. Matthews, H. S. Scott, D. de Kretser, M. O'Bryan, M. Blewitt, and E. Whitelaw. **2007**. Modifiers of epigenetic reprogramming show paternal effects in the mouse. *Nat Genet* 39:614-622.
Clark, J. M., and E. M. Eddy. **1975**. Fine structural observations on the origin and associations of primordial germ cells of the mouse. *Dev Biol* 47:136-155.
Clemente, E. J., R. A. Furlong, K. L. Loveland, and N. A. Affara. **2006**. Gene expression study in the juvenile mouse testis: identification of stage-specific molecular pathways during spermatogenesis. *Mamm Genome* 17:956-975.
Cobb, J., and M. A. Handel. **1998**. Dynamics of meiotic prophase I during spermatogenesis: from pairing to division. *Semin Cell Dev Biol* 9:445-450.
Codelia, V. A., P. Cisternas, and R. D. Moreno. **2008**. Relevance of caspase activity during apoptosis in pubertal rat spermatogenesis. *Mol Reprod Dev* 75:881-889.
Conaway, R. C., C. S. Brower, and J. W. Conaway. **2002**. Emerging roles of ubiquitin in transcription regulation. *Science* 296:1254-1258.
Finnish-German APECED Consortium. **1997**. An autoimmune disease, APECED, caused by mutations in a novel gene featuring two PHD-type zinc-finger domains. *Nat. Genet.* 17:399-403.
Cooke, H. J., and P. T. Saunders. **2002**. Mouse models of male infertility. *Nat Rev Genet* 3:790-801.
Cooper, T. G. **1998**. Interactions between epididymal secretions and spermatozoa. *J Reprod Fertil Suppl* 53:119-136.
Coucouvanis, E. C., S. W. Sherwood, C. Carswell-Crumpton, E. G. Spack, and P. P. Jones. **1993**. Evidence that the mechanism of prenatal germ cell death in the mouse is apoptosis. *Exp Cell Res* 209:238-247.
D'Abrizio, P., E. Baldini, P. F. Russo, L. Biordi, F. M. Graziano, N. Rucci, G. Properzi, S. Francavilla, and S. Ulisse. **2004**. Ontogenesis and cell specific localization of Fas ligand expression in the rat testis. *Int J Androl* 27:304-310.
Dahlmann, B. **2005**. Proteasomes. *Essays Biochem* 41:31-48.
Danial, N. N., and S. J. Korsmeyer. **2004**. Cell death: critical control points. *Cell* 116:205-219.
de Kretser, D. **2007**. *Endocrinology of the Male Reproductive System*.
de Kretser, D. M., K. L. Loveland, A. Meinhardt, D. Simorangkir, and N. Wreford. **1998**. Spermatogenesis. *Hum Reprod* 13 Suppl 1:1-8.
de Lamirande, E., and C. Gagnon. **1993**. Human sperm hyperactivation and capacitation as parts of an oxidative process. *Free Radic Biol Med* 14:157-166.
de Rooij, D. G., and P. de Boer. **2003**. Specific arrests of spermatogenesis in genetically modified and mutant mice. *Cytogenet Genome Res* 103:267-276.
de Rooij, D. G., and J. A. Grootegoed. **1998**. Spermatogonial stem cells. *Curr Opin Cell Biol* 10:694-701.
Deininger, P. L., J. V. Moran, M. A. Batzer, and H. H. Kazazian, Jr. **2003**. Mobile elements and mammalian genome evolution. *Curr Opin Genet Dev* 13:651-658.
DeJonge, C., C. Barratt. **2006**. *The Sperm Cell*. Cambridge University Press.
Deplus, R., C. Brenner, W. A. Burgers, P. Putmans, T. Kouzarides, Y. de Launoit, and F. Fuks. **2002**. Dnmt3L is a transcriptional repressor that recruits histone deacetylase. *Nucleic Acids Res* 30:3831-3838.
Derbinski, J., J. Gabler, B. Brors, S. Tierling, S. Jonnakuty, M. Hergenhahn, L. Peltonen, J. Walter, and B. Kyewski. **2005**. Promiscuous gene expression in thymic epithelial cells is regulated at multiple levels. *J Exp Med* 202:33-45.
Derbinski, J., A. Schulte, B. Kyewski, and L. Klein. **2001**. Promiscuous gene expression in medullary thymic epithelial cells mirrors the peripheral self. *Nat Immunol* 2:1032-1039.

DeVoss, J., Y. Hou, K. Johannes, W. Lu, G. I. Liou, J. Rinn, H. Chang, R. R. Caspi, L. Fong, and M. S. Anderson. **2006**. Spontaneous autoimmunity prevented by thymic expression of a single self-antigen. *J Exp Med* 203:2727-2735.
Devoss, J. J., A. K. Shum, K. P. Johannes, W. Lu, A. K. Krawisz, P. Wang, T. Yang, N. P. Leclair, C. Austin, E. C. Strauss, and M. S. Anderson. **2008**. Effector mechanisms of the autoimmune syndrome in the murine model of autoimmune polyglandular syndrome type 1. *J Immunol* 181:4072-4079.
Eblen, A., S. Bao, Z. M. Lei, S. T. Nakajima, and C. V. Rao. **2001**. The presence of functional luteinizing hormone/chorionic gonadotropin receptors in human sperm. *J Clin Endocrinol Metab* 86:2643-2648.
Eddahri, F., S. Denanglaire, F. Bureau, R. Spolski, W. J. Leonard, O. Leo, and F. Andris. **2008**. Interleukin-6 / STAT3 signalling regulates the ability of naive T cells to acquire B cell help capacities. *Blood*.
Eddy, E. M. **2002**. Male germ cell gene expression. *Recent Prog Horm Res* 57:103-128.
Egger, G., G. Liang, A. Aparicio, and P. A. Jones. **2004**. Epigenetics in human disease and prospects for epigenetic therapy. *Nature* 429:457-463.
Embree-Ku, M., D. Venturini, and K. Boekelheide. **2002**. Fas is involved in the p53-dependent apoptotic response to ionizing radiation in mouse testis. *Biol Reprod* 66:1456-1461.
Erkkila, K., K. Henriksen, V. Hirvonen, S. Rannikko, J. Salo, M. Parvinen, and L. Dunkel. **1997**. Testosterone regulates apoptosis in adult human seminiferous tubules in vitro. *J Clin Endocrinol Metab* 82:2314-2321.
Ferguson, B. J., C. Alexander, S. W. Rossi, I. Liiv, A. Rebane, C. L. Worth, J. Wong, M. Laan, P. Peterson, E. J. Jenkinson, G. Anderson, H. S. Scott, A. Cooke, and T. Rich. **2008**. AIRE's CARD revealed, a new structure for central tolerance provokes transcriptional plasticity. *J Biol Chem* 283:1723-1731.
Fontenot, J. D., and A. Y. Rudensky. **2005**. A well adapted regulatory contrivance: regulatory T cell development and the forkhead family transcription factor Foxp3. *Nat Immunol* 6:331-337.
French, L. E., M. Hahne, I. Viard, G. Radlgruber, R. Zanone, K. Becker, C. Muller, and J. Tschopp. **1996**. Fas and Fas ligand in embryos and adult mice: ligand expression in several immune-privileged tissues and coexpression in adult tissues characterized by apoptotic cell turnover. *J Cell Biol* 133:335-343.
Galonek, H. L., and J. M. Hardwick. 2006. Upgrading the BCL-2 network. *Nat Cell Biol* 8:1317-1319.
Gardner, J. M., J. J. Devoss, R. S. Friedman, D. J. Wong, Y. X. Tan, X. Zhou, K. P. Johannes, M. A. Su, H. Y. Chang, M. F. Krummel, and M. S. Anderson. **2008**. Deletional tolerance mediated by extrathymic Aire-expressing cells. *Science* 321:843-847.
Gatti, J. L., S. Castella, F. Dacheux, H. Ecroyd, S. Metayer, V. Thimon, and J. L. Dacheux. **2004**. Post-testicular sperm environment and fertility. *Anim Reprod Sci* 82-83:321-339.
Gavanescu, I., C. Benoist, and D. Mathis. **2008**. B cells are required for Aire-deficient mice to develop multi-organ autoinflammation: A therapeutic approach for APECED patients. *Proc Natl Acad Sci U S A* 105:13009-13014.
Gavanescu, I., B. Kessler, H. Ploegh, C. Benoist, and D. Mathis. **2007**. Loss of Aire-dependent thymic expression of a peripheral tissue antigen renders it a target of autoimmunity. *Proc Natl Acad Sci U S A* 104:4583-4587.
Gerton, J. **2005**. Chromosome cohesion: a cycle of holding together and falling apart. *PLoS Biol* 3:e94.
Ghosh, P. K., N. M. Biswas, and D. Ghosh. **1991**. Effect of lithium chloride on spermatogenesis and testicular steroidogenesis in mature albino rats: duration dependent response. *Life Sci* 48:649-657.
Ginsburg, M., M. H. Snow, and A. McLaren. **1990**. Primordial germ cells in the mouse embryo during gastrulation. *Development* 110:521-528.
Goll, M. G., and T. H. Bestor. **2005**. Eukaryotic cytosine methyltransferases. *Annu Rev Biochem* 74:481-514.
Gotter, J., B. Brors, M. Hergenhahn, and B. Kyewski. **2004**. Medullary epithelial cells of the human thymus express a highly diverse selection of tissue-specific genes colocalized in chromosomal clusters. *J Exp Med* 199:155-166.
Govin, J., C. Caron, C. Lestrat, S. Rousseaux, and S. Khochbin. **2004**. The role of histones in chromatin remodelling during mammalian spermiogenesis. *Eur J Biochem* 271:3459-3469.

Gowher, H., C. J. Stockdale, R. Goyal, H. Ferreira, T. Owen-Hughes, and A. Jeltsch. **2005**. De novo methylation of nucleosomal DNA by the mammalian Dnmt1 and Dnmt3A DNA methyltransferases. *Biochemistry* 44:9899-9904.
Gray, D. H., I. Gavanescu, C. Benoist, and D. Mathis. **2007**. Danger-free autoimmune disease in Aire-deficient mice. *Proc Natl Acad Sci U S A* 104:18193-18198.
Guermonprez, P., J. Valladeau, L. Zitvogel, C. Thery, and S. Amigorena. **2002**. Antigen presentation and T cell stimulation by dendritic cells. *Annu Rev Immunol* 20:621-667.
Gwynn, B., K. Lueders, M. S. Sands, and E. H. Birkenmeier. **1998**. Intracisternal A-particle element transposition into the murine beta-glucuronidase gene correlates with loss of enzyme activity: a new model for beta-glucuronidase deficiency in the C3H mouse. *Mol Cell Biol* 18:6474-6481.
Gylling, M., T. Tuomi, P. Bjorses, S. Kontiainen, J. Partanen, M. R. Christie, M. Knip, J. Perheentupa, and A. Miettinen. **2000**. ss-cell autoantibodies, human leukocyte antigen II alleles, and type 1 diabetes in autoimmune polyendocrinopathy-candidiasis-ectodermal dystrophy. *J Clin Endocrinol Metab* 85:4434-4440.
Hakuno, N., T. Koji, T. Yano, N. Kobayashi, O. Tsutsumi, Y. Taketani, and P. K. Nakane. **1996**. Fas/APO-1/CD95 system as a mediator of granulosa cell apoptosis in ovarian follicle atresia. *Endocrinology* 137:1938-1948.
Halonen, M., P. Eskelin, A. G. Myhre, J. Perheentupa, E. S. Husebye, O. Kampe, F. Rorsman, L. Peltonen, I. Ulmanen, and J. Partanen. **2002**. AIRE mutations and human leukocyte antigen genotypes as determinants of the autoimmune polyendocrinopathy-candidiasis-ectodermal dystrophy phenotype. *J Clin Endocrinol Metab* 87:2568-2574.
Halonen, M., H. Kangas, T. Ruppell, T. Ilmarinen, J. Ollila, M. Kolmer, M. Vihinen, J. Palvimo, J. Saarela, I. Ulmanen, and P. Eskelin. **2004**. APECED-causing mutations in AIRE reveal the functional domains of the protein. *Hum Mutat* 23:245-257.
Halonen, M., M. Pelto-Huikko, P. Eskelin, L. Peltonen, I. Ulmanen, and M. Kolmer. **2001**. Subcellular location and expression pattern of autoimmune regulator (Aire), the mouse orthologue for human gene defective in autoimmune polyendocrinopathy candidiasis ectodermal dystrophy (APECED). *J Histochem Cytochem* 49:197-208.
Hamazaki, Y., H. Fujita, T. Kobayashi, Y. Choi, H. S. Scott, M. Matsumoto, and N. Minato. **2007**. Medullary thymic epithelial cells expressing Aire represent a unique lineage derived from cells expressing claudin. *Nat Immunol* 8:304-311.
Hamer, G., I. Novak, A. Kouznetsova, and C. Hoog. **2008**. Disruption of pairing and synapsis of chromosomes causes stage-specific apoptosis of male meiotic cells. *Theriogenology* 69:333-339.
Hansen, R. S., C. Wijmenga, P. Luo, A. M. Stanek, T. K. Canfield, C. M. Weemaes, and S. M. Gartler. **1999**. The DNMT3B DNA methyltransferase gene is mutated in the ICF immunodeficiency syndrome. *Proc Natl Acad Sci U S A* 96:14412-14417.
Haoudi, A., O. J. Semmes, J. M. Mason, and R. E. Cannon. **2004**. Retrotransposition-Competent Human LINE-1 Induces Apoptosis in Cancer Cells With Intact p53. *J Biomed Biotechnol* 2004:185-194.
Harrison, J. C., and J. E. Haber. **2006**. Surviving the breakup: the DNA damage checkpoint. *Annu Rev Genet* 40:209-235.
Hata, K., M. Kusumi, T. Yokomine, E. Li, and H. Sasaki. **2006**. Meiotic and epigenetic aberrations in Dnmt3L-deficient male germ cells. *Mol Reprod Dev* 73:116-122.
Hata, K., M. Okano, H. Lei, and E. Li. **2002**. Dnmt3L cooperates with the Dnmt3 family of de novo DNA methyltransferases to establish maternal imprints in mice. *Development* 129:1983-1993.
Heckert, L. L., and M. D. Griswold. **1991**. Expression of follicle-stimulating hormone receptor mRNA in rat testes and Sertoli cells. *Mol Endocrinol* 5:670-677.
Heckert, L. L., and M. D. Griswold. **2002**. The expression of the follicle-stimulating hormone receptor in spermatogenesis. *Recent Prog Horm Res* 57:129-148.
Heino, M., P. Peterson, J. Kudoh, K. Nagamine, A. Lagerstedt, V. Ovod, A. Ranki, I. Rantala, M. Nieminen, J. Tuukkanen, H. S. Scott, S. E. Antonarakis, N. Shimizu, and K. Krohn. **1999**. Autoimmune regulator is expressed in the cells regulating immune tolerance in thymus medulla. *Biochem Biophys Res Commun* 257:821-825.
Heino, M., P. Peterson, J. Kudoh, N. Shimizu, S. E. Antonarakis, H. S. Scott, and K. Krohn. **2001**. APECED mutations in the autoimmune regulator (AIRE) gene. *Hum Mutat* 18:205-211.

Heino, M., P. Peterson, N. Sillanpaa, S. Guerin, L. Wu, G. Anderson, H. S. Scott, S. E. Antonarakis, J. Kudoh, N. Shimizu, E. J. Jenkinson, P. Naquet, and K. J. Krohn. **2000**. RNA and protein expression of the murine autoimmune regulator gene (Aire) in normal, RelB-deficient and in NOD mouse. *Eur J Immunol* 30:1884-1893.
Helling, R. B., H. M. Goodman, and H. W. Boyer. **1974**. Analysis of endonuclease R-EcoRI fragments of DNA from lambdoid bacteriophages and other viruses by agarose-gel electrophoresis. *J Virol* 14:1235-1244.
Helton, E. S., J. Zhang, and X. Chen. **2008**. The proline-rich domain in p63 is necessary for the transcriptional and apoptosis-inducing activities of TAp63. *Oncogene* 27:2843-2850.
Hershko, A., and A. Ciechanover. **1998**. The ubiquitin system. *Annu Rev Biochem* 67:425-479.
Hikim, A. P., Y. Lue, C. M. Yamamoto, Y. Vera, S. Rodriguez, P. H. Yen, K. Soeng, C. Wang, and R. S. Swerdloff. **2003**. Key apoptotic pathways for heat-induced programmed germ cell death in the testis. *Endocrinology* 144:3167-3175.
Hinton, B. T., M. A. Palladino, D. Rudolph, Z. J. Lan, and J. C. Labus. **1996**. The role of the epididymis in the protection of spermatozoa. *Curr Top Dev Biol* 33:61-102.
Hogquist, K. A., T. A. Baldwin, and S. C. Jameson. **2005**. Central tolerance: learning self-control in the thymus. *Nat Rev Immunol* 5:772-782.
Holdcraft, R. W., and R. E. Braun. **2004**. Hormonal regulation of spermatogenesis. *Int J Androl* 27:335-342.
Holdcraft, R. W., and R. E. Braun. **2004**. Androgen receptor function is required in Sertoli cells for the terminal differentiation of haploid spermatids. *Development* 131:459-467.
Holler, N., A. Tardivel, M. Kovacsovics-Bankowski, S. Hertig, O. Gaide, F. Martinon, A. Tinel, D. Deperthes, S. Calderara, T. Schulthess, J. Engel, P. Schneider, and J. Tschopp. **2003**. Two adjacent trimeric Fas ligands are required for Fas signaling and formation of a death-inducing signaling complex. *Mol Cell Biol* 23:1428-1440.
Hu, J. H., J. Jiang, Y. H. Ma, N. Yang, M. H. Zhang, M. Wu, J. Fei, and L. H. Guo. **2003**. Enhancement of germ cell apoptosis induced by ethanol in transgenic mice overexpressing Fas Ligand. *Cell Res* 13:361-367.
Hubert, F. X., S. A. Kinkel, K. E. Webster, P. Cannon, P. E. Crewther, A. I. Proeitto, L. Wu, W. R. Heath, and H. S. Scott. **2008**. A specific anti-Aire antibody reveals aire expression is restricted to medullary thymic epithelial cells and not expressed in periphery. *J Immunol* 180:3824-3832.
Huesmann, M., B. Scott, P. Kisielow, and H. von Boehmer. **1991**. Kinetics and efficacy of positive selection in the thymus of normal and T cell receptor transgenic mice. *Cell* 66:533-540.
Hurst, L. D., and H. Ellegren. **1998**. Sex biases in the mutation rate. *Trends Genet* 14:446-452.
Iguchi-Ariga, S. M., and W. Schaffner. **1989**. CpG methylation of the cAMP-responsive enhancer/promoter sequence TGACGTCA abolishes specific factor binding as well as transcriptional activation. *Genes Dev* 3:612-619.
Irving, N. G., D. E. Cabin, D. A. Swanson, and R. H. Reeves. **1994**. Gene order is conserved within the human chromosome 21 linkage group on mouse chromosome 10. *Genomics* 21:144-149.
Jeganathan, K. B., and J. M. van Deursen. **2006**. Differential mitotic checkpoint protein requirements in somatic and germ cells. *Biochem Soc Trans* 34:583-586.
Jiang, W., M. S. Anderson, R. Bronson, D. Mathis, and C. Benoist. **2005**. Modifier loci condition autoimmunity provoked by Aire deficiency. *J Exp Med* 202:805-815.
Johnnidis, J. B., E. S. Venanzi, D. J. Taxman, J. P. Ting, C. O. Benoist, and D. J. Mathis. **2005**. Chromosomal clustering of genes controlled by the aire transcription factor. *Proc Natl Acad Sci U S A* 102:7233-7238.
Junqueira, L., J. Carneiro. **2003**. *Basic Histology*. McGraw-Hill/Appleton & Lange.
Kaina, B. **2003**. DNA damage-triggered apoptosis: critical role of DNA repair, double-strand breaks, cell proliferation and signaling. *Biochem Pharmacol* 66:1547-1554.
Kaneda, M., M. Okano, K. Hata, T. Sado, N. Tsujimoto, E. Li, and H. Sasaki. **2004**. Essential role for de novo DNA methyltransferase Dnmt3a in paternal and maternal imprinting. *Nature* 429:900-903.
Kang-Decker, N., G. T. Mantchev, S. C. Juneja, M. A. McNiven, and J. M. van Deursen. **2001**. Lack of acrosome formation in Hrb-deficient mice. *Science* 294:1531-1533.
Kaufman, R. J. **2002**. Orchestrating the unfolded protein response in health and disease. *J Clin Invest* 110:1389-1398.

Kekalainen, E., H. Tuovinen, J. Joensuu, M. Gylling, R. Franssila, N. Pontynen, K. Talvensaari, J. Perheentupa, A. Miettinen, and T. P. Arstila. **2007**. A defect of regulatory T cells in patients with autoimmune polyendocrinopathy-candidiasis-ectodermal dystrophy. *J Immunol* 178:1208-1215.
Kishimoto, H., and J. Sprent. **1997**. Negative selection in the thymus includes semimature T cells. *J Exp Med* 185:263-271.
Kleene, K. C. **2001**. A possible meiotic function of the peculiar patterns of gene expression in mammalian spermatogenic cells. *Mech Dev* 106:3-23.
Klein, L., and B. Kyewski. **2000**. Self-antigen presentation by thymic stromal cells: a subtle division of labor. *Curr Opin Immunol* 12:179-186.
Knudson, C. M., K. S. Tung, W. G. Tourtellotte, G. A. Brown, and S. J. Korsmeyer. **1995**. Bax-deficient mice with lymphoid hyperplasia and male germ cell death. *Science* 270:96-99.
Kobayashi, H., A. Sato, E. Otsu, H. Hiura, C. Tomatsu, T. Utsunomiya, H. Sasaki, N. Yaegashi, and T. Arima. **2007**. Aberrant DNA methylation of imprinted loci in sperm from oligospermic patients. *Hum Mol Genet* 16:2542-2551.
Koh, A. S., A. J. Kuo, S. Y. Park, P. Cheung, J. Abramson, D. Bua, D. Carney, S. E. Shoelson, O. Gozani, R. E. Kingston, C. Benoist, and D. Mathis. **2008**. Aire employs a histone-binding module to mediate immunological tolerance, linking chromatin regulation with organ-specific autoimmunity. *Proc Natl Acad Sci U S A* 105:15878-15883.
Koji, T., and Y. Hishikawa. **2003**. Germ cell apoptosis and its molecular trigger in mouse testes. *Arch Histol Cytol* 66:1-16.
Kont, V., M. Laan, K. Kisand, A. Merits, H. S. Scott, and P. Peterson. **2008**. Modulation of Aire regulates the expression of tissue-restricted antigens. *Mol Immunol* 45:25-33.
Korsmeyer, S. J. **1995**. Regulators of cell death. *Trends Genet* 11:101-105.
Krajewski, S., M. Krajewska, A. Shabaik, T. Miyashita, H. G. Wang, and J. C. Reed. **1994**. Immunohistochemical determination of in vivo distribution of Bax, a dominant inhibitor of Bcl-2. *Am J Pathol* 145:1323-1336.
Krohn, K., R. Uibo, E. Aavik, P. Peterson, and K. Savilahti. **1992**. Identification by molecular cloning of an autoantigen associated with Addison's disease as steroid 17 alpha-hydroxylase. *Lancet* 339:770-773.
Kumar, P. G., M. Laloraya, C. Y. Wang, Q. G. Ruan, A. Davoodi-Semiromi, K. J. Kao, and J. X. She. 2001. The autoimmune regulator (AIRE) is a DNA-binding protein. *J Biol Chem* 276:41357-41364.
Kuroda, N., T. Mitani, N. Takeda, N. Ishimaru, R. Arakaki, Y. Hayashi, Y. Bando, K. Izumi, T. Takahashi, T. Nomura, S. Sakaguchi, T. Ueno, Y. Takahama, D. Uchida, S. Sun, F. Kajiura, Y. Mouri, H. Han, A. Matsushima, G. Yamada, and M. Matsumoto. **2005**. Development of autoimmunity against transcriptionally unrepressed target antigen in the thymus of Aire-deficient mice. *J Immunol* 174:1862-1870.
Kwon, J., K. Mochida, Y. L. Wang, S. Sekiguchi, T. Sankai, S. Aoki, A. Ogura, Y. Yoshikawa, and K. Wada. **2005**. Ubiquitin C-terminal hydrolase L-1 is essential for the early apoptotic wave of germinal cells and for sperm quality control during spermatogenesis. *Biol Reprod* 73:29-35.
Kyewski, B. **2008**. Immunology. A breath of Aire for the periphery. *Science* 321:776-777.
Kyewski, B., and J. Derbinski. **2004**. Self-representation in the thymus: an extended view. *Nat Rev Immunol* 4:688-698.
Kyewski, B., and L. Klein. **2006**. A central role for central tolerance. *Annu Rev Immunol* 24:571-606.
La Salle, S., C. Mertineit, T. Taketo, P. B. Moens, T. H. Bestor, and J. M. Trasler. **2004**. Windows for sex-specific methylation marked by DNA methyltransferase expression profiles in mouse germ cells. *Dev Biol* 268:403-415.
Lane, N., W. Dean, S. Erhardt, P. Hajkova, A. Surani, J. Walter, and W. Reik. **2003**. Resistance of IAPs to methylation reprogramming may provide a mechanism for epigenetic inheritance in the mouse. *Genesis* 35:88-93.
Lee, J., J. H. Richburg, S. C. Younkin, and K. Boekelheide. **1997**. The Fas system is a key regulator of germ cell apoptosis in the testis. *Endocrinology* 138:2081-2088.
Lees-Murdock, D. J., and C. P. Walsh. **2008**. DNA methylation reprogramming in the germ line. *Epigenetics* 3:5-13.
Leonard, F. **1946**. Chronic idiopathic hypoparathyroidism with superimposed Addison's disease in a child. *J Clin Endocrinol* 6:493-506.

Levanon, D., M. Brandeis, Y. Bernstein, and Y. Groner. **1995**. Common promoter features in human and mouse liver type phosphofructokinase gene. *Biochem Mol Biol Int* 35:929-936.
Li, J. Y., D. J. Lees-Murdock, G. L. Xu, and C. P. Walsh. **2004**. Timing of establishment of paternal methylation imprints in the mouse. *Genomics* 84:952-960.
Li, X. C., and J. C. Schimenti. **2007**. Mouse pachytene checkpoint 2 (trip13) is required for completing meiotic recombination but not synapsis. *PLoS Genet* 3:e130.
Liiv, I., A. Rebane, T. Org, M. Saare, J. Maslovskaja, K. Kisand, E. Juronen, L. Valmu, M. J. Bottomley, N. Kalkkinen, and P. Peterson. **2008**. DNA-PK contributes to the phosphorylation of AIRE: importance in transcriptional activity. *Biochim Biophys Acta* 1783:74-83.
Liston, A., S. Lesage, J. Wilson, L. Peltonen, and C. C. Goodnow. **2003**. Aire regulates negative selection of organ-specific T cells. *Nat Immunol* 4:350-354.
Lizama, C., I. Alfaro, J. G. Reyes, and R. D. Moreno. **2007**. Up-regulation of CD95 (Apo-1/Fas) is associated with spermatocyte apoptosis during the first round of spermatogenesis in the rat. *Apoptosis* 12:499-512.
Lockshin, R. A., and Z. Zakeri. **2004**. Caspase-independent cell death? *Oncogene* 23:2766-2773.
London, C. A., M. P. Lodge, and A. K. Abbas. **2000**. Functional responses and costimulator dependence of memory CD4+ T cells. *J Immunol* 164:265-272.
Los, M., C. Stroh, R. U. Janicke, I. H. Engels, and K. Schulze-Osthoff. **2001**. Caspases: more than just killers? *Trends Immunol* 22:31-34.
Ludwig, M., A. Katalinic, S. Gross, A. Sutcliffe, R. Varon, and B. Horsthemke. **2005**. Increased prevalence of imprinting defects in patients with Angelman syndrome born to subfertile couples. *J Med Genet* 42:289-291.
Maatouk, D. M., L. D. Kellam, M. R. Mann, H. Lei, E. Li, M. S. Bartolomei, and J. L. Resnick. **2006**. DNA methylation is a primary mechanism for silencing postmigratory primordial germ cell genes in both germ cell and somatic cell lineages. *Development* 133:3411-3418.
Marques, C. J., F. Carvalho, M. Sousa, and A. Barros. **2004**. Genomic imprinting in disruptive spermatogenesis. *Lancet* 363:1700-1702.
Marques, C. J., T. Francisco, S. Sousa, F. Carvalho, A. Barros, and M. Sousa. **2009**. Methylation defects of imprinted genes in human testicular spermatozoa. *Fertil Steril*.
Martianov, I., S. Brancorsini, A. Gansmuller, M. Parvinen, I. Davidson, and P. Sassone-Corsi. **2002**. Distinct functions of TBP and TLF/TRF2 during spermatogenesis: requirement of TLF for heterochromatic chromocenter formation in haploid round spermatids. *Development* 129:945-955.
Mathis, D., and C. Benoist. **2007**. A decade of AIRE. *Nat Rev Immunol* 7:645-650.
Matzuk, M. M., and D. J. Lamb. **2008**. The biology of infertility: research advances and clinical challenges. *Nat Med* 14:1197-1213.
McHeyzer-Williams, L. J., L. P. Malherbe, and M. G. McHeyzer-Williams. **2006**. Helper T cell-regulated B cell immunity. *Curr Top Microbiol Immunol* 311:59-83.
McLachlan, R. I. **2000**. The endocrine control of spermatogenesis. *Baillieres Best Pract Res Clin Endocrinol Metab* 14:345-362.
McLachlan, R. I., L. O'Donnell, S. J. Meachem, P. G. Stanton, D. M. de Kretser, K. Pratis, and D. M. Robertson. **2002**. Identification of specific sites of hormonal regulation in spermatogenesis in rats, monkeys, and man. *Recent Prog Horm Res* 57:149-179.
McLaren, A. **2003**. Primordial germ cells in the mouse. *Dev Biol* 262:1-15.
Meager, A., K. Visvalingam, P. Peterson, K. Moll, A. Murumagi, K. Krohn, P. Eskelin, J. Perheentupa, E. Husebye, Y. Kadota, and N. Willcox. **2006**. Anti-interferon autoantibodies in autoimmune polyendocrinopathy syndrome type 1. *PLoS Med* 3:e289.
Meistrich, M. L., B. Mohapatra, C. R. Shirley, and M. Zhao. **2003**. Roles of transition nuclear proteins in spermiogenesis. *Chromosoma* 111:483-488.
Mellor, J. **2006**. It takes a PHD to read the histone code. *Cell* 126:22-24.
Meloni, A., F. Incani, D. Corda, A. Cao, and M. C. Rosatelli. **2008**. Role of PHD fingers and COOH-terminal 30 amino acids in AIRE transactivation activity. *Mol Immunol* 45:805-809.
Meloni, A., R. Perniola, V. Faa, E. Corvaglia, A. Cao, and M. C. Rosatelli. **2002**. Delineation of the molecular defects in the AIRE gene in autoimmune polyendocrinopathy-candidiasis-ectodermal dystrophy patients from Southern Italy. *J Clin Endocrinol Metab* 87:841-846.

Mempel, T. R., M. J. Pittet, K. Khazaie, W. Weninger, R. Weissleder, H. von Boehmer, and U. H. von Andrian. **2006**. Regulatory T cells reversibly suppress cytotoxic T cell function independent of effector differentiation. *Immunity* 25:129-141.
Mendis-Handagama, S. M. **1997**. Luteinizing hormone on Leydig cell structure and function. *Histol Histopathol* 12:869-882.
Meng, X., M. Lindahl, M. E. Hyvonen, M. Parvinen, D. G. de Rooij, M. W. Hess, A. Raatikainen-Ahokas, K. Sainio, H. Rauvala, M. Lakso, J. G. Pichel, H. Westphal, M. Saarma, and H. Sariola. **2000**. Regulation of cell fate decision of undifferentiated spermatogonia by GDNF. *Science* 287:1489-1493.
Mittaz, L., C. Rossier, M. Heino, P. Peterson, K. J. Krohn, A. Gos, M. A. Morris, J. Kudoh, N. Shimizu, S. E. Antonarakis, and H. S. Scott. **1999**. Isolation and characterization of the mouse Aire gene. *Biochem Biophys Res Commun* 255:483-490.
Monney, L., C. A. Sabatos, J. L. Gaglia, A. Ryu, H. Waldner, T. Chernova, S. Manning, E. A. Greenfield, A. J. Coyle, R. A. Sobel, G. J. Freeman, and V. K. Kuchroo. **2002**. Th1-specific cell surface protein Tim-3 regulates macrophage activation and severity of an autoimmune disease. *Nature* 415:536-541.
Moreno, R. D., and C. P. Alvarado. **2006**. The mammalian acrosome as a secretory lysosome: new and old evidence. *Mol Reprod Dev* 73:1430-1434.
Morgan, H. D., F. Santos, K. Green, W. Dean, and W. Reik. **2005**. Epigenetic reprogramming in mammals. *Hum Mol Genet* 14 Spec No 1:R47-58.
Mori, C., N. Nakamura, D. J. Dix, M. Fujioka, S. Nakagawa, K. Shiota, and E. M. Eddy. **1997**. Morphological analysis of germ cell apoptosis during postnatal testis development in normal and Hsp 70-2 knockout mice. *Dev Dyn* 208:125-136.
Mullis, K., F. Faloona, S. Scharf, R. Saiki, G. Horn, and H. Erlich. **1986**. Specific enzymatic amplification of DNA in vitro: the polymerase chain reaction. *Cold Spring Harb Symp Quant Biol* 51 Pt 1:263-273.
Mullis, K. B., and F. A. Faloona. **1987**. Specific synthesis of DNA in vitro via a polymerase-catalyzed chain reaction. *Methods Enzymol* 155:335-350.
Munsterberg, A., and R. Lovell-Badge. **1991**. Expression of the mouse anti-mullerian hormone gene suggests a role in both male and female sexual differentiation. *Development* 113:613-624.
Murphy, K., P. Travers, and M. Walport. **2008**. *Janeway's Immunobiology*. Garland Science, Taylor & Francis Group, LLC.
Nagafuchi, S., H. Katsuta, R. Koyanagi-Katsuta, S. Yamasaki, Y. Inoue, K. Shimoda, Y. Ikeda, M. Shindo, E. Yoshida, T. Matsuo, Y. Ohno, K. Kogawa, K. Anzai, H. Kurisaki, J. Kudoh, M. Harada, and N. Shimizu. **2006**. Autoimmune regulator (AIRE) gene is expressed in human activated CD4+ T-cells and regulated by mitogen-activated protein kinase pathway. *Microbiol Immunol* 50:979-987.
Nagamine, K., P. Peterson, H. S. Scott, J. Kudoh, S. Minoshima, M. Heino, K. J. Krohn, M. D. Lalioti, P. E. Mullis, S. E. Antonarakis, K. Kawasaki, S. Asakawa, F. Ito, and N. Shimizu. **1997**. Positional cloning of the APECED gene. *Nat Genet* 17:393-398.
Naito, M., and M. Itoh. **2008**. Patterns of infiltration of lymphocytes into the testis under normal and pathological conditions in mice. *Am J Reprod Immunol* 59:55-61.
Nakao, M. **2001**. Epigenetics: interaction of DNA methylation and chromatin. *Gene* 278:25-31.
Neufeld, M., N. Maclaren, and R. Blizzard. 1980. Autoimmune polyglandular syndromes. *Pediatr Ann* 9:154-162.
Newmeyer, D. D., and S. Ferguson-Miller. **2003**. Mitochondria: releasing power for life and unleashing the machineries of death. *Cell* 112:481-490.
Nicolaides, N. C., S. J. Littman, P. Modrich, K. W. Kinzler, and B. Vogelstein. **1998**. A naturally occurring hPMS2 mutation can confer a dominant negative mutator phenotype. *Mol Cell Biol* 18:1635-1641.
Oakberg, E. F. **1971**. Spermatogonial stem-cell renewal in the mouse. *Anat Rec* 169:515-531.
Oatley, J. M., and R. L. Brinster. **2006**. Spermatogonial stem cells. *Methods Enzymol* 419:259-282.
Okano, M., D. W. Bell, D. A. Haber, and E. Li. **1999**. DNA methyltransferases Dnmt3a and Dnmt3b are essential for de novo methylation and mammalian development. *Cell* 99:247-257.
Ooi, S. K., C. Qiu, E. Bernstein, K. Li, D. Jia, Z. Yang, H. Erdjument-Bromage, P. Tempst, S. P. Lin, C. D. Allis, X. Cheng, and T. H. Bestor. **2007**. DNMT3L connects unmethylated lysine 4 of histone H3 to de novo methylation of DNA. *Nature* 448:714-717.

Org, T., F. Chignola, C. Hetenyi, M. Gaetani, A. Rebane, I. Liiv, U. Maran, L. Mollica, M. J. Bottomley, G. Musco, and P. Peterson. **2008**. The autoimmune regulator PHD finger binds to non-methylated histone H3K4 to activate gene expression. *EMBO Rep* 9:370-376.
Oven, I., N. Brdickova, J. Kohoutek, T. Vaupotic, M. Narat, and B. M. Peterlin. **2007**. AIRE recruits P-TEFb for transcriptional elongation of target genes in medullary thymic epithelial cells. *Mol Cell Biol* 27:8815-8823.
Page, S. L., and R. S. Hawley. **2004**. The genetics and molecular biology of the synaptonemal complex. *Annu Rev Cell Dev Biol* 20:525-558.
Palombella, V. J., O. J. Rando, A. L. Goldberg, and T. Maniatis. **1994**. The ubiquitin-proteasome pathway is required for processing the NF-kappa B1 precursor protein and the activation of NF-kappa B. *Cell* 78:773-785.
Panning, B., and R. Jaenisch. **1998**. RNA and the epigenetic regulation of X chromosome inactivation. *Cell* 93:305-308.
Park, H. H., Y. C. Lo, S. C. Lin, L. Wang, J. K. Yang, and H. Wu. **2007**. The death domain superfamily in intracellular signaling of apoptosis and inflammation. *Annu Rev Immunol* 25:561-586.
Paulsen, M., and A. C. Ferguson-Smith. **2001**. DNA methylation in genomic imprinting, development, and disease. *J Pathol* 195:97-110.
Payne, A. H., and G. L. Youngblood. **1995**. Regulation of expression of steroidogenic enzymes in Leydig cells. *Biol Reprod* 52:217-225.
Perheentupa, J. **2002**. APS-I/APECED: the clinical disease and therapy. *Endocrinol Metab Clin North Am* 31:295-320, vi.
Perheentupa, J. **2006**. Autoimmune polyendocrinopathy-candidiasis-ectodermal dystrophy. *J Clin Endocrinol Metab* 91:2843-2850.
Peterson, P., K. Nagamine, H. Scott, M. Heino, J. Kudoh, N. Shimizu, S. E. Antonarakis, and K. J. Krohn. **1998**. APECED: a monogenic autoimmune disease providing new clues to self-tolerance. *Immunol Today* 19:384-386.
Peterson, P., T. Org, and A. Rebane. **2008**. Transcriptional regulation by AIRE: molecular mechanisms of central tolerance. *Nat Rev Immunol*.
Peterson, P., and L. Peltonen. **2005**. Autoimmune polyendocrinopathy syndrome type 1 (APS1) and AIRE gene: new views on molecular basis of autoimmunity. *J Autoimmun* 25 Suppl:49-55.
Peterson, P., J. Pitkanen, N. Sillanpaa, and K. Krohn. **2004**. Autoimmune polyendocrinopathy candidiasis ectodermal dystrophy (APECED): a model disease to study molecular aspects of endocrine autoimmunity. *Clin Exp Immunol* 135:348-357.
Petronczki, M., M. F. Siomos, and K. Nasmyth. **2003**. Un menage a quatre: the molecular biology of chromosome segregation in meiosis. *Cell* 112:423-440.
Pickart, C. M. **2001**. Mechanisms underlying ubiquitination. *Annu Rev Biochem* 70:503-533.
Pitkanen, J., V. Doucas, T. Sternsdorf, T. Nakajima, S. Aratani, K. Jensen, H. Will, P. Vahamurto, J. Ollila, M. Vihinen, H. S. Scott, S. E. Antonarakis, J. Kudoh, N. Shimizu, K. Krohn, and P. Peterson. **2000**. The autoimmune regulator protein has transcriptional transactivating properties and interacts with the common coactivator CREB-binding protein. *J Biol Chem* 275:16802-16809.
Pitkanen, J., A. Rebane, J. Rowell, A. Murumagi, P. Strobel, K. Moll, M. Saare, J. Heikkila, V. Doucas, A. Marx, and P. Peterson. **2005**. Cooperative activation of transcription by autoimmune regulator AIRE and CBP. *Biochem Biophys Res Commun* 333:944-953.
Pontynen, N., A. Miettinen, T. P. Arstila, O. Kampe, M. Alimohammadi, O. Vaarala, L. Peltonen, and I. Ulmanen. **2006**. Aire deficient mice do not develop the same profile of tissue-specific autoantibodies as APECED patients. *J Autoimmun* 27:96-104.
Porter, M. E., and W. S. Sale. **2000**. The 9 + 2 axoneme anchors multiple inner arm dyneins and a network of kinases and phosphatases that control motility. *J Cell Biol* 151:F37-42.
Print, C. G., and K. L. Loveland. **2000**. Germ cell suicide: new insights into apoptosis during spermatogenesis. *Bioessays* 22:423-430.
Print, C. G., K. L. Loveland, L. Gibson, T. Meehan, A. Stylianou, N. Wreford, D. de Kretser, D. Metcalf, F. Kontgen, J. M. Adams, and S. Cory. **1998**. Apoptosis regulator bcl-w is essential for spermatogenesis but appears otherwise redundant. *Proc Natl Acad Sci U S A* 95:12424-12431.
Purohit, S., P. G. Kumar, M. Laloraya, and J. X. She. **2005**. Mapping DNA-binding domains of the autoimmune regulator protein. *Biochem Biophys Res Commun* 327:939-944.

Ramadan, S., A. Terrinoni, M. V. Catani, A. E. Sayan, R. A. Knight, M. Mueller, P. H. Krammer, G. Melino, and E. Candi. **2005**. p73 induces apoptosis by different mechanisms. *Biochem Biophys Res Commun* 331:713-717.

Ramsey, C., O. Winqvist, L. Puhakka, M. Halonen, A. Moro, O. Kampe, P. Eskelin, M. Pelto-Huikko, and L. Peltonen. **2002**. Aire deficient mice develop multiple features of APECED phenotype and show altered immune response. *Hum Mol Genet* 11:397-409.

Rannikki, A. S., F. P. Zhang, and I. T. Huhtaniemi. **1995**. Ontogeny of follicle-stimulating hormone receptor gene expression in the rat testis and ovary. *Mol Cell Endocrinol* 107:199-208.

Reik, W., and J. Walter. **2001**. Genomic imprinting: parental influence on the genome. *Nat Rev Genet* 2:21-32.

Revenkova, E., M. Eijpe, C. Heyting, C. A. Hodges, P. A. Hunt, B. Liebe, H. Scherthan, and R. Jessberger. **2004**. Cohesin SMC1 beta is required for meiotic chromosome dynamics, sister chromatid cohesion and DNA recombination. *Nat Cell Biol* 6:555-562.

Riccioli, A., L. Salvati, A. D'Alessio, D. Starace, C. Giampietri, P. De Cesaris, A. Filippini, and E. Ziparo. **2003**. The Fas system in the seminiferous epithelium and its possible extra-testicular role. *Andrologia* 35:64-70.

Riccioli, A., D. Starace, A. D'Alessio, G. Starace, F. Padula, P. De Cesaris, A. Filippini, and E. Ziparo. **2000**. TNF-alpha and IFN-gamma regulate expression and function of the Fas system in the seminiferous epithelium. *J Immunol* 165:743-749.

Rinderle, C., H. M. Christensen, S. Schweiger, H. Lehrach, and M. L. Yaspo. **1999**. AIRE encodes a nuclear protein co-localizing with cytoskeletal filaments: altered sub-cellular distribution of mutants lacking the PHD zinc fingers. *Hum Mol Genet* 8:277-290.

Robaire, B., and N. A. Henderson. **2006**. Actions of 5alpha-reductase inhibitors on the epididymis. *Mol Cell Endocrinol* 250:190-195.

Rodenhiser, D., and M. Mann. **2006**. Epigenetics and human disease: translating basic biology into clinical applications. *Cmaj* 174:341-348.

Rodewald, H. R. **2008**. Thymus organogenesis. *Annu Rev Immunol* 26:355-388.

Rodriguez, I., C. Ody, K. Araki, I. Garcia, and P. Vassalli. **1997**. An early and massive wave of germinal cell apoptosis is required for the development of functional spermatogenesis. *Embo J* 16:2262-2270.

Rosatelli, M. C., A. Meloni, A. Meloni, M. Devoto, A. Cao, H. S. Scott, P. Peterson, M. Heino, K. J. Krohn, K. Nagamine, J. Kudoh, N. Shimizu, and S. E. Antonarakis. **1998**. A common mutation in Sardinian autoimmune polyendocrinopathy-candidiasis-ectodermal dystrophy patients. *Hum Genet* 103:428-434.

Ruan, Q. G., K. Tung, D. Eisenman, Y. Setiady, S. Eckenrode, B. Yi, S. Purohit, W. P. Zheng, Y. Zhang, L. Peltonen, and J. X. She. **2007**. The autoimmune regulator directly controls the expression of genes critical for thymic epithelial function. *J Immunol* 178:7173-7180.

Ruan, Q. G., C. Y. Wang, J. D. Shi, and J. X. She. **1999**. Expression and alternative splicing of the mouse autoimmune regulator gene (Aire). *J Autoimmun* 13:307-313.

Rucker, E. B., 3rd, P. Dierisseau, K. U. Wagner, L. Garrett, A. Wynshaw-Boris, J. A. Flaws, and L. Hennighausen. **2000**. Bcl-x and Bax regulate mouse primordial germ cell survival and apoptosis during embryogenesis. *Mol Endocrinol* 14:1038-1052.

Russell, L. D., Robert A. Ettlin; Amiya P. Sinha Hikmi, Eric D. Clegg. **1990**. *Histological and histopathological evaluation of the testis*. Cache River Press.

Russell, L. D., H. Chiarini-Garcia, S. J. Korsmeyer, and C. M. Knudson. **2002**. Bax-dependent spermatogonia apoptosis is required for testicular development and spermatogenesis. *Biol Reprod* 66:950-958.

Russell, L. D., J. Warren, L. Debeljuk, L. L. Richardson, P. L. Mahar, K. G. Waymire, S. P. Amy, A. J. Ross, and G. R. MacGregor. **2001**. Spermatogenesis in Bclw-deficient mice. *Biol Reprod* 65:318-332.

Ruwanpura, S. M., R. I. McLachlan, P. G. Stanton, K. L. Loveland, and S. J. Meachem. **2008**. Pathways involved in testicular germ cell apoptosis in immature rats after FSH suppression. *J Endocrinol* 197:35-43.

Saiki, R. K., S. Scharf, F. Faloona, K. B. Mullis, G. T. Horn, H. A. Erlich, and N. Arnheim. **1985**. Enzymatic amplification of beta-globin genomic sequences and restriction site analysis for diagnosis of sickle cell anemia. *Science* 230:1350-1354.

Sakaguchi, S., T. Yamaguchi, T. Nomura, and M. Ono. **2008**. Regulatory T cells and immune tolerance. *Cell* 133:775-787.
Sakkas, D., G. C. Manicardi, and D. Bizzaro. **2003**. Sperm nuclear DNA damage in the human. *Adv Exp Med Biol* 518:73-84.
Sanborn, B. M., A. Steinberger, R. K. Tcholakian, and E. Steinberger. **1977**. Direct measurement of androgen receptors in cultured Sertoli cells. *Steroids* 29:493-502.
Santos, F., B. Hendrich, W. Reik, and W. Dean. **2002**. Dynamic reprogramming of DNA methylation in the early mouse embryo. *Dev Biol* 241:172-182.
Sato, K., K. Nakajima, H. Imamura, T. Deguchi, S. Horinouchi, K. Yamazaki, E. Yamada, Y. Kanaji, and K. Takano. **2002**. A novel missense mutation of AIRE gene in a patient with autoimmune polyendocrinopathy, candidiasis and ectodermal dystrophy (APECED), accompanied with progressive muscular atrophy: case report and review of the literature in Japan. *Endocr J* 49:625-633.
Sato, K., U. Sato, S. Tateishi, K. Kubo, R. Horikawa, T. Mimura, K. Yamamoto, and H. Kanda. **2004**. Aire downregulates multiple molecules that have contradicting immune-enhancing and immune-suppressive functions. *Biochem Biophys Res Commun* 318:935-940.
Schaefer, C. B., S. K. Ooi, T. H. Bestor, and D. Bourc'his. **2007**. Epigenetic decisions in mammalian germ cells. *Science* 316:398-399.
Schlecht, U., P. Demougin, R. Koch, L. Hermida, C. Wiederkehr, P. Descombes, C. Pineau, B. Jegou, and M. Primig. **2004**. Expression profiling of mammalian male meiosis and gametogenesis identifies novel candidate genes for roles in the regulation of fertility. *Mol Biol Cell* 15:1031-1043.
Schneider, G., F. Ahlhelm, K. Altmeyer, S. Aliani, K. Remberger, H. Schoenhofen, B. Kramann, and M. Uder. **2001**. Rare pseudotumors of the urinary bladder in childhood. *Eur Radiol* 11:1024-1029.
Schulz, R., K. Woodfine, T. R. Menheniott, D. Bourc'his, T. Bestor, and R. J. Oakey. **2008**. WAMIDEX: a web atlas of murine genomic imprinting and differential expression. *Epigenetics* 3:89-96.
Scott, H. S., M. Heino, P. Peterson, L. Mittaz, M. D. Lalioti, C. Betterle, A. Cohen, M. Seri, M. Lerone, G. Romeo, P. Collin, M. Salo, R. Metcalfe, A. Weetman, M. P. Papasavvas, C. Rossier, K. Nagamine, J. Kudoh, N. Shimizu, K. J. Krohn, and S. E. Antonarakis. **1998**. Common mutations in autoimmune polyendocrinopathy-candidiasis-ectodermal dystrophy patients of different origins. *Mol Endocrinol* 12:1112-1119.
Seaman, F., P. Sawhney, C. J. Giammona, and J. H. Richburg. **2003**. Cisplatin-induced pulse of germ cell apoptosis precedes long-term elevated apoptotic rates in C57/BL/6 mouse testis. *Apoptosis* 8:101-108.
Shaman, J. A., R. Prisztoka, and W. S. Ward. **2006**. Topoisomerase IIB and an extracellular nuclease interact to digest sperm DNA in an apoptotic-like manner. *Biol Reprod* 75:741-748.
Shi, J. D., C. Y. Wang, M. P. Marron, Q. G. Ruan, Y. Q. Huang, J. C. Detter, and J. X. She. **1999**. Chromosomal localization and complete genomic sequence of the murine autoimmune regulator gene (Aire). *Autoimmunity* 31:47-53.
Shima, J. E., D. J. McLean, J. R. McCarrey, and M. D. Griswold. **2004**. The murine testicular transcriptome: characterizing gene expression in the testis during the progression of spermatogenesis. *Biol Reprod* 71:319-330.
Shimodaira, H., A. Yoshioka-Yamashita, R. D. Kolodner, and J. Y. Wang. **2003.** Interaction of mismatch repair protein PMS2 and the p53-related transcription factor p73 in apoptosis response to cisplatin. *Proc Natl Acad Sci U S A* 100:2420-2425.
Shinohara, T., M. R. Avarbock, and R. L. Brinster. **2000**. Functional analysis of spermatogonial stem cells in Steel and cryptorchid infertile mouse models. *Dev Biol* 220:401-411.
Shovlin, T. C., D. Bourc'his, S. La Salle, A. O'Doherty, J. M. Trasler, T. H. Bestor, and C. P. Walsh. **2007**. Sex-specific promoters regulate Dnmt3L expression in mouse germ cells. *Hum Reprod* 22:457-467.
Sofikitis, N., N. Giotitsas, P. Tsounapi, D. Baltogiannis, D. Giannakis, and N. Pardalidis. **2008**. Hormonal regulation of spermatogenesis and spermiogenesis. *J Steroid Biochem Mol Biol* 109:323-330.
Stallock, J., K. Molyneaux, K. Schaible, C. M. Knudson, and C. Wylie. **2003**. The pro-apoptotic gene Bax is required for the death of ectopic primordial germ cells during their migration in the mouse embryo. *Development* 130:6589-6597.

Stein, R., A. Razin, and H. Cedar. **1982**. In vitro methylation of the hamster adenine phosphoribosyltransferase gene inhibits its expression in mouse L cells. *Proc Natl Acad Sci U S A* 79:3418-3422.
Suetake, I., Y. Morimoto, T. Fuchikami, K. Abe, and S. Tajima. **2006**. Stimulation effect of Dnmt3L on the DNA methylation activity of Dnmt3a2. *J Biochem* 140:553-559.
Sullivan, R., G. Frenette, and J. Girouard. **2007**. Epididymosomes are involved in the acquisition of new sperm proteins during epididymal transit. *Asian J Androl* 9:483-491.
Sutovsky, P., R. Moreno, J. Ramalho-Santos, T. Dominko, W. E. Thompson, and G. Schatten. **2001**. A putative, ubiquitin-dependent mechanism for the recognition and elimination of defective spermatozoa in the mammalian epididymis. *J Cell Sci* 114:1665-1675.
Suzuki, E., Y. Kobayashi, O. Kawano, K. Endo, H. Haneda, H. Yukiue, H. Sasaki, M. Yano, M. Maeda, and Y. Fujii. **2008**. Expression of AIRE in thymocytes and peripheral lymphocytes. *Autoimmunity* 41:133-139.
Taams, L. S., E. P. Boot, W. van Eden, and M. H. Wauben. **2000**. 'Anergic' T cells modulate the T-cell activating capacity of antigen-presenting cells. *J Autoimmun* 14:335-341.
Takahama, Y. **2006**. Journey through the thymus: stromal guides for T-cell development and selection. *Nat Rev Immunol* 6:127-135.
Tam, P. P., and M. H. Snow. **1981**. Proliferation and migration of primordial germ cells during compensatory growth in mouse embryos. *J Embryol Exp Morphol* 64:133-147.
Tao, Y., R. Kupfer, B. J. Stewart, C. Williams-Skipp, C. K. Crowell, D. D. Patel, S. Sain, and R. I. Scheinman. **2006**. AIRE recruits multiple transcriptional components to specific genomic regions through tethering to nuclear matrix. *Mol Immunol* 43:335-345.
Tegelenbosch, R. A., and D. G. de Rooij. **1993**. A quantitative study of spermatogonial multiplication and stem cell renewal in the C3H/101 F1 hybrid mouse. *Mutat Res* 290:193-200.
Thorne, H. V. **1966**. Electrophoretic separation of polyoma virus DNA from host cell DNA. *Virology* 29:234-239.
Thorpe, E., and H. Handley. **1929**. Chronic tetany and chronic mycelial stomatitis in a child aged four and one-half years. *Am J Dis Child* 38:328–338.
Trambas, C. M., and G. M. Griffiths. **2003**. Delivering the kiss of death. *Nat Immunol* 4:399-403.
Trasler, J. M. **2006**. Gamete imprinting: setting epigenetic patterns for the next generation. *Reprod Fertil Dev* 18:63-69.
Turner, T. T., C. E. Jones, S. S. Howards, L. L. Ewing, B. Zegeye, and G. L. Gunsalus. **1984**. On the androgen microenvironment of maturing spermatozoa. *Endocrinology* 115:1925-1932.
Uchida, D., S. Hatakeyama, A. Matsushima, H. Han, S. Ishido, H. Hotta, J. Kudoh, N. Shimizu, V. Doucas, K. I. Nakayama, N. Kuroda, and M. Matsumoto. **2004**. AIRE functions as an E3 ubiquitin ligase. *J Exp Med* 199:167-172.
Ulmanen, I., M. Halonen, T. Ilmarinen, and L. Peltonen. **2005**. Monogenic autoimmune diseases - lessons of self-tolerance. *Curr Opin Immunol* 17:609-615.
Underhill, D. M., M. Bassetti, A. Rudensky, and A. Aderem. **1999**. Dynamic interactions of macrophages with T cells during antigen presentation. *J Exp Med* 190:1909-1914.
Vasileva, A., D. Tiedau, A. Firooznia, T. Muller-Reichert, and R. Jessberger. **2009**. Tdrd6 Is Required for Spermiogenesis, Chromatoid Body Architecture, and Regulation of miRNA Expression. *Curr Biol*.
Veldhoen, M., and B. Stockinger. **2006**. TGFbeta1, a "Jack of all trades": the link with pro-inflammatory IL-17-producing T cells. *Trends Immunol* 27:358-361.
Vergouwen, R. P., S. G. Jacobs, R. Huiskamp, J. A. Davids, and D. G. de Rooij. **1991**. Proliferative activity of gonocytes, Sertoli cells and interstitial cells during testicular development in mice. *J Reprod Fertil* 93:233-243.
Villasenor, J., C. Benoist, and D. Mathis. **2005**. AIRE and APECED: molecular insights into an autoimmune disease. *Immunol Rev* 204:156-164.
Vogl, A. W., D. C. Pfeiffer, D. Mulholland, G. Kimel, and J. Guttman. **2000**. Unique and multifunctional adhesion junctions in the testis: ectoplasmic specializations. *Arch Histol Cytol* 63:1-15.
Wang, R. A., P. K. Nakane, and T. Koji. **1998**. Autonomous cell death of mouse male germ cells during fetal and postnatal period. *Biol Reprod* 58:1250-1256.
Watanabe, N., Y. H. Wang, H. K. Lee, T. Ito, Y. H. Wang, W. Cao, and Y. J. Liu. **2005**. Hassall's corpuscles instruct dendritic cells to induce CD4+CD25+ regulatory T cells in human thymus. *Nature* 436:1181-1185.

Webster, K. E., M. K. O'Bryan, S. Fletcher, P. E. Crewther, U. Aapola, J. Craig, D. K. Harrison, H. Aung, N. Phutikanit, R. Lyle, S. J. Meachem, S. E. Antonarakis, D. M. de Kretser, M. P. Hedger, P. Peterson, B. J. Carroll, and H. S. Scott. **2005**. Meiotic and epigenetic defects in Dnmt3L-knockout mouse spermatogenesis. *Proc Natl Acad Sci U S A* 102:4068-4073.
Whitaker, J., B. Landing, V. Esselborn, and R. Williams. **1956**. The syndrome of familial juvenile hypoadrenocorticism, hypoparathyroidism and superficial moniliasis. *J Clin Endocrinol Metab* 16.
Wing, S. S. **2003**. Deubiquitinating enzymes--the importance of driving in reverse along the ubiquitin-proteasome pathway. *Int J Biochem Cell Biol* 35:590-605.
Winqvist, O., F. A. Karlsson, and O. Kampe. **1992**. 21-Hydroxylase, a major autoantigen in idiopathic Addison's disease. *Lancet* 339:1559-1562.
Wojcik, C., M. Benchaib, J. Lornage, J. C. Czyba, and J. F. Guerin. **2000**. Proteasomes in human spermatozoa. *Int J Androl* 23:169-177.
Wouters-Tyrou, D., A. Martinage, P. Chevaillier, and P. Sautiere. **1998**. Nuclear basic proteins in spermiogenesis. *Biochimie* 80:117-128.
Wright, A., W. W. Reiley, M. Chang, W. Jin, A. J. Lee, M. Zhang, and S. C. Sun. **2007**. Regulation of early wave of germ cell apoptosis and spermatogenesis by deubiquitinating enzyme CYLD. *Dev Cell* 13:705-716.
Xu, J. P., X. Li, E. Mori, M. W. Guo, I. Matsuda, H. Takaichi, T. Amano, and T. Mori. **1999**. Expression of Fas-Fas ligand in murine testis. *Am J Reprod Immunol* 42:381-388.
Yamamoto, A., K. Kitamura, D. Hihara, Y. Hirose, S. Katsuyama, and Y. Hiraoka. **2008**. Spindle checkpoint activation at meiosis I advances anaphase II onset via meiosis-specific APC/C regulation. *J Cell Biol* 182:277-288.
Yamazaki, Y., M. R. Mann, S. S. Lee, J. Marh, J. R. McCarrey, R. Yanagimachi, and M. S. Bartolomei. **2003**. Reprogramming of primordial germ cells begins before migration into the genital ridge, making these cells inadequate donors for reproductive cloning. *Proc Natl Acad Sci U S A* 100:12207-12212.
Yang, Y., and X. Yu. **2003**. Regulation of apoptosis: the ubiquitous way. *Faseb J* 17:790-799.
Yoder, J. A., and T. H. Bestor. **1998**. A candidate mammalian DNA methyltransferase related to pmt1p of fission yeast. *Hum Mol Genet* 7:279-284.
Yoder, J. A., N. S. Soman, G. L. Verdine, and T. H. Bestor. **1997**. DNA (cytosine-5)-methyltransferases in mouse cells and tissues. Studies with a mechanism-based probe. *J Mol Biol* 270:385-395.
Yoshida, S., M. Sukeno, T. Nakagawa, K. Ohbo, G. Nagamatsu, T. Suda, and Y. Nabeshima. **2006**. The first round of mouse spermatogenesis is a distinctive program that lacks the self-renewing spermatogonia stage. *Development* 133:1495-1505.
Yoshida, S., A. Takakura, K. Ohbo, K. Abe, J. Wakabayashi, M. Yamamoto, T. Suda, and Y. Nabeshima. **2004**. Neurogenin3 delineates the earliest stages of spermatogenesis in the mouse testis. *Dev Biol* 269:447-458.
Yuan, L., J. G. Liu, J. Zhao, E. Brundell, B. Daneholt, and C. Hoog. **2000**. The murine SCP3 gene is required for synaptonemal complex assembly, chromosome synapsis, and male fertility. *Mol Cell* 5:73-83.
Zamudio, N. M., S. Chong, and M. K. O'Bryan. **2008**. Epigenetic regulation in male germ cells. *Reproduction* 136:131-146.
Zeng, M., L. Narayanan, X. S. Xu, T. A. Prolla, R. M. Liskay, and P. M. Glazer. **2000**. Ionizing radiation-induced apoptosis via separate Pms2- and p53-dependent pathways. *Cancer Res* 60:4889-4893.
Zheng, S., T. T. Turner, and J. J. Lysiak. **2006**. Caspase 2 activity contributes to the initial wave of germ cell apoptosis during the first round of spermatogenesis. *Biol Reprod* 74:1026-1033.
Zlotogora, J., and M. S. Shapiro. **1992**. Polyglandular autoimmune syndrome type I among Iranian Jews. *J Med Genet* 29:824-826.
Zuklys, S., G. Balciunaite, A. Agarwal, E. Fasler-Kan, E. Palmer, and G. A. Hollander. **2000**. Normal thymic architecture and negative selection are associated with Aire expression, the gene defective in the autoimmune-polyendocrinopathy-candidiasis-ectodermal dystrophy (APECED). *J Immunol* 165:1976-1983.

Curriculum Vitae

PERSONAL INFO

Address
Email
Phone
Born June 2nd 1973, Mering, Germany

EDUCATION

2009 Ph.D. candidate
Ludwig-Maximilians-University Munich; Advisor: Prof. Elisabeth Weiss
University of California San Francisco; Advisor: Prof. Matthias Wabl

2001 M.S., Biology
Ludwig-Maximilians-University Munich
Major: Human Genetics and Anthropology

1994 Abitur
Rudolf-Diesel Gymnasium Augsburg, Germany

WORK EXPERIENCE

current Strategist
Eight Inc., San Francisco, CA
• Market research and analysis
• Strategic outreach
• Business Development

2007-2008 Consultant
Claudia Schaller Consulting, Germany
• Market research and analysis
• Branding and strategy
• Business development

2001-2007 Junior Research Specialist
University of California San Francisco
• Research
• Scientific writings and presentation

1993-1996 Assistant Department Manager
H&M, Germany
• Management and presentation of fashion merchandise
• Accounting

ADDITIONAL TRAINING

2007 Integrated Marketing, Market Research, Branding Strategies
San Francisco State University College of Extended Learning

2007 Project Management
San Francisco State University College of Extended Learning

2005 Professional Communication Skills
San Francisco State University College of Extended Learning

2005 Corporate Finance Skills Course
Center for Bioentrepreneurship, University of California San Francisco

Publication

Schaller, C.E., C.W. Wang, G. Beck-Engeser G., L. Goss, H.S. Scott, M.S. Anderson, and M. Wabl. 2008. Expression of Aire and the Early Wave of Apoptosis in Spermatogenesis. J Immunol. 2008 Feb 1;180(3):1338-43.

Danksagung

Ein herzliches Dankeschön an Professor Matthias Wabl für die Bereitstellung des interessanten Themas und die jahrelange wissenschaftliche Unterstützung.

Ein großes Danke ebenso an Professor Elisabeth Weiss für die stets freundliche Hilfe bei dieser externen Promotion.

A big thank you to the “Wabl lab”, especially to Dr. Tobias Gerdes!

Das größte Dankeschön gilt meinen Eltern und Markus Diebel für die lange und liebevolle Hilfe während der letzten Jahre!